

12-2020

ELECTRICAL IDENTIFICATION OF INNATE IMMUNE CELLS

Rasha Ayman Nasser

Follow this and additional works at: https://scholarworks.uaeu.ac.ae/all_theses



Part of the [Medical Immunology Commons](#)

Recommended Citation

Nasser, Rasha Ayman, "ELECTRICAL IDENTIFICATION OF INNATE IMMUNE CELLS" (2020). *Theses*. 771.
https://scholarworks.uaeu.ac.ae/all_theses/771

This Thesis is brought to you for free and open access by the Electronic Theses and Dissertations at Scholarworks@UAEU. It has been accepted for inclusion in Theses by an authorized administrator of Scholarworks@UAEU. For more information, please contact mariam_aljaberi@uaeu.ac.ae.

United Arab Emirates University

College of Medicine and Health Sciences

Department of Medical Microbiology

ELECTRICAL IDENTIFICATION OF INNATE IMMUNE CELLS

Rasha Ayman Nasser

This thesis is submitted in partial fulfilment of the requirements for the degree of
Master of Medical Sciences (Microbiology and Immunology)

Under the Supervision of Professor Bassam R. Ali

December 2020

Declaration of Original Work

I, Rasha Ayman Nasser, the undersigned, a graduate student at the United Arab Emirates University (UAEU), and the author of this thesis entitled “*Electrical Identification of Innate Immune Cells*”, hereby, solemnly declare that this thesis is my own original research work that has been done and prepared by me under the supervision of Professor Bassam R. Ali in the College of Medicine & Health Sciences at UAEU. This work has not previously been presented or published, or formed the basis for the award of any academic degree, diploma or a similar title at this or any other university. Any materials borrowed from other sources (whether published or unpublished) and relied upon or included in my thesis have been properly cited and acknowledged in accordance with appropriate academic conventions. I further declare that there is no potential conflict of interest with respect to the research, data collection, authorship, presentation and/or publication of this thesis.

Student's Signature: _____



Date: 9-12-2020

Copyright © 2020 Rasha Ayman Nasser
All Rights Reserved

Advisory Committee

1) Advisor: Bassam R. Ali

Title: Professor

Department of Pathology

College of Medicine and Health Sciences

2) Co-advisor: Mahmoud Al-Ahmad

Title: Associate Professor

Department of Electrical Engineering

College of Engineering

3) Member: Lihadh Al-Gazali

Title: Professor

Department of Pediatrics

College of Medicine and Health Sciences

Approval of the Master Thesis

This Master Thesis is approved by the following Examining Committee Members:

- 1) Advisor (Committee Chair): Bassam R. Ali

Title: Professor

Department of Pathology

College of Medicine and Health Sciences

Signature  Date 2nd of January 2021

- 2) Member: Mahmoud Al-Ahmad

Title: Associate Professor

Department of Electrical Engineering

College of Engineering

Signature  Date 2nd January 2021

- 3) Member: Mariam Al-Shamsi

Title: Associate Professor

Department of Medical Microbiology

College of Medicine and Health Sciences

Signature  Date 3rd January, 2021

- 4) Member (External Examiner): Kinda Khalaf

Title: Associate Professor

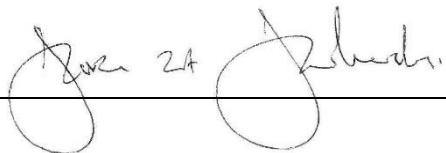
Department of Biomedical Engineering

Institution: Khalifa University of Science and Technology, UAE

Signature  Date 3/2/2021

This Master Thesis is accepted by:

Dean of the College of Medicine and Health Sciences: Professor Janusz Jankowski

Signature  _____ Date 4/3/2021 _____

Dean of the College of Graduate Studies: Professor Ali Al-Marzouqi

Signature  _____ Date 4/4/2021 _____

Copy _____ of _____

Abstract

This thesis is concerned with the electrical characterization of the key players of the innate immune cells. Innate immunity is basically the nonspecific immune response that is triggered by any foreign body that attacks the human system. The key players of the innate immune system are mainly dendritic cells and macrophages. Accurately classifying these cell types helps us understand the mechanism of the immune system thereby enabling the development of models to improve new prospects for the therapeutics and diagnostics. The characterization described in this thesis is based on extracting the capacitance for each biological cell using I-V curves. The main aim of this thesis is to overcome the drawbacks of the conventional techniques used to characterize and differentiate between these immune cells. The main challenges with the conventional techniques are the problem of cross-referencing and lack of biological identity for each cell. A matlab mathematical model was developed to extract the capacitance from the I-V curves obtained from the DropSens machine. The results obtained display the concept of immunophenotyping, meaning the ability to accurately define and characterize the different types of cells.

Our results for the capacitance are in concordance with the area for each cell type and the published literature.

Keywords: Innate immunity, adaptive immunity, THP-1, dendritic cells, macrophages, electrical characterization, I-V curves, capacitance, image processing, flowcytometry.

Title and Abstract (in Arabic)

تعريف خلايا المناعة باستخدام الكشف الكهربائي

الملخص

تُعنى هذه الأطروحة بالتوصيف و التعريف الكهربائي للخلايا المناعية الأساسية. يعتمد التعريف على السعة الكهربائية لكل خلية بيولوجية باستخدام منحنيات التيار و الجهد. الهدف الرئيسي من هذه الأطروحة هو التغلب على عيوب التقنيات التقليدية المستخدمة في تمييز الخلايا المناعية. المشكلة الرئيسية في التقنيات التقليدية هي مشكلة ازدواجية المرجعية للخلايا أي عدم وجود هوية بيولوجية لكل خلية. تم تطوير نموذج رياضي باستخدام matlab لاستخراج السعة الكهربائية من منحنيات التيار و الجهد التي تم الحصول عليها من آلة DropSens. تعرض النتائج التي تم الحصول عليها مفهوم التوصيف المناعي ، مما يعني القدرة على تحديد وتوصيف أنواع الخلايا المختلفة بدقة. تكمن أهمية هذا العمل في القدرة على تصنيف الخلايا المناعية وتمكينها من تحسين آفاق جديدة للعلاجات.

تتوافق نتائجنا الخاصة بالسعة الكهربائية مع نتائجنا الخاصة بالمساحة لكل خلية والنتائج الموجودة في المراجع العلمية.

مفاهيم البحث الرئيسية: المناعة الفطرية، المناعة التكيفية، السعة الكهربائية، منحنيات التيار و معالجة الصور، قياس التدفق في الخلايا الجهد.

Acknowledgements

My thanks go to my supervisors Dr. Mahmoud Al-Ahmad and Professor Bassam Ali for helping me throughout this journey, for their guidance and endless support. It has been a very tough journey and I wouldn't have made it this far without you helping me every step of the way.

Special and sincere thank you to my parents Ayman and Eman for their unconditional love and support through this journey and every journey in my life, I am very grateful to be your daughter. I owe you all my successes and my accomplishments. Thank you to my siblings Ruba, Aya, Ragheb and Faris for always being there for me. To my husband Ahmad, thank you for being the man you are, for being my love, my support and for being my home. Thank you to my best friend Hala and my friends and colleagues for their support throughout this journey.

Dedication

To my beloved parents, my dear husband and family

Table of Contents

Title	i
Declaration of Original Work	ii
Copyright	iii
Advisory Committee	iv
Approval of the Master Thesis	v
Abstract	vii
Title and Abstract (in Arabic)	viii
Acknowledgements	ix
Dedication	x
Table of Contents	xi
List of Tables	xiii
List of Figures	xiv
List of Abbreviations	xv
Chapter 1: Introduction	1
1.1 Overview	1
1.2 Statement of the Problem	2
1.3 Relevant Literature for the Biological System	2
1.3.1 Innate Versus Adaptive Immune System	2
1.3.2 Physical Barriers	4
1.3.3 Mechanical Defenses	5
1.3.4 Chemical Defenses	5
1.3.5 Microbiota	5
1.3.6 Antigen Presenting Cells (APCs)	5
1.3.7 Adaptive Immune System	9
1.3.8 The Lymphatic System	12
1.4 Relevant Literature for the Electrical Methods	15
1.4.1 Image Processing in Biological Applications	15
1.4.2 Image Analysis	17
1.4.3 An Overview of Electrical Characterization in Biological Systems	18
1.4.4 Electrical Parameters Extracted from Electrical Signals	19
1.4.5 Different Electrical Techniques Used for Electrical Characterization	19

1.4.6 Different Electrical Methods Used for Electrical Characterization.....	24
1.4.7 Current-Voltage.....	25
1.4.8 Capacitance-Voltage	25
1.4.9 Difference Between C-V and I-V.....	25
1.5 Potential Contributions and Limitations of the Study.....	26
Chapter 2: Methods	28
2.1 Research Design.....	28
2.1.1 Biological Set-Up.....	29
2.1.2 Electrical Measurement Set-Up	30
2.1.3 Capacitance Extraction Using Matlab Code	32
2.1.4 Image Acquisition and Processing	33
2.1.5 Flowcytometry	33
Chapter 3: Results and Discussion.....	34
3.1 Overview	34
3.2 Flow Cytometry	34
3.3 Image Processing	39
3.4 Electrochemical Characterization	41
3.4.1 System Optimization	41
3.4.2 Electrochemical Experiment	79
Chapter 4: Conclusions	84
Chapter 5: Challenges and Future work.....	85
References	86
Appendix.....	96

List of Tables

Table 1: Comparison of surface markers and functions between the main cells, Dendritic cells and Macrophages	8
Table 2: Comparison for the different imaging techniques	17
Table 3: Comparison between I-V and C-V techniques	26
Table 4: Markers used for immune cells and their specifications.....	36
Table 5: Dropsens configuration for Estep and Srate optimization. Srate as the only variable.....	41
Table 6: Dropsens configuration for Estep and Srate optimization. Estep and Srate as the variables.....	51
Table 7: Functionality for each cable.....	66

List of Figures

Figure 1: The interaction of the innate and adaptive immune systems.....	3
Figure 2: Dendritic cell (Left) Macrophage (Right)	8
Figure 3: Interaction between dendritic cell and T cell	12
Figure 4: Lymphatic system with the main lymphatic organs, thymus gland, spleen and lymph nodes spread in the body	15
Figure 5: Overlapping of markers between Macrophages and Dendritic cells.....	27
Figure 6: Representation of the experimental approach of this project.	28
Figure 7: Cable connections for the dropsense technology.	31
Figure 8: Average mean fluorescent intensity of different cell markers.....	36
Figure 9: Mean fluorescent intensity for CD197 for THP-1 cells	37
Figure 10: Mean fluorescent intensity for CD197 for DCs and Macrophages	38
Figure 11: The average area of each cell	40
Figure 12: A: THP-1 B: Dendritic cells C: Macrophages, D, E, F after selection.....	40
Figure 13: I-V curves (A-H) obtained from Dropsens software	42
Figure 14: I-V curves (A-L) obtained from Dropsens software	52
Figure 15: Screen printed electrode	64
Figure 16: Connection between the system and the software	65
Figure 17: I-V curves (A-L) obtained from the different cable connections.	67
Figure 18: I-V curve for the three types of cells using drop sense technology.....	80
Figure 19: Capacitance-time curve for the three types of cells before de-embedding.....	81
Figure 20: Capacitance-time curve for the three types of cells after de-embedding.....	82
Figure 21: Capacitance vs concentration for the three types of cells.....	83

List of Abbreviations

DC	Dendritic Cells
mDC	Mature Dendritic Cells
I	Current
V	Voltage
APC	Antigen Presenting Cell
MHC	Major Histocompatibility Complex
TCR	T-Cell Receptor
PCR	Polymerase Chain Reaction
TD	T-cell Dependent antigen
TI	T-cell Independent antigen
CV	Capacitance-Voltage
IV	Current-Voltage
FBS	Fetal Bovine Serum
PMA	Phorbol 12-Myristate-13-acetate

Chapter 1: Introduction

1.1 Overview

During assessments of diseases, it is essential to identify and categorize diseases based on their systematic method of action and to subsequently re-evaluate the importance of the functional analysis of the host's response represented by the innate immune cells. Classifying the innate immune system players is a key step to comprehensively and quantitatively evaluate the interactions between the innate immune system and the adaptive immune system, thereby enabling the development of models to predict behavior and improve new prospects for the therapeutics and diagnostics. Rapid development in technologies that allow the accurate and rapid classification of cell types in action provided insights into the field of innate immunity and established the action of some therapies [1-3]. This thesis aims to offer a novel approach in characterizing and differentiating between the two most important cell types of the innate immune system, namely the dendritic cells and macrophages. Scientists have been using known and conventional techniques in defining these two cells such as Western blotting, FACs analysis, immunohistochemistry and Polymerase Chain Reaction (PCR). These techniques and approaches have proven their efficiencies and utilities. However, they are time consuming, costly, require highly trained technicians and most importantly have little reliability since the markers used to differentiate between these two cell types overlap significantly. In this thesis, we are presenting a characterization method that uses the current-voltage curves to extract the capacitance for each cell type and to use it as an identification tool.

1.2 Statement of the Problem

The innate immune system is a complex system that is comprised of the physical barriers, mechanical defenses, microbiota and effector cells [4]. In practice, the process of differentiating between the two key players of the innate immune cell, macrophages and dendritic cells, *in vitro* is not straightforward [5]. It has heavily relied on cell-surface markers assumed to be solely present on one cell type and not the other. However, growing evidence suggests that many cell surface markers previously used to differentiate between these two cell types overlap [6]. This further complicates our understanding of the mononuclear innate system and confirms the need for a more reliable system to distinguish between these two key immune cell types. Scientists have been using conventional techniques such as Western blotting [7], flow cytometry (FACs) [8], immunohistochemistry [9] and PCR [10] to differentiate between dendritic cells (DCs) and macrophages. Flow cytometry, the most common technique used in classifying immune cells, segregates cell types based on cell-surface-markers expressed on their outer cell membranes. However, growing evidence suggests that when it is used to compare between DCs and macrophages, the markers overlap and display lack of specificity.

1.3 Relevant Literature for the Biological System

1.3.1 Innate Versus Adaptive Immune System

The human immune system is divided into two main categories, innate and adaptive immune systems [11]. Figure 1 displays the main components of each system; the innate and adaptive immune systems meet at specific immunological locations that will be explained later in the thesis. The different components, characteristics and traits of each category can overlap. Clear definitions for the subcategories of these two main

categories are not mutually exclusive due to the properties these different cells share. Innate immunity can be defined by the nonspecific immune response that is triggered by the chemical properties of the antigen; the foreign body that attacks the immune system. The key players of the innate immune system are the antigen presenting cells (APCs) [4]. Antigen presentation requires special heterogeneous immune cells that capture the antigen, process it and present it to the adaptive immune system at specific immunological locations.

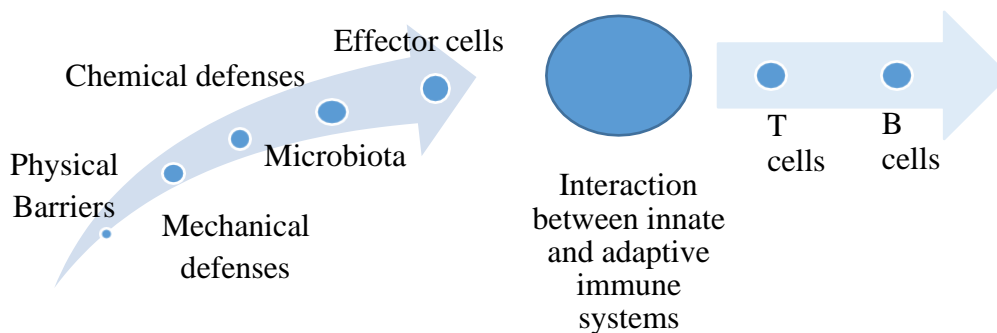


Figure 1: The interaction of the innate and adaptive immune systems.

The innate immune system starts with the physical barriers and ends with the effector cells that are the joining point between the innate and adaptive immune systems. Effector cells of the innate immune system interact with the adaptive immune system at specific immunological locations.

The mechanism adopted by the APCs involves recognizing and processing and the antigen into fragments that are later presented on Major Histocompatibility Complex (MHC) molecules for T cell recognition [12]. Usually the innate immune response arises instantly or within a short time of the antigen's presence in the body. Although the APCs play the most important role at the innate immune system, they are also supported with the physical barriers of the physiological system, mechanical defenses and the microbiota which we will be presenting in the next section [13].

1.3.2 Physical Barriers

Physical barriers are a representation of the basic form of the innate immune system [4]. They can be divided into several important components.

- a. The physical barrier - the skin: The complexity of the skin is evident when studying its composition of three different layers; epidermis, dermis and hypodermis, which strengthen its capability to defend the body from foreign pathogens [14]. Keratin that comprises the top layer of the skin supports the system against bacterial enzyme degradation. The frequent shedding of this layer removes any attached microbes and provides continuous protection against microbial attacks [15]. In theory, compromising the skin barrier by a wounds, skin burns and even insect bites are the ways for pathogens to enter a host and proliferate.
- b. Mucous Membranes: These are the linings that cover the inside of the internal organs and produce secretions to support the innate immune system. Mucous membranes secretions provide protection from debris and small microbes. However, it is the actual mechanical action of the membranes that pushes the pathogens outside the body [16]. The physiological structure of the mucous membranes depends on their location. Lungs have hair-like structures, called cilia, with mucous secretions to trap and flush the out microbes [17]. The digestive tract on the other side contracts in an action called peristalsis to excrete pathogens and microbes in the feces.
- c. Cell junctions that make up different tissues in the body; are classified into three main groups' tight junctions where cells are connected by

joined areas of the plasma membrane, desmosomes where cells are connected by the actin filaments and gap junctions that are connective tunnels between two cells [18, 19].

1.3.3 Mechanical Defenses

Preventing the microbes from taking up space inside the body is carried out using mechanical defenses developed by the body. In addition to the examples mentioned in the mucous membranes in the previous sections, the process of flushing-by urine and tears ensures the purging of some toxins and pathogens [20].

1.3.4 Chemical Defenses

The body produces defensive chemicals to protect itself from pathogens. Chemical defenses are found in different parts of the body. The skin secretes bactericidal chemicals enhancing the skin as the first line of defense. Also, the mucous membrane's secretions contain gastric juices that dissolve most bacteria. Finally the acidity produced by the urine and the vaginal secretions inhibit the growth of bacteria [21].

1.3.5 Microbiota

The microbiota is not only essential for the human development but it plays an important role in defense against pathogens. Their main role in defense is by competing with the invading pathogens on binding sites and nutrients [22, 23].

1.3.6 Antigen Presenting Cells (APCs)

APC's are classically defined as cells that present antigenic peptides on specific proteins called MHC molecules [24]. Their role is to bind the fragments of the antigens and present them to T cells to mount the appropriate immune response [25]. APC's are crucial because the adaptive immune system gets activated only through the

interaction that happens between MHC molecules and T cell receptors (TCR) [26]. The three main types of Professional APCs are dendritic cells, macrophages and B cells. All are of hematopoietic origin. Although both macrophages and dendritic cells are antigen presenting cells, they differ in their function. Dendritic cells are specialized for surveillance and detection of pathogens and, as their name suggests, have elongated structures arising from the cell called dendrites. It is important to note that the dendrites increase the surface area of the dendritic cells compared to the cell's volume [27, 28]. Dendritic cells originate from the bone marrow and are resident in tissues that are in contact with the external environment [16]. They also circulate in the blood while in their immature state before activation and migration. Dendritic cells are categorized into two groups: myeloid dendritic cells (mDCs) with their subsets mDC-1 that is specialized for T-cell activation, and mDC-2 that fights infections caused by wounds [27]. Plasmacytoid dendritic cells share characteristics of plasma and mDCs, and they secrete significant amounts of interferon-alpha [29]. Like dendritic cells, macrophages patrol for pathogens and they take different forms at different body parts. The second and very important role macrophages play is phagocytosis of microbial substances, pathogens and even cancer cells. The final role for macrophages is in regulating the immune system by releasing cytokines for anti-inflammation [28, 30, 31]. This is clearly displayed in the two subsets of macrophages: M1 and its role in phagocytosis and inflammation, and M2 that function for homeostasis, wound healing and for the activation of repair mechanisms [32]. In healthy tissues, macrophages circulate in the blood as monocytes or are already resident in different tissues (the type of macrophage depends on their tissue location). As the body is responding to an infection, monocytes leave the blood circulation towards the site of injury/disease by a process called leukocytes extravasation [28, 33]. The movement of monocytes is regulated by

chemotaxis and once they are activated, they release cytokines to attract more immune cells [34]. Once monocytes encounter the pathogen, they undergo changes and differentiate to become macrophages. Phagocytosis is the process by which macrophages eliminate pathogens, microbes and dead cells. Phagocytosed microbes are contained into a vacuole called phagosome that fuses with another organelle called lysosome to form phagolysosome [35]. The lysosome is a membranous structure containing degradative enzymes that acts on degrading the engulfed microbes. Table 1 is a comparison between the two main APCs dendritic cells and macrophages and it explains the markers used to characterize each cell, as the table summarizes surface markers CD11c, CD11b, MHCII are for both DCs and macrophages. CD68 is also used for both cells however it highly displayed on macrophages. On the other hand DC-sign can only characterize DCs and not macrophages. In addition, Table 1 summarizes the functionality for each cell, DCs are stronger in stimulating T cells, antigen presentation and migration to lymph nodes. However, macrophages are stronger than DCs in phagocytosis.

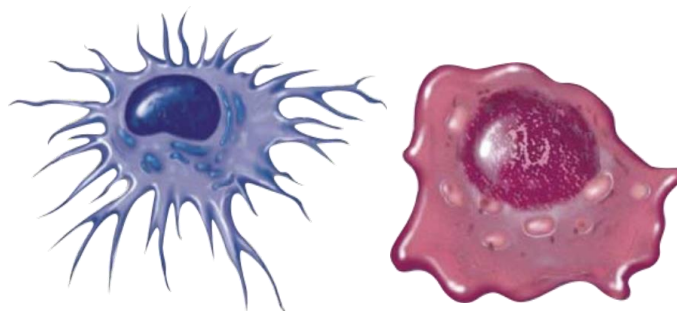


Figure 2: Dendritic cell (Left) Macrophage (Right). Dendritic cells have elongations called dendrites. Macrophages are larger in size and lack the elongations.

Table 1: Comparison of surface markers and functions between the main cells, Dendritic Cells and Macrophages. XX: very strong, X: strong.

Markers		
Surface Markers	Dendritic cells	Macrophages
CD11c	X	X
CD11b	X	X
MHCII	X	X
CD68	X	XX
DC-Sign	X	
Functions		
Functional Characteristics	Dendritic cells	Macrophages
T-Cell stimulation	XX	X
Antigen Presentation	XX	X
Phagocytosis	X	XX
Cytotoxicity	X	X
Migration	XX	X

1.3.7 Adaptive Immune System

Both macrophages and dendritic cells are the link between the innate and adaptive immune system [29, 36]. Following encounter and engulfing of the pathogen, APCs migrate to lymph nodes to activate a specific response by the adaptive immune system. The adaptive immune system consists of lymphocytes that originate from the bone marrow and are found circulating the blood and home into lymphoids tissue [37].

The adaptive immune system is categorized into two main types of cells T and B cells. Both originating from the bone marrow. T cells travel to thymus and mature there, whereas B cells remain and mature in the bone marrow [37, 38]. T cells are distinguishable by the presence of a T cell receptor that recognizes the antigen presented on histocompatibility complexes on antigen presenting cells. Different responses emerge from T cells which contributes to shaping, regulating and controlling the variation of the immune system [39]. Studies have summarized the role of T cells in several main groups, T helper cells (CD 4+ T cell) which express CD4 on their surfaces CD4 does not play role in antigen recognition but plays role in signal transduction following antigen recognition by T cells. Once T helper cells are activated they proliferate, secrete cytokines for the direction of other T cells subtypes [40]. Subtypes of CD4+ T helper cells such as Th1, Th2, Th 17 produce various cytokines that supports responses against different invaders including intracellular bacteria, viruses and cancer [41]. They aid in the differentiation and induction of antibodies production by B cells. They also play an important role in the defense against helminths and pathogens at the mucosal barrier. CD4+ T cells only help activate and propagate the response of the adaptive immune system, however the second main category of T cell, called cytotoxic T cells or CD8+, directly kills virus infected cells and tumors [42]. CD8+ T kill cells after the recognition of peptides presented on MHC

I on target cells surfaces [43]. Killing is then triggered by the release of cytotoxic proteins. Granzymes and perforins work together as the perforin penetrates and polymerizes on the surface of target cells to form a pore like structure, allowing the granzymes to enter and induce programmed cell death [44]. The other way CD8+ T cells induces killing is through the Fas ligand expressed on some target cells. After the binding of CD8 + T cells and the infected cell through the Fas/Fas ligand, caspase gets activated and leads to apoptosis in the target cell [45]. All the pathways explained previously for CD8+ T cells requires direct cell contact; however, CD8+ T cells can induce killing by the secretion of IFN- γ and tumor necrosis factor- α [44]. These cytokines binds to their receptors on the target cell and activate the caspase cascade leading to cell death. The above three main ways summarize the pathways taken for CD8+ T cells to kill cells. These ways are crucial for the study of tumor regression and they are considered in many therapeutic treatments for enhancing cancer treatment. Our immune system orchestrates a way to respond faster to foreign pathogens through responses by memory T cells. Memory T cells recall previous encounters with antigens and enhance the response rate by minimizing the time required for antigen recognition and therefore faster induction of inflammation [46]. Upon activation, T cells differentiate into memory and effector T cells. There are different types of memory T cells : 1. Central memory T cells: with high expression of CCR7 and CD44 which is used to distinguish between naïve and memory T cells, and usually found in lymph node and peripheral circulation, 2. Effector memory T cells: lack CCR7 but express CD45RO, and are found in peripheral circulation and tissues 3. Tissue Resident memory T cells: they do not circulate and are resident in specific tissues. Deep understating of the fundamental mechanisms that regulate memory T cell function and

development help scientists in designing vaccines and therapeutic options for immune-mediated diseases [47].

Humoral immunity is an important component of the adaptive immune system and is governed by B lymphocytes. Humoral immunity is defined by the secretion of antibodies by B cells. Unlike T cells, B cells express B cell receptors on their surfaces that allow direct antigen recognition by B cells, consequently triggering the immune response. This was previously mentioned in the sections covering APC, but it is very important to remark that B cells are antigen presenting cells as well [48].

For every antigen there is an antibody produced by a certain B cell. Antigens recognized by B cells can be classified into two groups. Antigens that need the help of T cells to activate B cells and these are mainly peptides and are known as T cell-dependent antigens (TD) [38]. The other types of antigens, such as lipids, nucleic acids, polysaccharides, does not need the help of T cells to activate B cells, known as T cell independent antigen (TI).

TD antigens, bind to the B cell through B cell receptor, enter the cell by endocytosis, gets degraded by certain enzymes and presented on MHC molecules to be recognized T helper cells.

Antigen recognition by T cells induces T cell activation and cytokines secretions such as IL-4, IL-21 which serve to co-stimulate B cells for proliferation, immunoglobulin class switching and somatic hypermutation [38]. Upon B cell activation, they undergo a process to initially produce short lived antibodies for immediate response and protection, and next produce long-lived plasma cells for the memory B cell reservoir.

The difference between TD and TI antigens is mainly the type of antigen whether it is a peptide or something else as well is the response time, responses to TI are faster because they do not require T cells help. However, antibodies produced to combat these antigens have lower affinity and less functionality than the ones produced in response to TD antigens [49].

In the following sections, the role of the lymphatic system in transporting white blood cells to and from the lymph nodes and in transporting antigen presenting cells from the site of interaction with antigens to the lymph nodes for the required immune reaction will be explored.

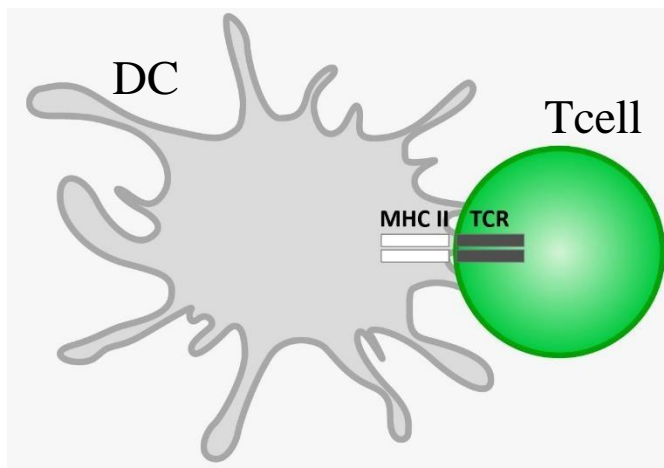


Figure 3: Interaction between dendritic cell and T cell. This is to activate the adaptive immune system. The interaction occurs between the MHCII in DCs and TCR on T cells.

1.3.8 The Lymphatic System

The lymphatic system is made up of connected network of tissues and circulating cells. The systems mainly consist of lymphatic vessels that are connected to the lymph nodes where the activation of T cells takes place [50].

Our body contains hundreds of lymph nodes, surrounding the lungs, the heart and these nodes are embedded around the body in many tissues.

The main lymphatic organs:

- a. Thymus: is the primary lymphoid organ and is made up of lobules that are divided by the epithelium. It is surrounded by the capsule providing it with blood supply [51]. The thymus is divided into several regions that are the corticomedullary junction, the cortex, the subcapsular zone and finally the medulla. In the postnatal thymus circulating progenitors migrate to the corticomedullary junction through the enriched vasculature that surrounds it [52]. Interactions between the progenitor cells and the vasculature are regulated by adhesive proteins; PSGL1 expressed on progenitor cells and P-selectin expressed on the epithelium [53]. Immature T cells do not express either CD4 nor CD8 antigen and these are the double negative cells. There the thymocytes go through negative selection, this process is divided into 4 main stages DN1, DN2, DN3, DN4. From there they migrate to the cortex regulated by chemokines, CXCR4 and CCR7, further migration is mediated by CCR9 signals. During migration thymocytes develop pre-TCR receptor, which is then followed by proliferation. Signals then initiate further development into double positive for the thymocytes to express both CD4 and CD8 co-receptors and signals to complete the assembly of the TCR complex [54]. These generated thymocytes are motile and interact with the generated TCR with peptide MHC complex, this starts the negative and positive selection to get mature T cells with either CD8 or CD4 receptors [55]. The single positive selected cells are attracted to the medulla, and they spend around 12 days there before being transported out of the thymus. Negative selection is the process by which self-tolerance takes place and the single positive thymocytes are further selected by dendritic cells that present self-antigens. This selection leads to the deletion of

tissue specific antigen T cells, and the generation of regulatory T cells [56]. Finally these mature T cells travel back to the corticomedullary junction and are then released into the periphery equipped with the necessary tools to mount the immune responses.

- b. The spleen: the largest organ of the lymphatic system that is responsible for keeping the balance of the fluids in the body. It is a soft purple organ that is divided into the red and the white pulps separated by the perifollicular zone. The main function of the red pulp is to filter the blood of antigens, microorganisms and defective or worn-out RBCs [57]. On the other hand the white pulp which is the smaller part of the spleen consists of lymphoid tissue with designated areas for B and T cells. APCs enter the spleen via blood to initiate immunological interactions through presenting captured antigens to T lymphocytes [58]. Once the inflammation started T lymphocytes change their number, dynamics and location and go to the white pulp to initiate the adaptive immune response [59]. The periarteriolar lymphoid sheath (PALS) in the white pulp contains T cells Trafficking of T cells is regulated through binding of CCR7 and its ligands CCL19 and CCL21. On the other hand the B cells are concentrated in follicles that also contain mixture of cells that are important for their survival and activation [58]. The marginal zone or the interface between the red pulp and the white pulp contains antigen presenting cells such as dendritic cells that capture the antigens and present them to T cells in the white pulp.
- c. Lymph nodes: are filters for the lymph that circulates the biological system. they are the major site for the interaction between APCs and lymphocytes that

reside in the lymph nodes. The act of filtration played by the lymph nodes is supported by their distribution all over the body and the connection between the lymph nodes with the lymphatic vessels [60]. The structure of the lymph node is relatively simple compared to that of the spleen and thymus. Lymph nodes are made up of the outer cortex and the inner medulla that are surrounded in a fibrous capsule.

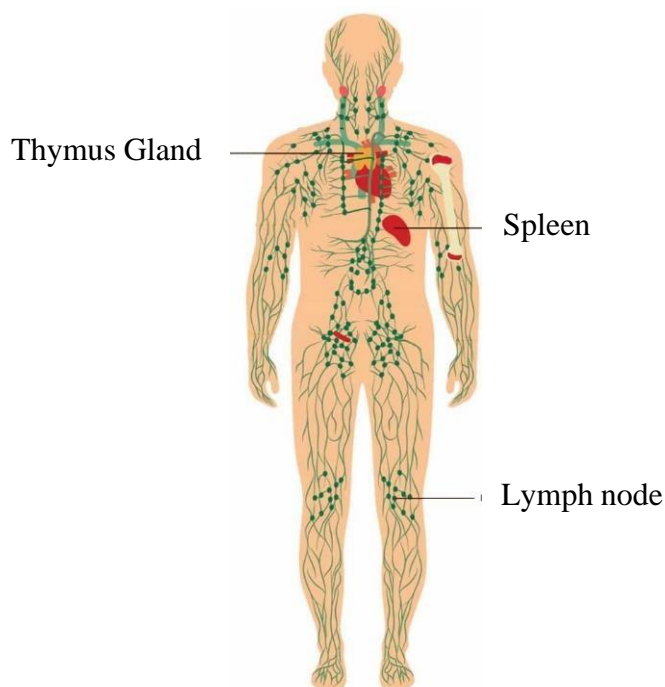


Figure 4: Lymphatic system with the main lymphatic organs, thymus gland, spleen and lymph nodes spread in the body.

1.4 Relevant Literature for the Electrical Methods

1.4.1 Image Processing in Biological Applications

Image processing has become a vital tool in biological applications for quantifying the phenotypic differences between various cell populations. Screening biological samples has given scientists a deep insight into the biological systems and their diverse processes such as gene expression, protein modification or interaction, signal transduction and irregular RNA interference and mutations. Imaging starts with

the principle of extracting the physical parameters of the sample such as the area, density and morphological properties [61]. Consequently the data obtained from these images allow the mathematical modeling of biological kinetics and the studying of biochemical signaling networks [62]. The main imaging techniques used for cellular studies are fluorescent microscopy, multiphoton microscopy, atomic and electron microscopy [61]. The fluorescent microscope is mainly used for the visualization of the sub-cellular structures and their compartmentalization [63]. It works by capturing the emissions of the excited biological samples using fluorophores. Multiphoton microscopy follows the same principle but is mainly used for living samples and can image at a deeper scale in comparison to the fluorescent microscopy [64]. On the other hand atomic force microscopy uses Hooke's law (principle in physics that explains that the force used to compress or extend a spring is proportional to the same distance [65]) to acquire the image from the sample [66]. The image is a representation of the forces between the sample and the tip of the probe that scans its surface, the forces measured vary between chemical, magnetic, electrostatic and mechanical contact forces. Lastly the electron microscopy uses an electron beam to image the object and magnifies it using electromagnetic fields [67]. Table 2 contains a comparison with the uses, advantages and limitations of the previously explained techniques.

Table 2: Comparison for the different imaging techniques.

Name	Usage	Advantage	Limitation
Fluorescent Multiphoton	Visualize sub-cellular structures	High and specific identification	Photobleaching
Atomic Force Microscope (AFM)	Map cell surface	No special treatment is needed for the sample	Mechanical forces may damage the sample
Electron Microscope (EM)	Screening for protein structures	High resolution	Requires long time to prepare sample / does not work on living samples

1.4.2 Image Analysis

Quantitative results are obtained by the different available software that are coupled with the imaging acquisition techniques [68]. The analysis of the results depends on the advances of the algorithms and processing of the software used. In general, the applications of these software include analyzing the stained tissues, gels and getting the physical and morphological data of the sample [69]. After capturing the sample image with the microscope, the software initiates the segmentation process, where the object is located and the boundaries are drawn along the object [70]. The main goal of this process is to simplify the image for quantification. Phenotypes quantification is the critical step that follows, the software manages to quantify the image and get data like, sample size, distances between the objects, spatial distributions and in case of live imaging, tracking the sample movement [71]. Phenotypes and data collected from experiments conducted by scientists were then collected and categorized in shared databases [69]. This platform was an avenue for users to browse and inquire about their own experiments and for other scientists to

develop the more efficient analysis software. Additional experiments like western blot, FACS, PCR along with the imaging data give scientists a better picture on the biological process.

Existing methods throughout the years have helped biologists get the data regarding the biological experiment conducted. However, these methods have their limitations and this is why the science is shifting towards using and developing image acquisition and analysis techniques.

1.4.3 An Overview of Electrical Characterization in Biological Systems

Recent years have witnessed a substantial growth in new techniques and technologies that allowed the detailed study of cells as well as their characteristics and functions. Scientists mainly focused on studying cells' electrical and chemical properties due to the importance and roles of these properties in biological cell activity [72]. These electrical properties are very important because they give insight into the changing biochemical and biophysical properties of the cell that control their interactions with other cells and their interactions with the environment [73]. Over the years, many studies have been carried out to extract biological data from electrical measurements. Useful examples are the resting and membrane potential from the nervous system and ECG of the heart. Electrical characterization expanded to study single cells, viruses, DNA and even blood samples [74]. The electrical characterization starts with the process of passing a current through a sample, whether it is a single cell or a tissue and measure the voltage, the parameters extracted depend on the analysis used.

1.4.4 Electrical Parameters Extracted from Electrical Signals

The information and data of electrical current is presented as electrical signals. Electrical signals can either be interpretation, transformation, perceived functions or any observable change in quantity [75]. An electrical signal can either be a voltage or a current that delivers the information required. Signals can visually be represented as waveforms; when the voltage or current output is plotted over time. The plot represented can be demonstrated in various ways, in other words there are many types of electrical waveforms that can be categorized into two distinctive groups [76]. The unidirectional waveform, electrical waves flow in one direction only and the bi-directional waveform where electrical waves alternate from the positive to the negative direction. There are three main properties that can be conducted from the waveforms. The first important property extracted from a signal is the frequency, which is the number of cycles per second. Peak voltage (the amplitude) is the highest voltage reached by the signal, and it is measured in volts. The time taken for the signal to complete one cycle is the time period and it is measured in seconds. From the time another property is calculated which is the frequency; the number of cycles per second, it is measured in hertz [77].

1.4.5 Different Electrical Techniques Used for Electrical Characterization

Fast emerging technologies have been developed and advanced by the scientists in the past few decades to study the biophysical properties of cells and to make extensive influences to biology and the clinical research field. These include:

A. Radiography

Radiography is wide-ranging term that covers imaging techniques that requires the use of either ionizing radiation or non-ionizing radiation for the purpose of internal body parts characterization. The process of radiography begins with a generator producing certain type of radiation that is absorbed by the object of study [78]. The outcome is then captured by a detector. There are two types of detectors computed detection and digital detection. For the first type cassettes are used to collect the signal and transform it into digits than can be then displayed on a screen. The second type does not use cassettes. However, the radiation hits a set of hardware that directly digitizes the signals for the user to read as images. The image presented depends on the radiological density of the object under study. Objects with higher density absorb the radiation more and their output appears whiter than less dense objects [79].

B. Ultrasound

Unlike radiography, ultrasound imaging relies on the usage of high-frequency sound waves to characterize internal objects in the body rather than ionizing radiation [80]. The advantage of this technique is mainly in acquiring real-time imaging that shows the movement and fluids flowing inside the body. The frequency waves are transduced through a gel that is applied on the object of study, the source of the waves are a probe that is directly placed on the object. The output of this process depends on the amplitude (strength) of the signal produced and the time needed for the wave to reach the organ to produce the image [78, 81].

C. Magnetic Resonance Imaging

Magnetic Resonance Imaging is a non-invasive imaging technique that uses strong magnetic field to produce high quality images of internal body parts [78, 82]. This technology is based on exciting protons in the tissue fluids and then detecting the change in the direction of their rotational axis. The proton excitation happens due to the force of a strong magnetic field. The high force pulls the protons out of their state of rest, once the force is turned off the sensors detect the energy released from the protons. The output of the image depends on the chemical and physical properties of the object [82].

D. Thermal Imaging

An innovative way to characterize objects based on their emitted heat (heat signature of objects) [83]. The warmer the object, the higher the radiation is emitted. The technology works with heat sensors that detects temperature differences and to translate heat signals into electronic images that can be read by the user. The outcome is presented as a thermal image, that shows mainly black and white colors, where black presents cold objects and the white areas represents hot objects. The depth of grey shows the variation between the two states [84].

E. Radiofrequency Radiation

Radiofrequency indicates the presence of electric and magnetic waves, both types of energy moving together. This is referred to as the electromagnetic spectrum, it can be expressed either in V/m (volts per meter) to express the strength of an electric field or A/m (Amperes per meter) to express the strength of the magnetic field. The radiofrequency waves are characterized by the wavelength – the distance needed to complete one cycle- and the frequency. Radiofrequency radiation with limited and FDA approved frequencies can be used to create images to characterize the internal

body parts. An amplifier is used to produce the energy and a software control the absorption rate in patients to avoid any side effects. The image depends on the objects capability to dissolve excess heat, this is expressed in specific absorption rate (SAR) [85].

F. Electrical Impedance Tomography (EIT)

This technique has the advantages of being portable, low cost and getting the output images faster. EIT works by assessing the electrical properties of the internal body organs without invasive measurements. The science behind this technique is to get the data based on permittivity and conductivity distribution inside the object after applying current into the object and measuring the voltage. The voltage output is used to solve inverse problems that aid in building the big picture needed for object characterization [86].

G. Impedance Flow cytometry

Impedance Flow cytometry is a powerful analytical tool in cell biology for analysis and identification of cells. Two large electrodes are connected with a long chamber, the biological samples then flow through the chamber that has a current flow, and this will displace the conductive fluid and alters the resistance after decreasing the current, hence classifying the samples based on their size [87].

For tissue engineering various types of electric techniques are used for cell manipulation and characterization whether it is electrical [88] optical [89, 90], ultrasound [91] magnetic [92] and are undergoing constant advancements.

Examples of these techniques:

a. Scanning Electron Microscopy

This technique uses an electron beam to create an image. The image created gives information about the topography and composition of the object under study. The device works by producing electrons from a column, then these electrons get accelerated to pass through a combination of lenses to produce a focused beam that hits the sample surface. The image is produced by the secondary electrons that are the outcome of the beam hitting the sample surface. The signal of the secondary electrons is then collected by one or several detectors to form the desired images [93].

b. Transmission Electron Microscopy

A very powerful tool used in the area of material science. It is used widely to study the development and growth of layers, their composition and defects. It contains a high-resolution option that allows the user to analyze the quality, shape and size of the sample under study. Transmission electron microscopy focuses beam of electrons through a condenser lens and then the beam hit the sample of study. The sample then allows part of the beam to be transmitted, depending on the thickness and transparency of the sample. The transmitted portion of the beam gets focused into an image on a screen or a coupled device camera for the user to study and observe [94].

c. Scanning Tunneling Microscopy

This device works by applying an electrical voltage to the sample of study through a small tip. The image provides detailed information about the samples atomic organization. Scanning tunneling microscopy works based on three main principles [95]. The quantum mechanical effect that allows the user to see the surface.

Piezoelectric effect which is the generation of an electric charge due to an applied mechanical stress [96]. This effect allows the user to precisely control the tip. Finally the feedback loop that monitors the current that passes through the tip and coordinates with the tips' movement.

d. Dynamic Light Scattering

The concept of dynamic light scattering is to collect and detect the fluctuations scattered by the light from hitting the sample of study. The advantage of this technique is that it gives full picture on the particle size distribution and movement [97].

e. Absorption Spectroscopy

Absorption spectroscopy is a technique that characterizes materials based on their absorption of radiation. The most common way to do so is by focusing a beam of light on the sample of study and then detecting the radiation that passes through it and using this information to calculate absorption [98].

1.4.6 Different Electrical Methods Used for Electrical Characterization

Both Current-Voltage (I-V); current is the rate of the charge flow in a circuit at a certain point, voltage is the difference potential of charge between two specific points. (Current is the effect and voltage is the cause) [99].

Capacitance-Voltage (C-V); capacitance is the ability of a material to store an electric charge, that is after the voltage is applied [100]. These measurements are important in characterizing different materials in different areas.

Several techniques and approaches have been introduced in the past years under the concept of applying short voltage pulses and extracting the current output to study the desired object or material. Full I-V or C-V curves obtained gives scientists deep insight and information regarding the material under study and analysis.

1.4.7 Current-Voltage

The relationship between the direct current (DC) through an electronic device and the DC voltage across its terminals is called a current–voltage characteristic of the device [101]. The IV curve of an electrical component can be measured with an instrument called a curve tracer. The transconductance and early voltage of a transistor are examples of parameters traditionally measured from the device's I–V curve. While I–V curves are applicable to any electrical system, they find wide use in the field of biological electricity [101], particularly in the sub-field of electrophysiology. In this case, the voltage refers to the voltage across a biological membrane, a membrane potential, and the current is the flow of charged ions through channels in this membrane. The current is determined by the conductance of these channels [102].

1.4.8 Capacitance-Voltage

Many researchers practice CV testing to regulate semiconductor parameters. Moreover, CV measurements are also extensively used to characterize other types of devices and technologies such as Bipolar junction transistors (BJTs) (current amplifiers used widely in electronic equipment such as mobile phones and televisions [103]), Junction field effect transistor (JFETs) (mainly used to control the electric behaviour of devices) compound devices and other materials [100]. These measurements are useful for lithography, etching, cleaning, dielectric and polysilicon depositions, and metallization as well. After device fabrication, CV measurements are used to characterize threshold voltages and other parameters during reliability and basic device testing and to model device performance.

1.4.9 Difference Between C-V and I-V

Both CV and IV techniques are used to characterise the materials and devices, however, they have many variations as follows:

Table 3: Comparison between I-V and C-V techniques.

Current-Voltage	Capacitance-Voltage
It is the current versus voltage characteristic of a given sample.	It is the capacitance behaviour of a given sample over the voltage range.
<ul style="list-style-type: none"> • Linear and non-linear • Negative and positive resistance • Active and passive • Hysteresis and single valued 	No types as such
<p>Pros:</p> <p>I–V curves are applicable to any electrical system such as circuits, biological samples, etc.</p>	<p>Pros:</p> <ul style="list-style-type: none"> • Reliability engineers use CV measurements to monitor process parameters and to analyse failure mechanisms. • Yield enhancement engineers use it to enhance the processes and device performances.
<p>Problems:</p> <p>Temperature dependent</p>	<p>Problems:</p> <p>Capacitance-voltage signature values can vary from one experimental setup to another [74].</p>
<p>Parameters:</p> <ul style="list-style-type: none"> • Device Parameters • Performance Parameters 	<p>Parameters:</p> <ul style="list-style-type: none"> • Dielectric Constant • Capacitance density

1.5 Potential Contributions and Limitations of the Study

It is very important to study the role of each cell type whether they propagate a response to inflammation or injury or a response against disease process such as cancer. This is a key area as both of these cells control the leukocyte population and

their responses, hence controlling which cell to activate based on the pathological agents.

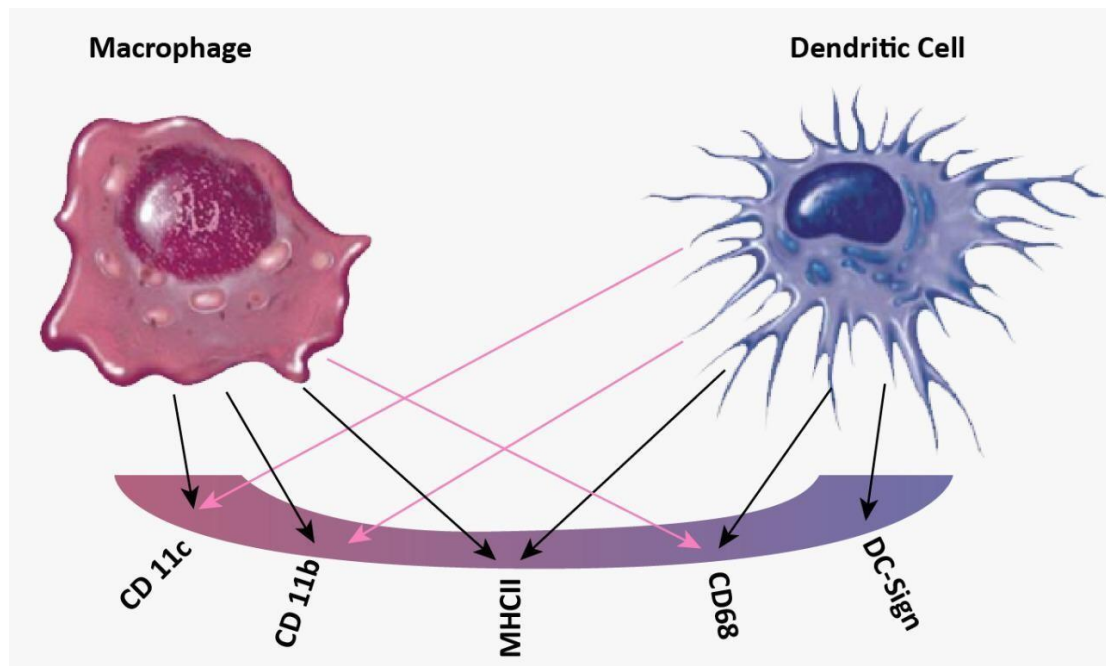


Figure 5: Overlapping of markers between Macrophages and Dendritic cells. Dendritic cells and Macrophages share the same surface markers CD11c, CD11b, MHCII, CD68.

In this thesis a new easy and efficient approach to fully differentiate between dendritic cells and macrophages is suggested. Distinguishing between these cell types based on their electrical characteristics and energy will ensure a better classification of the innate immune cells during their steady state and inflammatory conditions in different tissues and in playing different roles.

This will eliminate the constant confusion faced by scientists due to lack of specificity of cell markers as shown in Figure 5, as these cells share several markers in common and it is not always easy to differentiate between them.

Chapter 2: Methods

2.1 Research Design

The approach presented in this thesis depends on using image processing and electrochemical characterization to distinguish between the different innate immune cells. The process begins with the biological setup of differentiating the THP-1 cells into macrophages and dendritic cells.

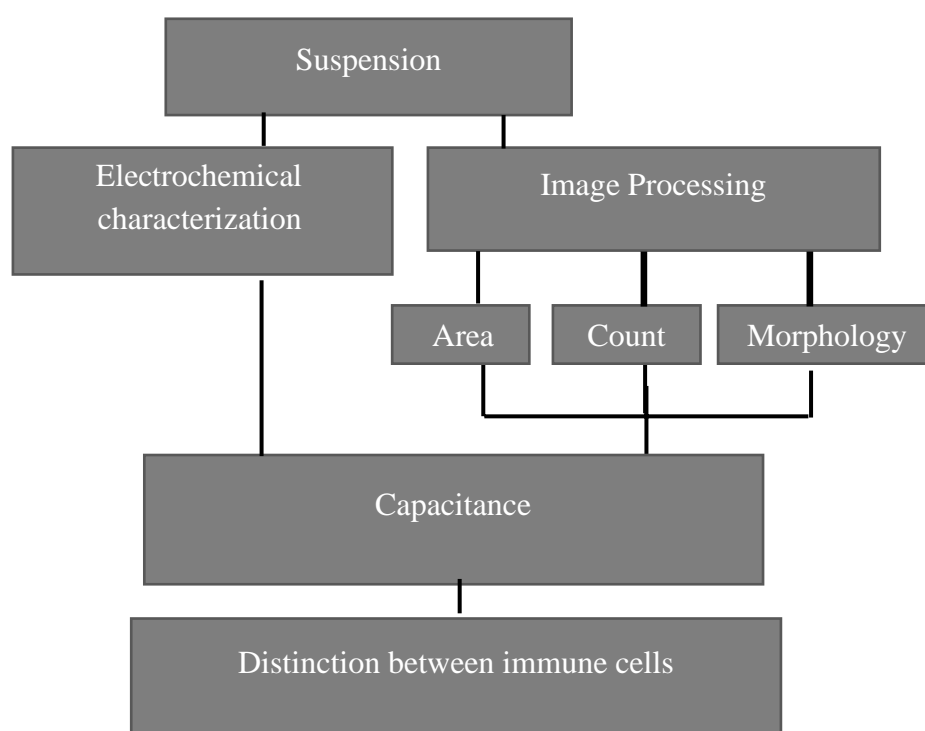


Figure 6: Representation of the experimental approach of this project. The experiment starts with the biological differentiation of cells and preparing them in suspensions. Followed by electrochemical characterization of the samples to extract the capacitance. The data is supported by the image processing experiments that gives the area, count and morphology for each cell. All experiments together give the distinction between the two types of immune cells.

2.1.1 Biological Set-Up

Human monocytic THP-1 cell line were obtained from ATCC (Manassas, VA, USA) [104] and were cultured in RPMI-1640 media supplemented with 10% fetal bovine serum (FBS), 1% sodium pyruvate, 0.01% of mercaptoethanol and 1% penicillin/streptomycin at 37°C, 5% CO₂ and 95% humidity. After that THP-1 cells were differentiated into DCs and macrophages using activators According to the following protocols:

- A. Differentiation of THP-1 to Dendritic cells: THP-1 cells were harvested by centrifugation, then resuspended in culture medium supplemented with 10% FBS at a concentration of 2×10^5 cells/ml and transferred to a final volume of 20 ml into 200 ml tissue culture flasks. To induce differentiation, rhIL-4 (200 ng=3000 IU/ml) and rhGM-CSF (100 ng/ml =1500 IU/ml), rhTNF- α (20 ng/ml = 2000 IU/ml) and 200 ng/ml ionomycin were added to the Fetal Bovine Serum (FBS) free media [105].
- B. Differentiation of THP-1 to Macrophages: Differentiating and activation protocols of THP-1-derived macrophages were adapted and modified from *Genin et al.* [106]. THP-1 cells were terminally differentiated into uncommitted macrophages (MPMA) with 300 nM Phorbol 12-Myristate 13-Acetate (PMA; Sigma-Aldrich, Germany) in RPMI 1640 media without FBS supplement. After 6 h, differentiating media was removed. Cells were washed with phosphate-buffered saline (PBS) and transferred to well plates in the incubator for 24 h in RPMI 1640 without FBS supplement and PMA. Afterwards, cell activation was induced by adding treating cells for 48 h into pro-inflammatory macrophages (M_{LPS/IFN γ}) with 10 pg/mL lipopolysaccharide (LPS; Sigma, USA) and 20 ng/mL IFN γ (Biolegend, San Diego, CA, USA), or

into anti-inflammatory macrophages (MIL-4/IL-13) with 20 ng/mL interleukin 4 (IL-4; Biolegend, USA) and 20 ng/mL interleukin 13 (IL-13; Biolegend, USA).

2.1.2 Electrical Measurement Set-Up

A.1 System Optimization for E-step and Srate:

All measurements were carried out at room temperature. Electrochemical measurements were performed with a μ STAT 400 potentiostat (is a portable hardware device that can control a three electrode cell used for electroanalytical experiments) (Metrohm DropSens, Spain) [107], controlled by Dropview software. The DRP-110 chip was used and only 100 μ l of the FBS media was used for the optimization at 37°C. Technique: Cyclic Voltammetry (The current measured after applying a certain voltage in an electrochemical cell [108]) and the constants in the system are:

Ebegin: the initial voltage applied, Evxt1: the range of the voltage (positive value), Evxt2: the range of the voltage (negative value), Estep: difference in voltage between two points, nscans: number of times the voltage is applied, Current Range: the range of current values

The variables are: the Srate and the voltage frequency

A.2 System Optimization for the coaxial cable:

All measurements were carried out at room temperature. Electrochemical measurements were performed with a μ STAT 400 potentiostat (Metrohm DropSens, Spain) [107], controlled by Dropview software. The coaxial cable was used to find the correct connection. Drinking water was used.

Technique: Cyclic Voltammetry and the constants in the system are:

Ebegin=0 Evxt1=0.9 Evxt2=-0.9 Estep=0.002 Srate=0.04

B. Electrical Experiment:

Instead of electrodes, a coaxial cable was used to measure the samples. As presented in Figure 7, the cables are connected as explained below:

- The Red cable (working electrode 1) with the red cable
- The Blue cable (reference) and the black cable (counter electrode) with the black cable

The cables were taped on the table for a steady measurement and the coaxial cable was taped on the wall opposite to the system as presented in Figure 6.

Cyclic voltammetry measurement was performed between 0.9 V to -0.9 V, E_{step} of 0.002 and S_{rate} of 0.04. Cells were prepared using RPMI full media supplemented with 10% FBS. After the activation process, cells were centrifuged and prepared at different dilutions from 10 to 10^6 per 500 μl . Data was extracted directly from drop view using the cyclic voltammetry technique. The results exported were current vs voltage.

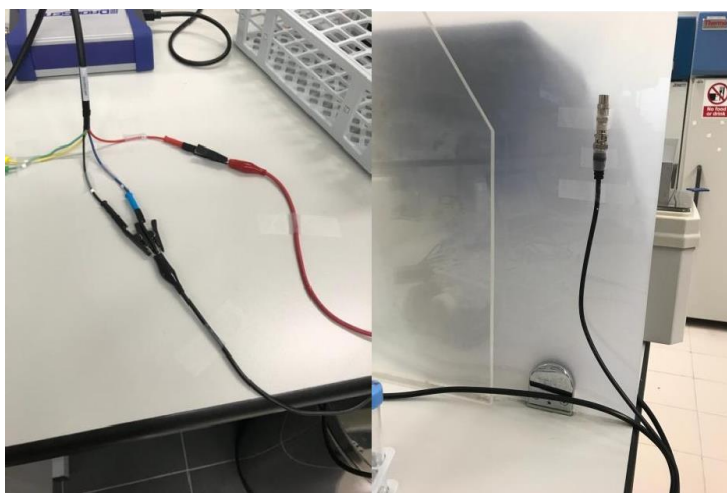


Figure 7: Cable connections for the dropsense technology. Five cables are connected from the machine to two cables in the software. Coaxial cable is held at the wall (500 μl of the sample is added inside the cable).

2.1.3 Capacitance Extraction Using Matlab Code

The approach presented in this thesis depends on using image processing and electrical characterization to distinguish between the different innate immune cells. After collecting the data using μ STAT 400 potentiostat, calculation was done after solving the non-homogenous linear equation that was obtained originally from ohms' law:

$$Q = cV(1)$$

Where $Q = \text{instantaneous charge}$

$c = \text{capacitance in farads}$

$v = \text{voltage}$

After differentiation of above law the following equation was obtained:

$$i(t) = \frac{dV(t)}{dt} = c \frac{dV(t)}{dt} + v \frac{dc(t)}{dt} (2)$$

From the data we extracted from drop-view

The known values are:

- $i(t) = \text{the current} - \text{the output from the y axis}$
- $v(t) = \text{the voltage} - \text{the input from the x axis}$
- $dv(t)/dt = \text{the rate of voltage change}$

Solving the non-homogenous linear equation, the following equation was obtained:

$$y = e^{-\int f(x)dx} \int e^{\int f(x)dx} r(x)dx + c (3)$$

Where

$y = c(t) \text{ Capacitance}$

$f(x) = dv(t)/dt \text{ rate of voltage}$

$$r(x) = i(t) / v(t) \text{ Current / voltage}$$

Using a matlab code with the final equation (3) values of capacitance for our biological cells were calculated.

2.1.4 Image Acquisition and Processing

Images were captured using Olympus Fluorescent Microscope and quantified using ImageJ Software (National Institute of health, USA) [109]. The software was used to obtain the ratio of THP-1 to dendritic cells, THP-1 to Macrophages.

2.1.5 Flowcytometry

Cultured cells were washed, suspended at 3×10^4 in 200 μ l cold FACS solution (DPBS; Gibco-Invitrogen) and incubated with FITC- or PE- conjugated monoclonal antibodies (that are explained elaborately in the results section) or appropriate isotypic controls for 30 mins. Cells were then washed twice and resuspended in 300 μ l of cold FACS solution. Stained cells were analyzed with (BD Accuri C6 plus). Cell debris were excluded from the analysis by setting a gate on forward and side scatter that included only viable cells. Results were processed using FlowJo Software.

Chapter 3: Results and Discussion

3.1 Overview

The experiment is divided into four main parts, the biological setup, Flow cytometry, image acquisition and analysis and finally the electrical measurements. The main goal of this thesis is to tackle the problem of cross referencing faced by the conventional techniques in important immune cell types. The experiments started with the differentiation process followed by the flow cytometry experiments, to present the data of the fluorescent markers and the draw-back of not being able to clearly differentiate between the three types of immune cells, THP-1, Macrophages and Dendritic cells [110]. The immune system consists of several cell types that interact with each other, secrete cytokines and modulate the immune response. Scientists use cell- surface specific biomarkers that are targeted to define these different cells. Immunophenotyping is the term used for identifying and quantifying immune cells, this is usually done by flow cytometry, Western blotting and PCR. The most common method used is flow cytometry, however as we previously explained flow cytometry's huge drawback is the lack of specificity of these biomarkers for each cell type and therefore the currently used markers to differentiate between cells does not provide accurate results [64]. Moreover, flow cytometry analyze the data by giving statistical significance to values but fails to interpret it into biological significance.

3.2 Flow Cytometry

To demonstrate the applicability of the proposed approach, THP-1 cells were cultured in RPMI-1640 media, then differentiated them into either DCs or macrophages according to established and published protocols. The differentiation was carried out based on Berges et al. protocol, using the activators specified therein

[105]. To validate the differentiation of monocytes, cell surface markers fluorescence was evaluated using flow cytometry, based on their surface self-antigens. Table 4 summarizes the markers used and the specificity of each marker. As presented in Table 4, the markers used to specify each type of immune cell are not specific for one type of cells which leads to the huge drawback of cross-referencing. Figure 8 illustrates the results of our flow cytometry experiments. To begin with, CD 83 represents an important marker that is specific for dendritic cells. However, the results show that there is no significant difference between DCs and THP-1 or macrophages, and this is supported by a study carried out by D Ferenbach and J. Hughes [6]. On the other hand, CD197 expression only shows differences between macrophages against THP-1 and DCs against THP-1. This can be attributed to CD197 being a marker for antigen presenting cells, so it cannot be used to classify the different types of antigen presenting cells. As for HLA-DR marker expression, it is presented on all the three types of immune cells [111, 106], hence there was no difference with the flow cytometry results. CD1c is a marker for dendritic cells, as shown in Table 4, this is supported by the results as they can classify DCs from macrophages but not from THP-1 cells. Whereas, CD 11c is a marker for all three cells [112] and as per the results there are no differences between these cells, using this marker. Figure 9 and 10 explains the gating process of the flowcytometry experiments, showing the process of cell selection. Debris were excluded and only stained cells were selected. Figure 9 presents the gating for THP-1 cells and the data then is displayed as histogram, 10-A and 10-B shows the gating for dendritic cells and macrophages. The peak on the right are THP-1 cells while the peaks on the left are for macrophages and dendritic cells.

Table 4: Markers used for immune cells and their specifications.

Marker	Specificity	Reference
CD83	Marker for mature DCs and very weak for THP-1	[42]
CD-197	Receptor for T-cells, B cells, Natural killer cells and DCs	[36]
HLA-DR	Recognizes T cells, Dendritic cells, Macrophages and B cells	[111]
CD-1c	Subset of B cells and Dendritic cells	[29]
CD-11c	For monocytes, macrophages, dendritic cells, Natural killer cells, T and B cells	[31]

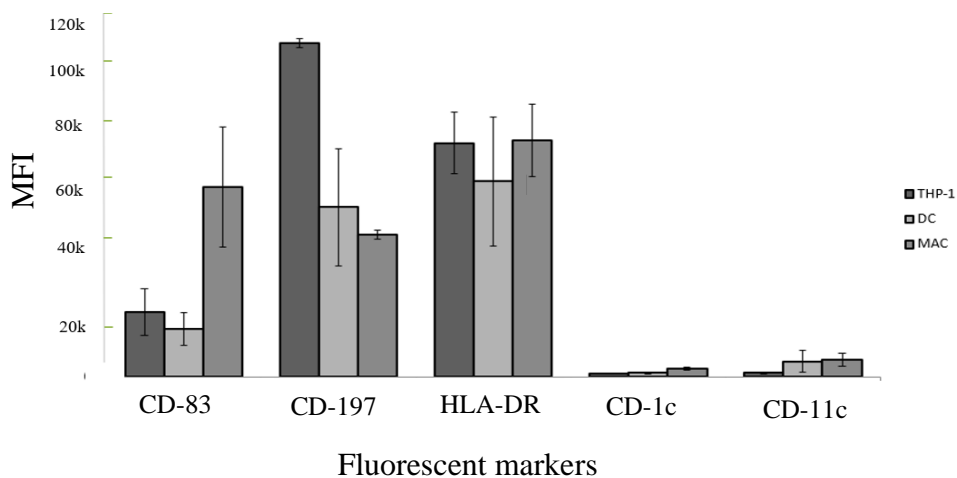


Figure 8: Average mean fluorescent intensity of different cell markers. This was done for the three cells, THP-1, Dendritic cells, and Macrophages. The expression of the surface markers CD-83, CD-197, HLA-DR, DC-1c and CD-11c on THP-1 cells and the differentiated dendritic cells and macrophages were analyzed. A T test with p-value of 0.05 was done. There was only significance ($p < 0.05$) when comparing CD-197 in DC vs THP-1 and Mac vs THP-1. The Y axis are the different fluorescent markers used Also there was significance ($p < 0.05$) when comparing DC-1c in DC vs Mac and Mac vs THP-1. For the rest of the comparisons ($p > 0.05$) meaning there was no significance in comparing between the three types of cells.

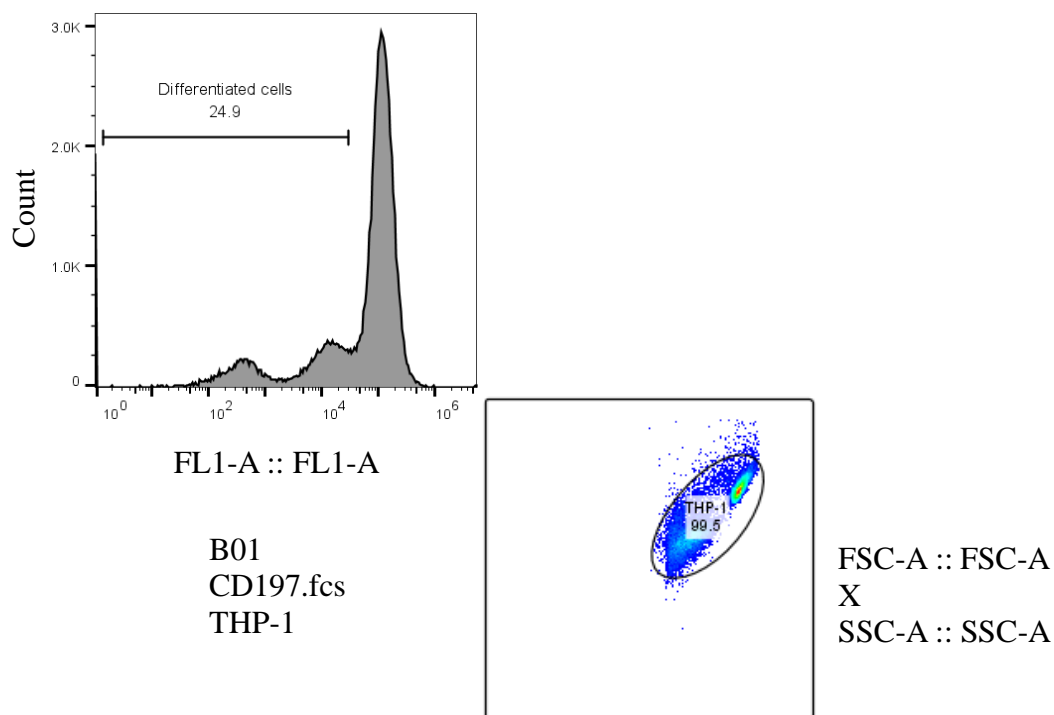


Figure 9: Mean fluorescent intensity for CD197 for THP-1 cells. The peak on the right reads for THP-1 cells.

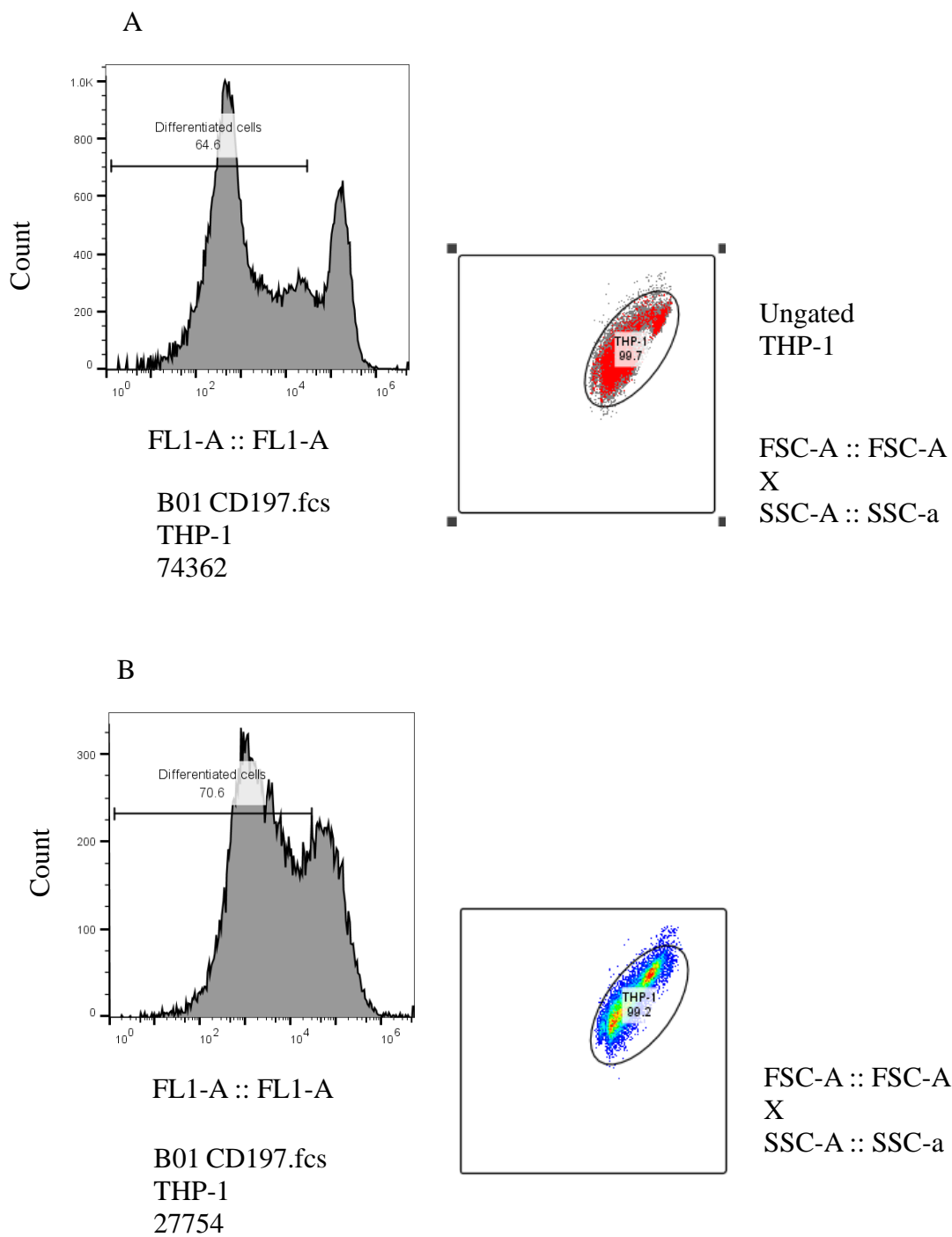


Figure 10: Mean fluorescent intensity for CD197 for DCs and Macrophages. After gating it from THP-1 cells in Figure 9 (The peak on the left reads for Dendritic cells and Macrophages)

3.3 Image Processing

As shown previously Flowcytometry does not give any biological significance to the immune cells, neither it classifies them accurately [64, 110]. Hence, image segmentation was used in the following experiments that will help with the electrical characterization for accurate immune cell identification. This method consists of analyzing the cells based on the visual data supported by their morphological and structural differences. The ImageJ software successfully manages to segment the images, recognize the cells, differentiate the different types of cells, and calculate the area. The morphology and structure of the three types of immune cells are demonstrated in Figure 12. The THP-1 cells can be easily distinguished from DC by their round structure without elongations. Once activated, the non-adherent THP1 cells differentiate to adherent cells that are morphologically different from their inactive forms. On the other hand, macrophages and DCs take more space to spread out, owing to the larger size of the former and the presence of dendrites in the latter Figure 12. Figure 12 (D-F) shows the detailed selection of immune cells using the software. The software highlights the morphological differences-(marked in yellow); by marking the outside boarder of the cell.

After the selection of each cell, the software automatically calculates the area of the cell. We have obtained the results from different images to statistically compare the area of each cell. Figure 11 shows that macrophages are the highest in area and the THP-1s are the lowest due to their rounded shape. This is supported by the data from the literature [112, 113].

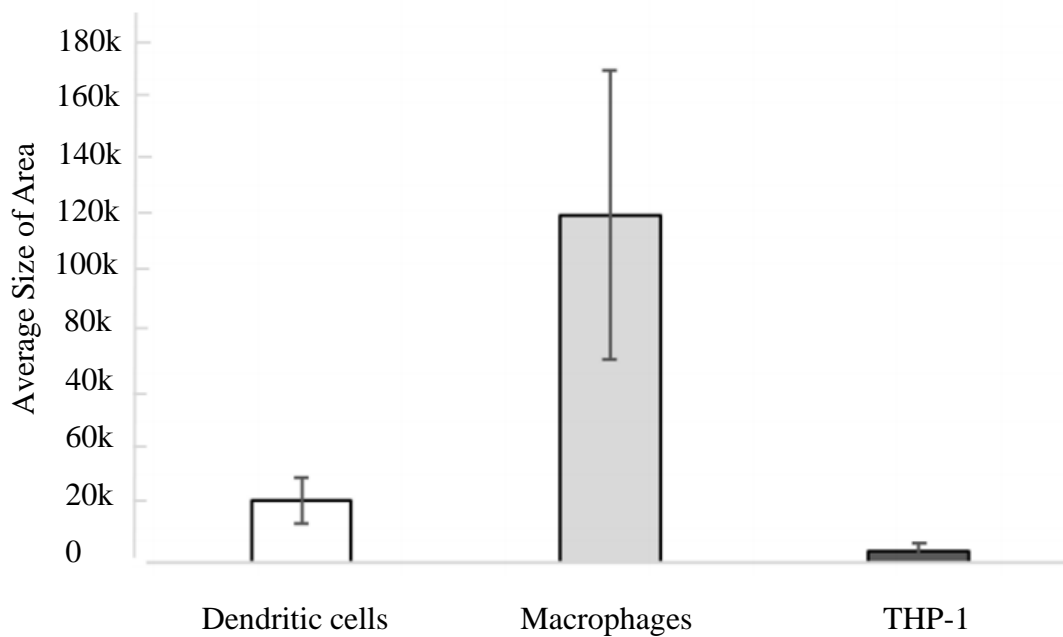


Figure 11: The average area of each cell. Macrophages have the largest area, followed by DCs and THP-1 cells.

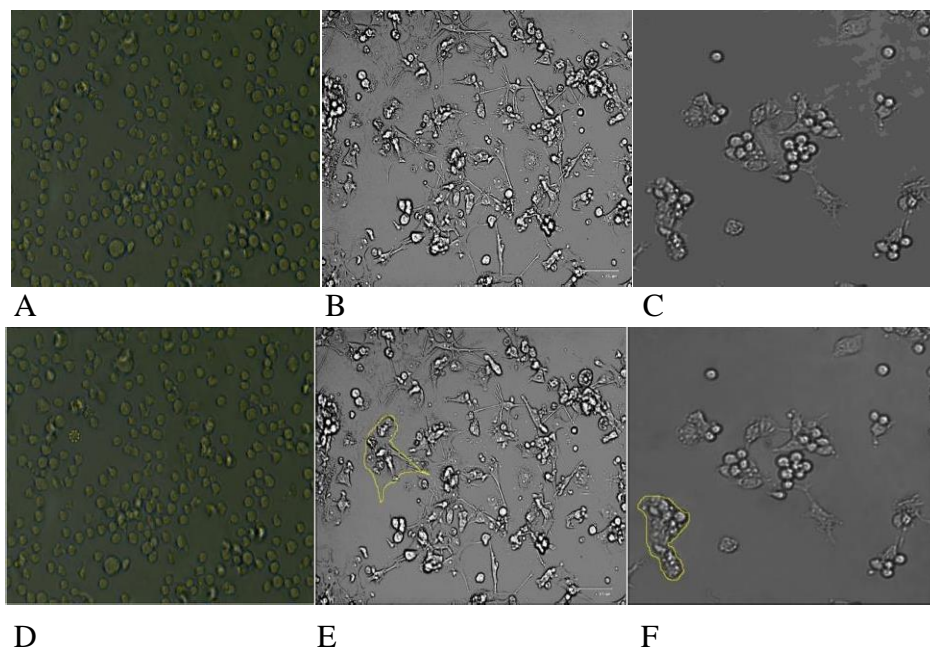


Figure 12: A: THP-1 B: Dendritic cells C: Macrophages, D, E, F after selection. Using Image J software to calculate the area of cells. THP-1 cells (A, D) have round shape and are suspended in the media, DCs are attached and spread their dendrites in the flask (B, E). Macrophages (C,F) are also adherent but without the elongations of the DCs.

3.4 Electrochemical Characterization

3.4.1 System Optimization

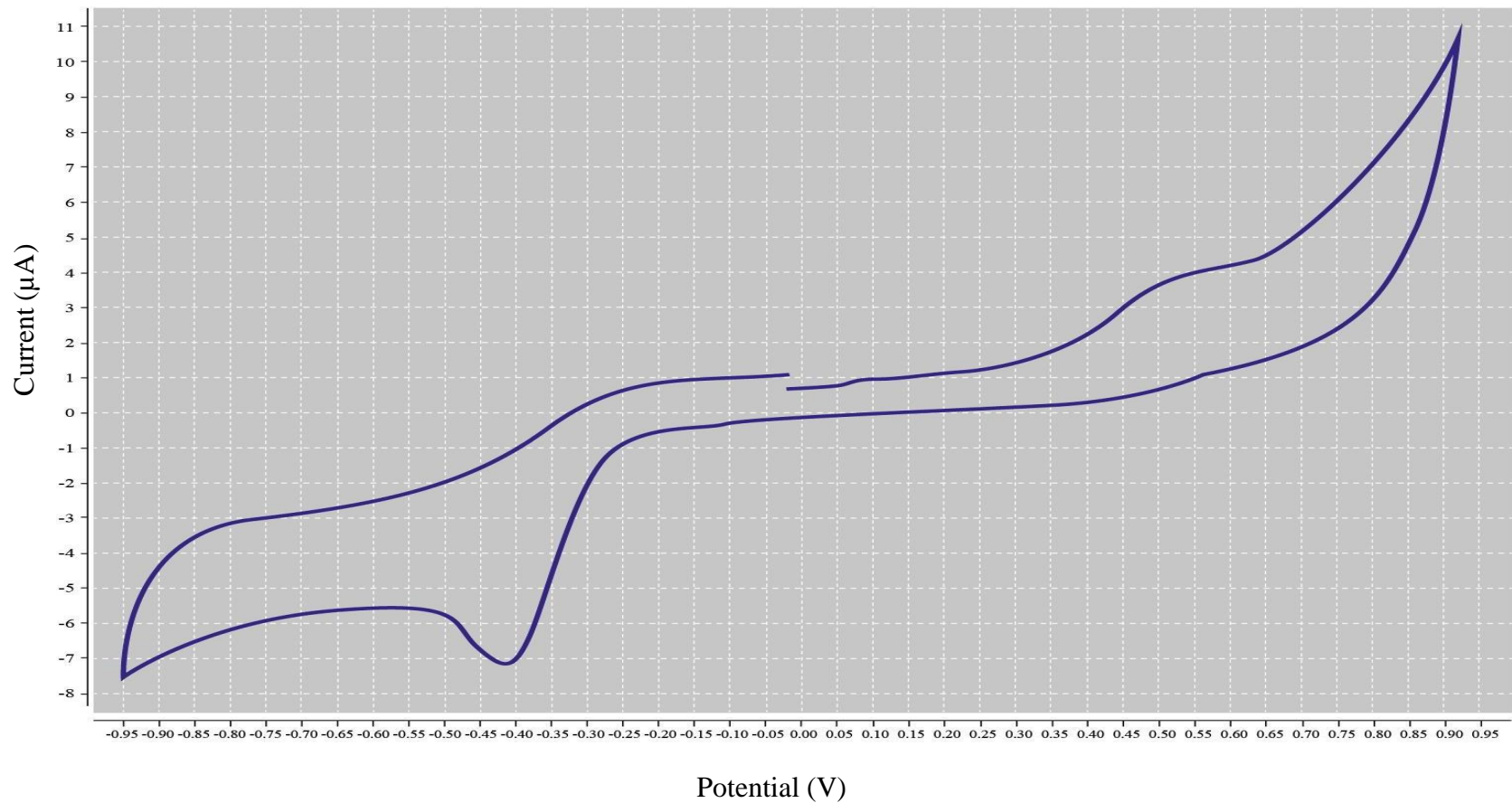
To optimize the system and to figure out the correct configuration for the upcoming experiments, two main optimization experiments we done, one to choose the value for the E-step and Srate. The second optimization experiment aimed to decide on the best connection method (using a chip or using a coaxial cable).

A. Optimization for E-step and Srate

E-step is defined as the difference in voltage between two points at different distances from the source of energy . Srate is the voltage frequency. Table 5 displays the configuration used to optimize and chose the best value for Estep and Srate. The table shows the value of the voltage that initiates the experiment (Ebegin) and it is equal to zero. The voltage then oscillates from 0.9 to -0.9 (Evxt1, Evxt2). The Estep value here is constant as well with a value of 0.002 The variable here is the Srate.

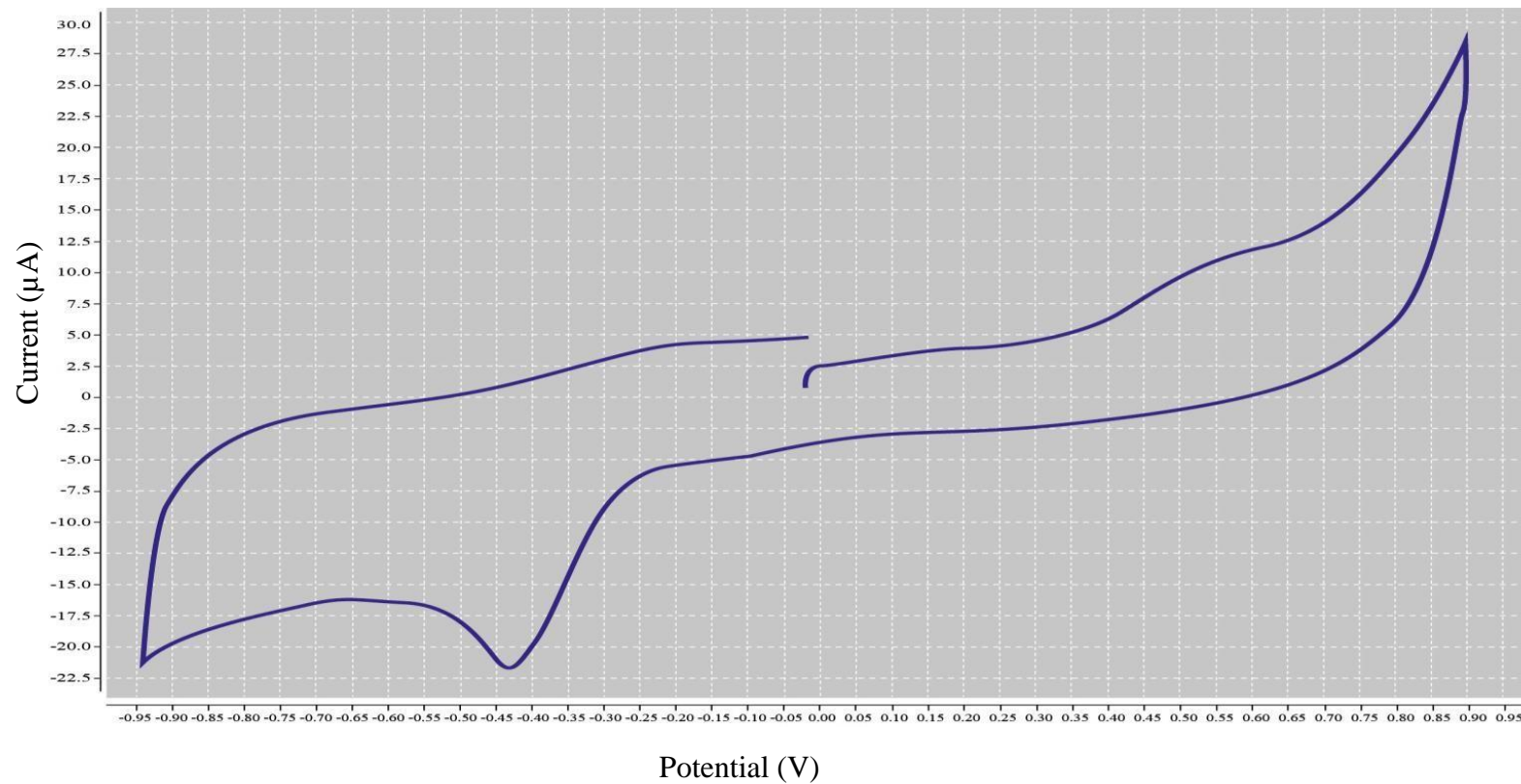
Table 5: Dropsens configuration for Estep and Srate optimization. Srate as the only variable.

#	Ebegin	Evxt1	Evxt2	Estep	Srate
1	0	0.9	-0.9	0.002	0.004
2	0	0.9	-0.9	0.002	0.02
3	0	0.9	-0.9	0.002	0.04
4	0	0.9	-0.9	0.002	0.09
5	0	0.9	-0.9	0.002	0.2
6	0	0.9	-0.9	0.002	0.5
7	0	0.9	-0.9	0.002	1
8	0	0.9	-0.9	0.002	2



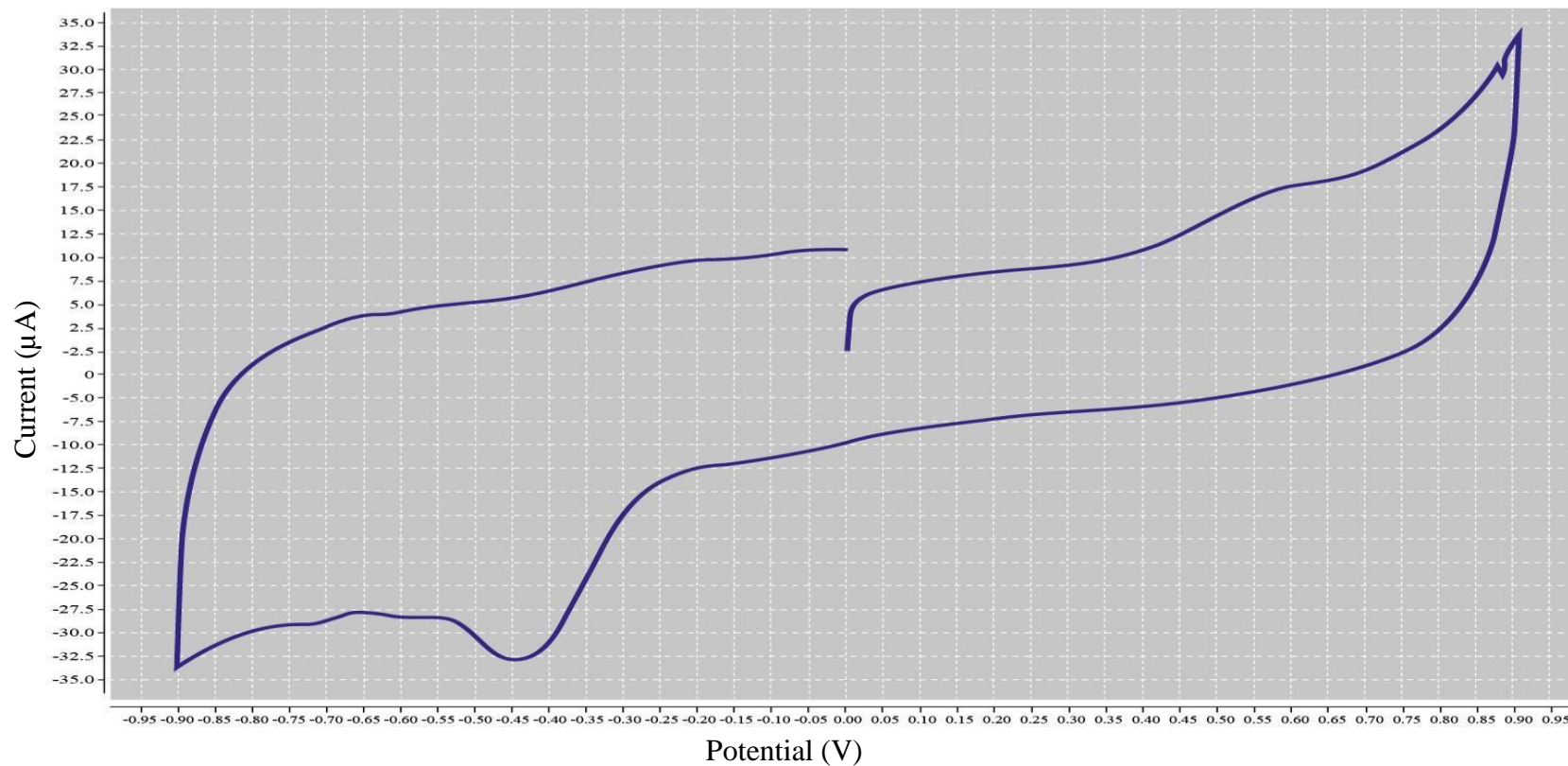
A: E-Step: 0.002 - Srate: 0.004

Figure 13: I-V curves (A- H) obtained from Dropsens software. Using different values for Srate. No accurate data are shown with high values of Srate as shown in graphs G and H. No sufficient flow of current in graphs A and B. Figure C gives I-V curve that is absent of the charging and discharging effects.



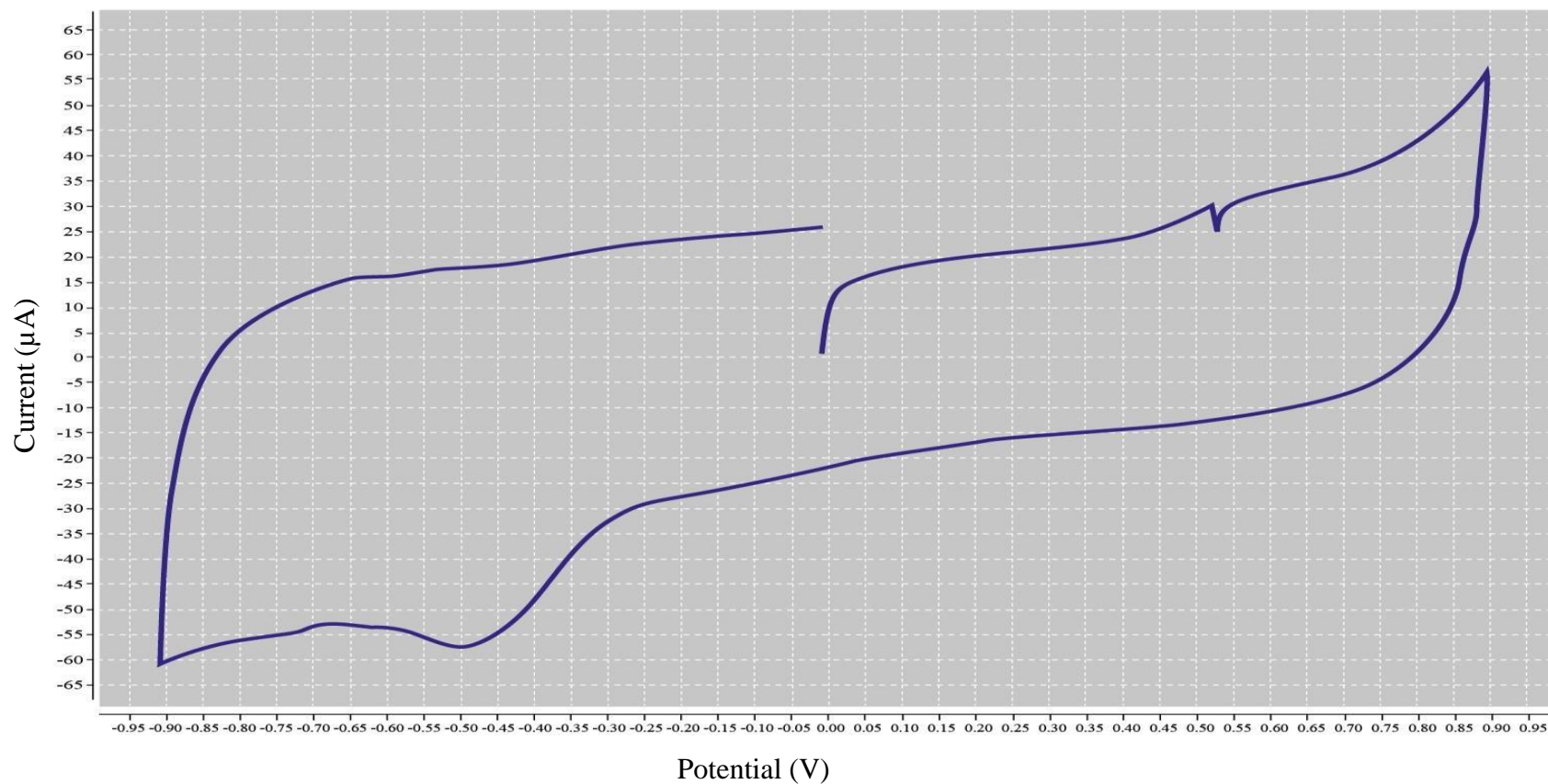
B: E-Step: 0.002 - Srate: 0.02

Figure 13: I-V (A-H) curves obtained from Dropsens software. Using different values for Srate. No accurate data are shown with high values of Srate as shown in graphs G and H. No sufficient flow of current in graphs A and B. Figure C gives I-V curve that is absent of the charging and discharging effects (Continued).



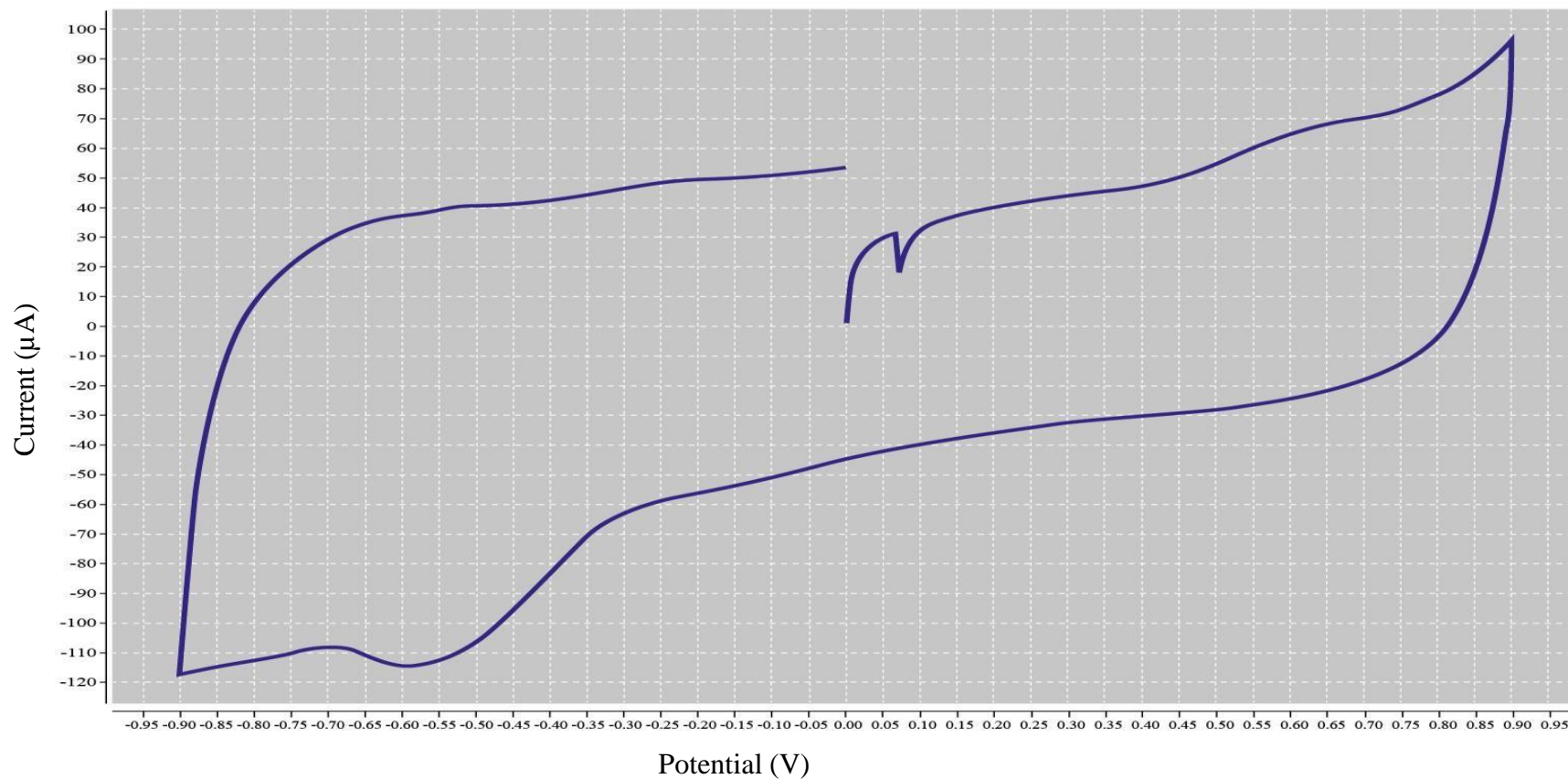
C: E-Step: 0.002 - Srate: 0.04

Figure 13: I-V (A-H) curves obtained from Dropsens software. Using different values for Srate. No accurate data are shown with high values of Srate as shown in graphs G and H. No sufficient flow of current in graphs A and B. Figure C gives I-V curve that is absent of the charging and discharging effects (Continued).



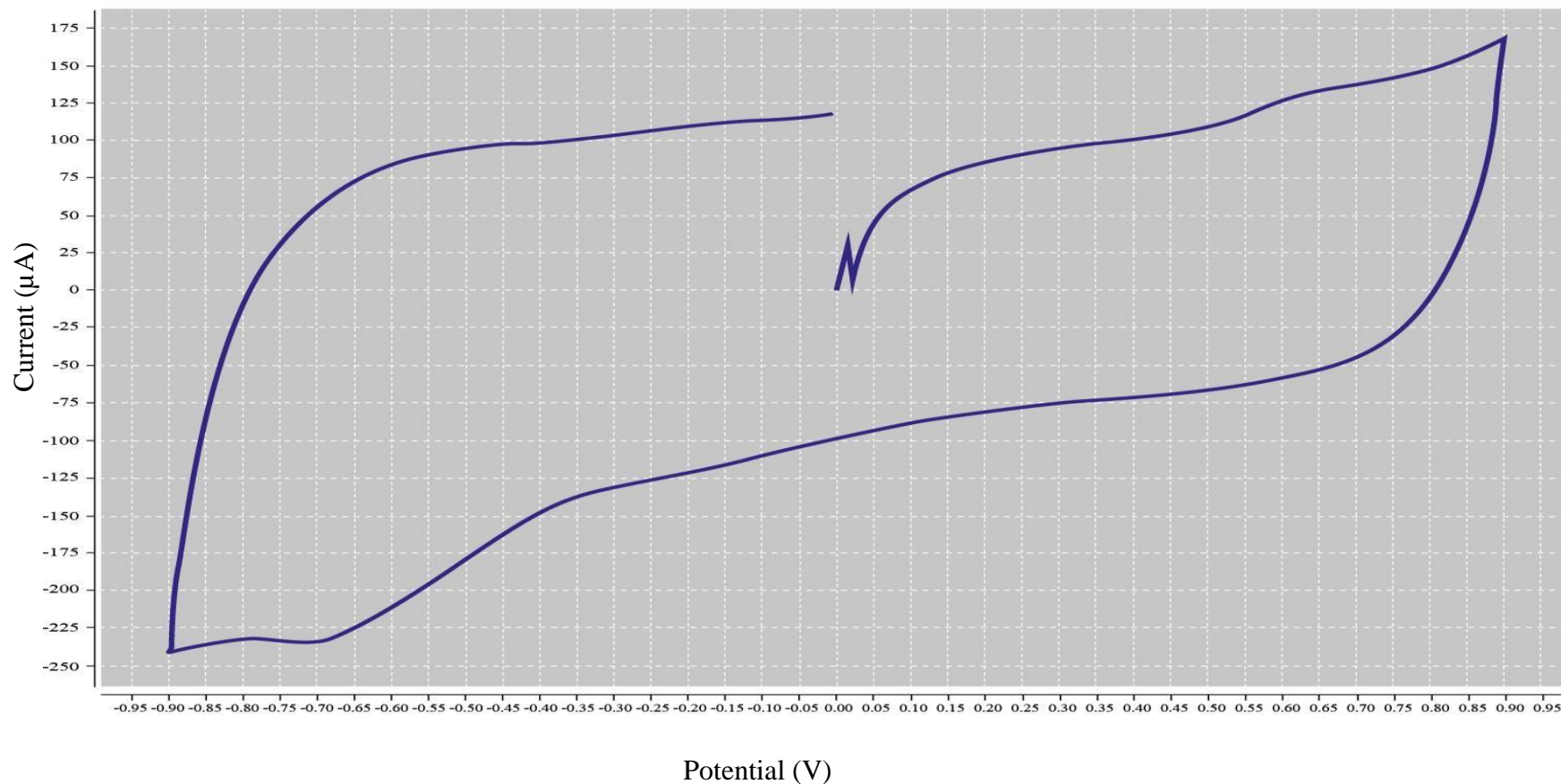
D: E-Step: 0.002 - Srate: 0.09

Figure 13: I-V (A-H) curves obtained from Dropsens software. Using different values for Srate. No accurate data are shown with high values of Srate as shown in graphs G and H. No sufficient flow of current in graphs A and B. Figure C gives I-V curve that is absent of the charging and discharging effects (Continued).



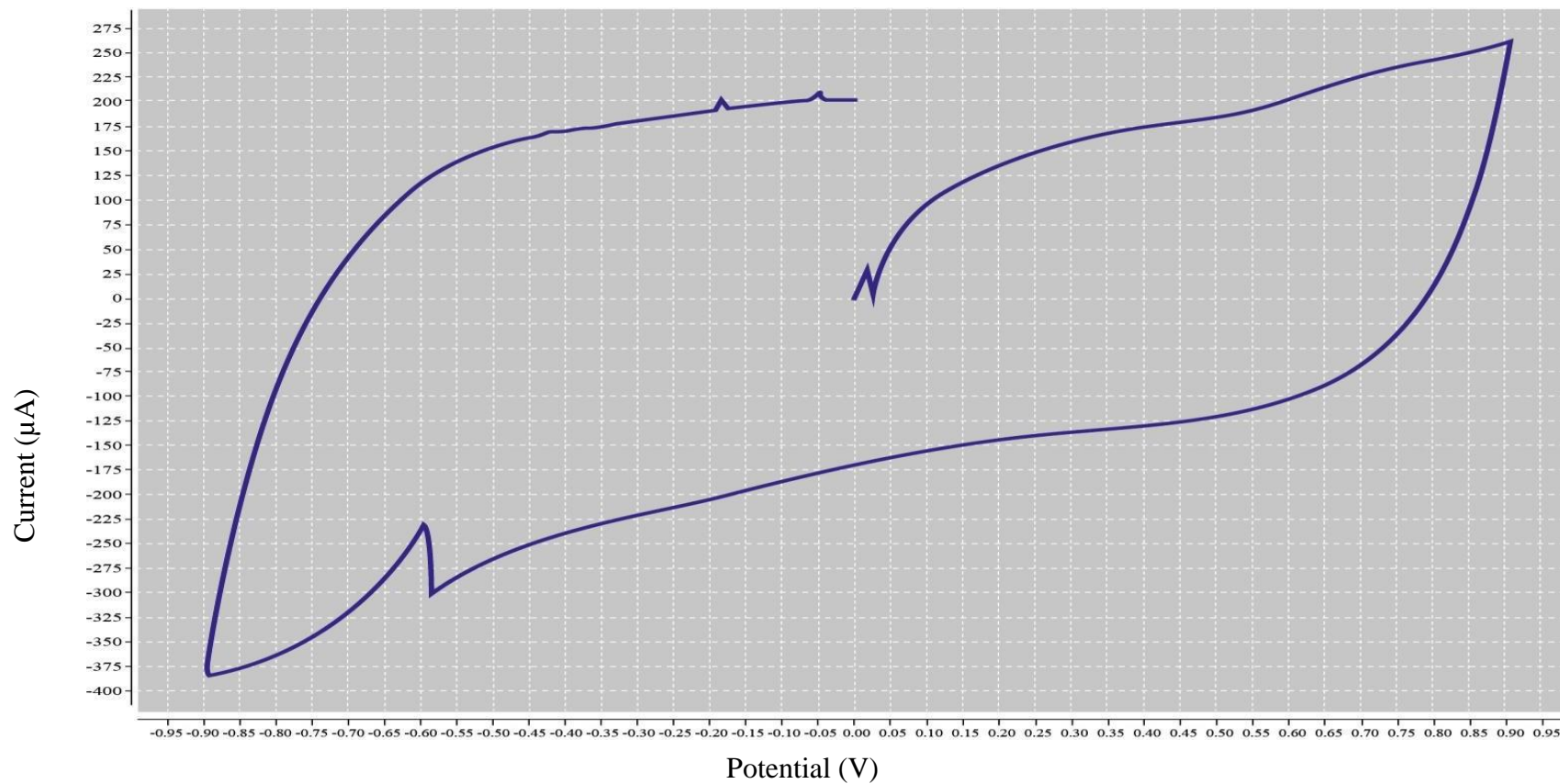
E: E-Step: 0.002 - Srate: 0.2

Figure 13: I-V (A-H) curves obtained from Dropsens software. Using different values for Srate. No accurate data are shown with high values of Srate as shown in graphs G and H. No sufficient flow of current in graphs A and B. Figure C gives I-V curve that is absent of the charging and discharging effects (Continued).



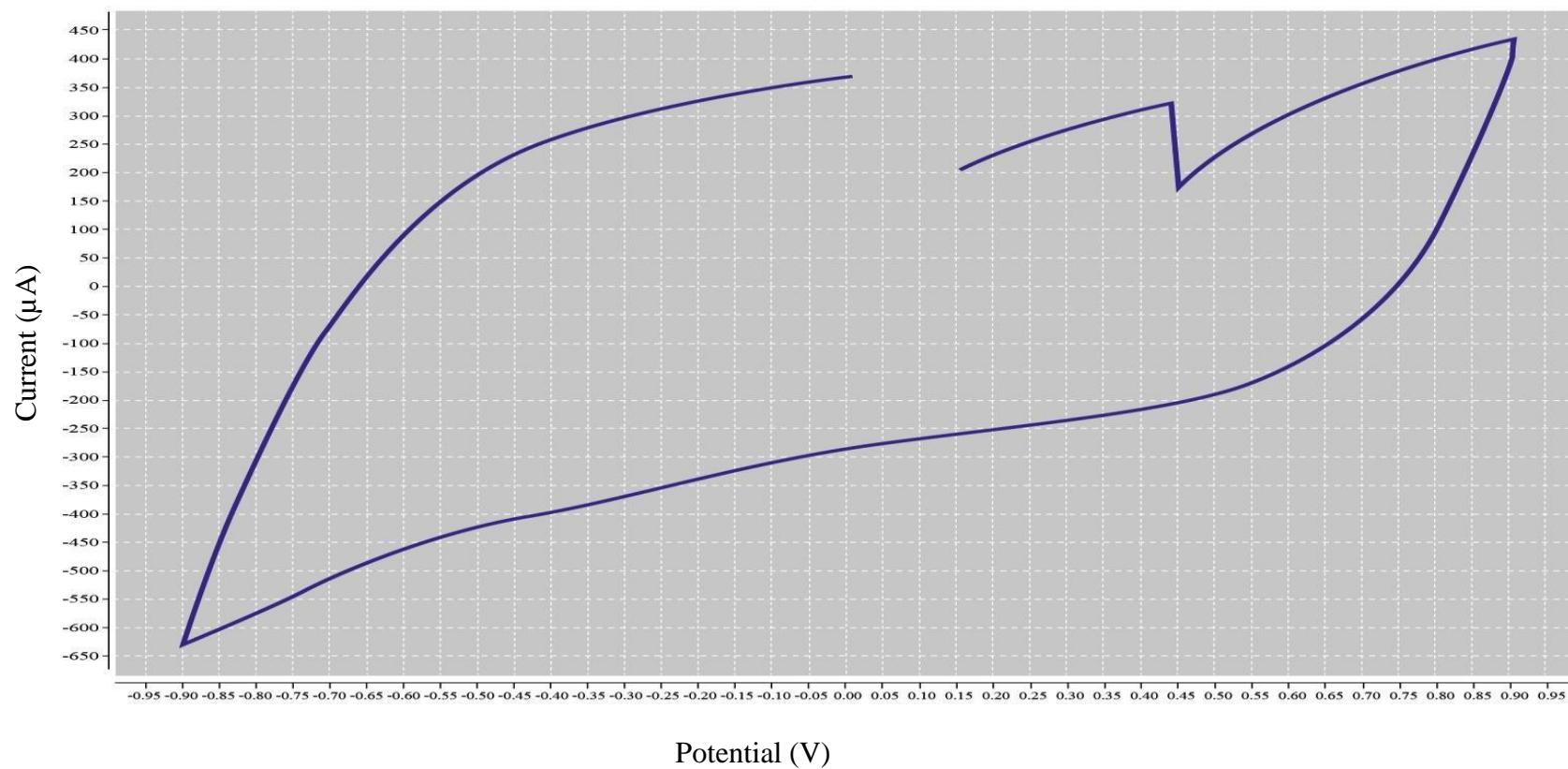
F: E-Step: 0.002 - Srate: 0.5

Figure 13: I-V (A-H) curves obtained from Dropsens software. Using different values for Srate. No accurate data are shown with high values of Srate as shown in graphs G and H. No sufficient flow of current in graphs A and B. Figure C gives I-V curve that is absent of the charging and discharging effects (Continued).



G: E-Step: 0.002 - Srate: 1

Figure 13: I-V (A-H) curves obtained from Dropsens software. Using different values for Srate. No accurate data are shown with high values of Srate as shown in graphs G and H. No sufficient flow of current in graphs A and B. Figure C gives I-V curve that is absent of the charging and discharging effects (Continued)



H: E-Step: 0.002 - Srate: 2

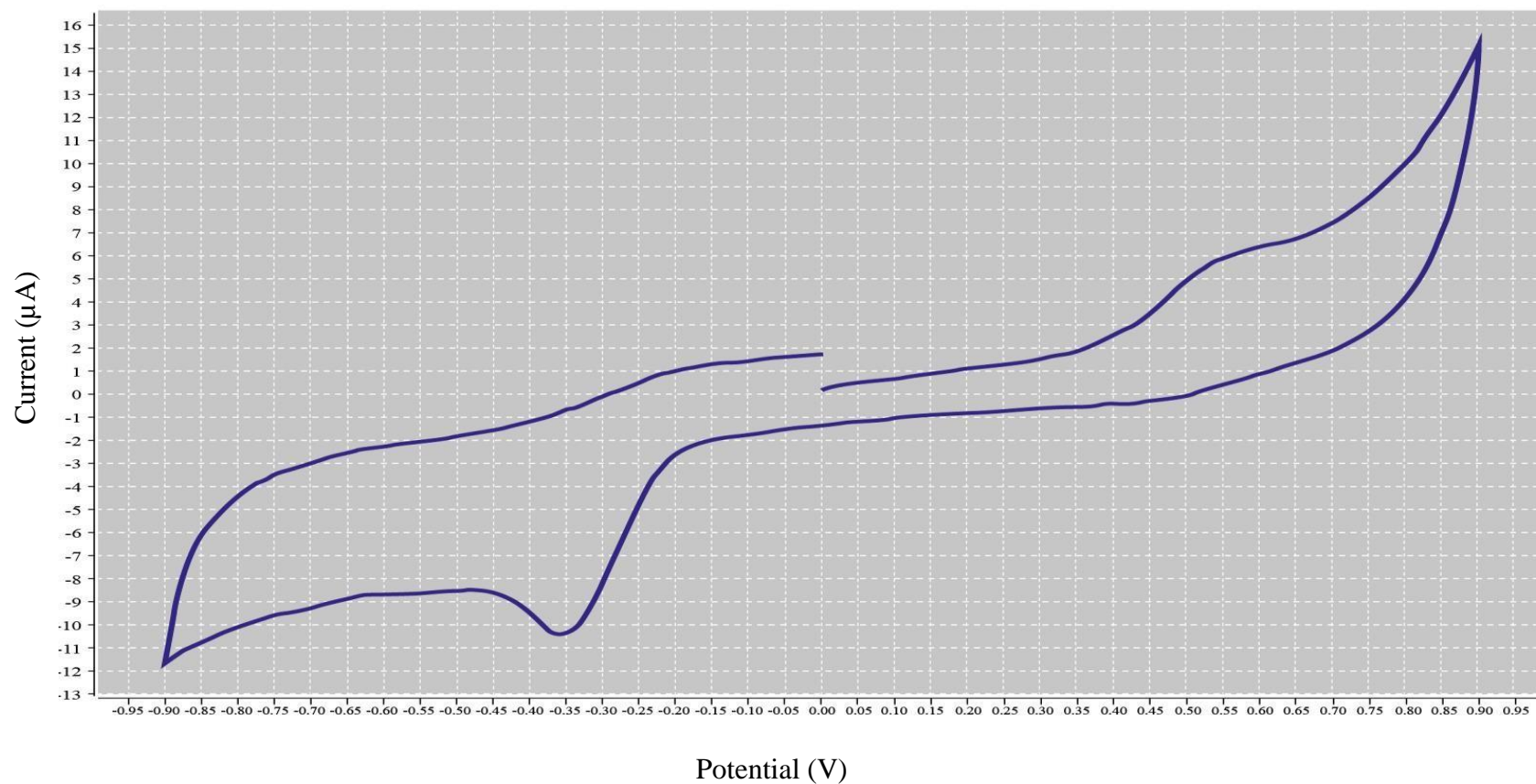
Figure 13: I-V (A-H) curves obtained from Dropsens software. Using different values for Srate. No accurate data are shown with high values of Srate as shown in graphs G and H. No sufficient flow of current in graphs A and B. Figure C gives I-V curve that is absent of the charging and discharging effects (Continued).

The common behavior of capacitors is to charge and discharge as a function of time. An alternating current with a high frequency would not sufficiently allow a capacitor material to charge/discharge (and would thereby behave as a resistor). In other words the graph loses the details and no accurate data can be obtained as shown in Figures 13 (G and H). On the other hand, a capacitor in an alternating current with zero frequency (effectively a DC current) would charge/discharge, and no longer allow a current to flow subsequently. Furthermore, this scenario would be damaging to the cells as shown in Figures 13 (A and B). It is for this fundamental behavior of capacitors that an Srate values that would give us I-V curves that are absent of the time-dependent charging and discharging effects was used, that would thus give us the highest resolution of capacitance which would further aid to distinguish cells, these are represented in Figures 13s)C and D).

To further validate our data, both the values for the Estep and Srate were changed. Table 6 displays the configuration used for the second optimization experiment. This experiment had the E begin, Evxt1, Evxt2 constants and the values are presented in the table. The values for Estep and Srate are variables are presented. The goal of this experiment is to study the graphs when changing the values of the Estep and Srate in parallel. It is important to study the effect of the Estep on the quality of the graphs and the data that can obtained from them.

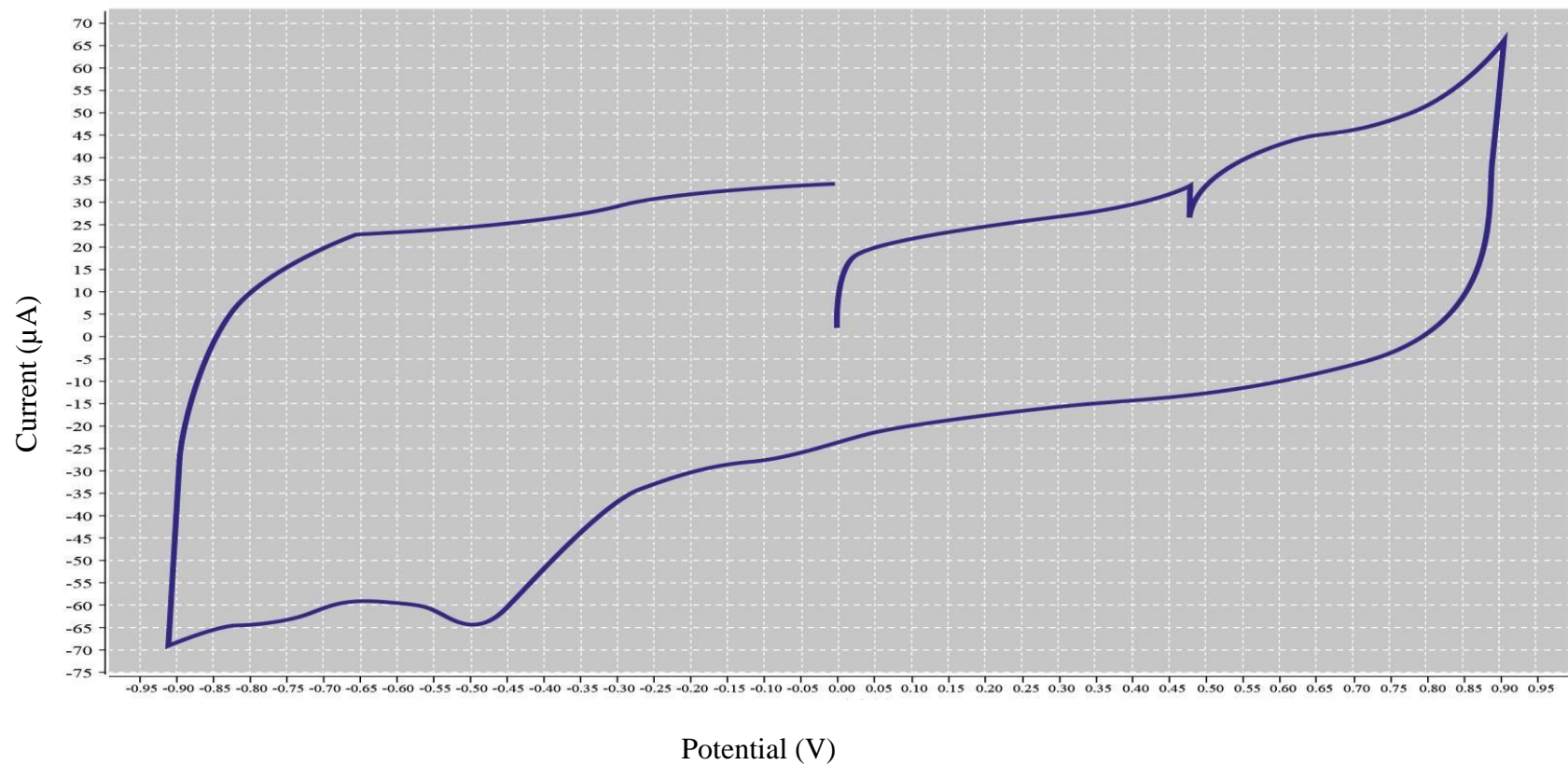
Table 6: Dropsens configuration for Estep and Srate optimization. Estep and Srate as the variables.

#	Ebegin	Evxt1	Evxt2	Estep	Srate
1	0	0.9	-0.9	0.009	0.009
2	0	0.9	-0.9	0.001	0.001
3	0	0.9	-0.9	0.009	0.09
4	0	0.9	-0.9	0.09	0.09
5	0	0.9	-0.9	0.01	0.1
6	0	0.9	-0.9	0.1	0.1
7	0	0.9	-0.9	0.001	0.9
8	0	0.9	-0.9	0.01	0.9
9	0	0.9	-0.9	0.1	0.9
10	0	0.9	-0.9	0.001	1
11	0	0.9	-0.9	0.01	1
12	0	0.9	-0.9	0.01	2



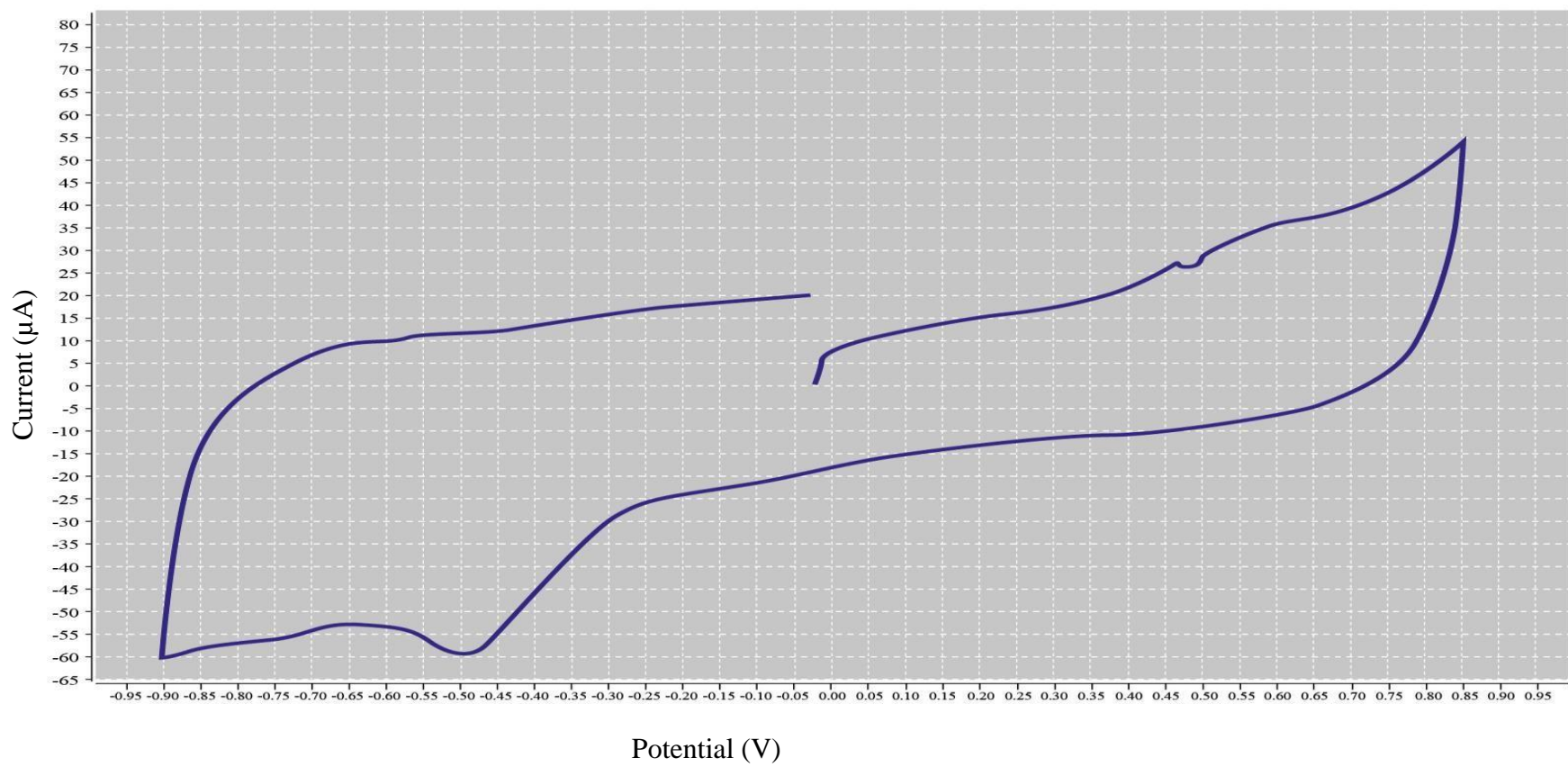
A: E-Step: 0.009 - Srate: 0.009

Figure 14: I-V curves (A-L) obtained from Dropsens software. Using different values for Estep and Srate. Low values of Srate and Estep does not allow proper flow of current as shown in A. High values of Srate does not allow sufficient charge of the sample as shown in G to L. Equal values of Estep and Srate do not give correct shape for cyclic voltammetry graph as shown in D and E.



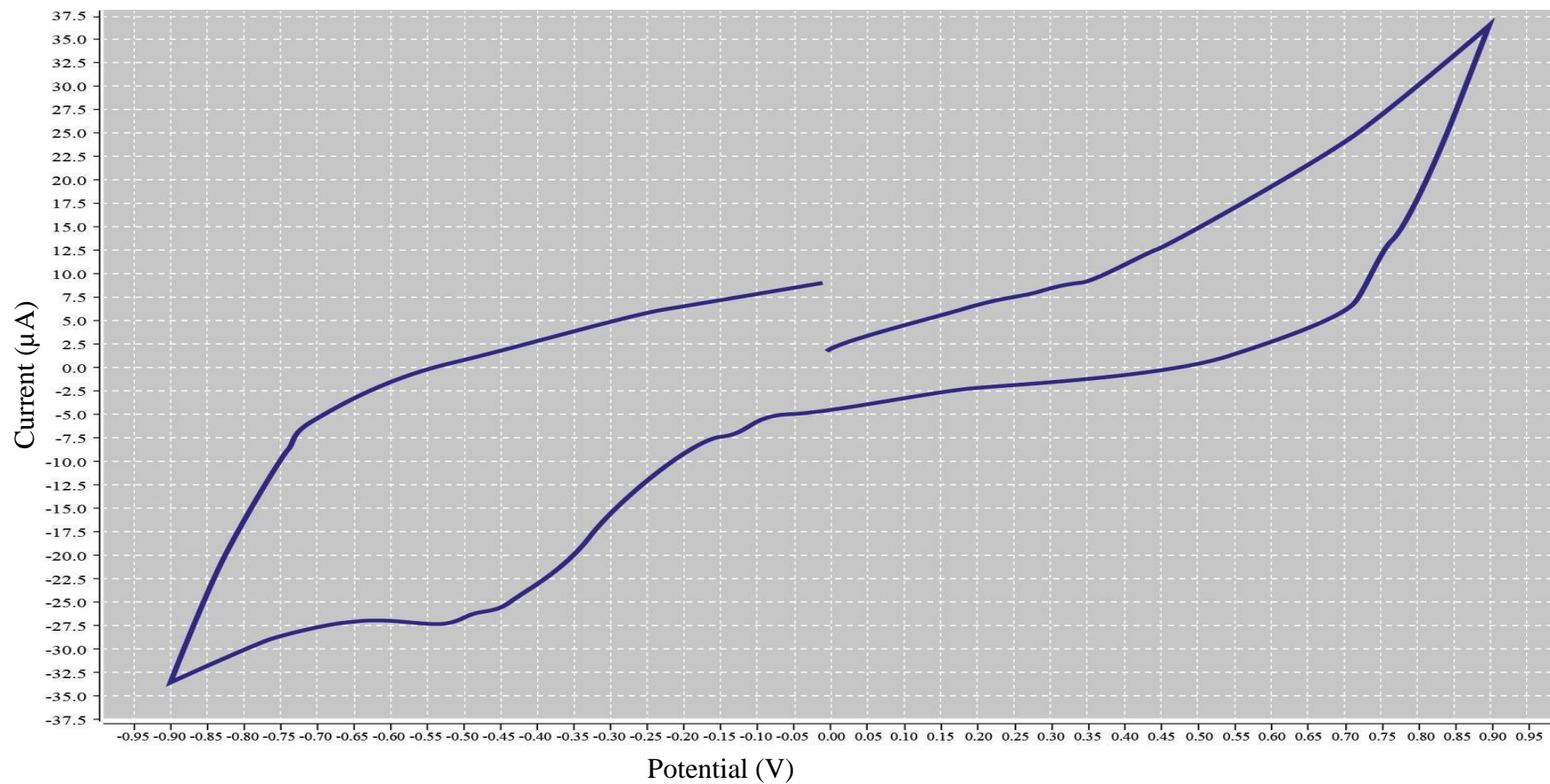
B: E-Step: 0.001 - Srate: 0.001

Figure 14: I-V curves (A-L) obtained from Dropsens software. Using different values for Estep and Srate. Low values of Srate and Estep does not allow proper flow of current as shown in A. High values of Srate does not allow sufficient charge of the sample as shown in G to L. Equal values of Estep and Srate do not give correct shape for cyclic voltammetry graph as shown in D and E (Continued).



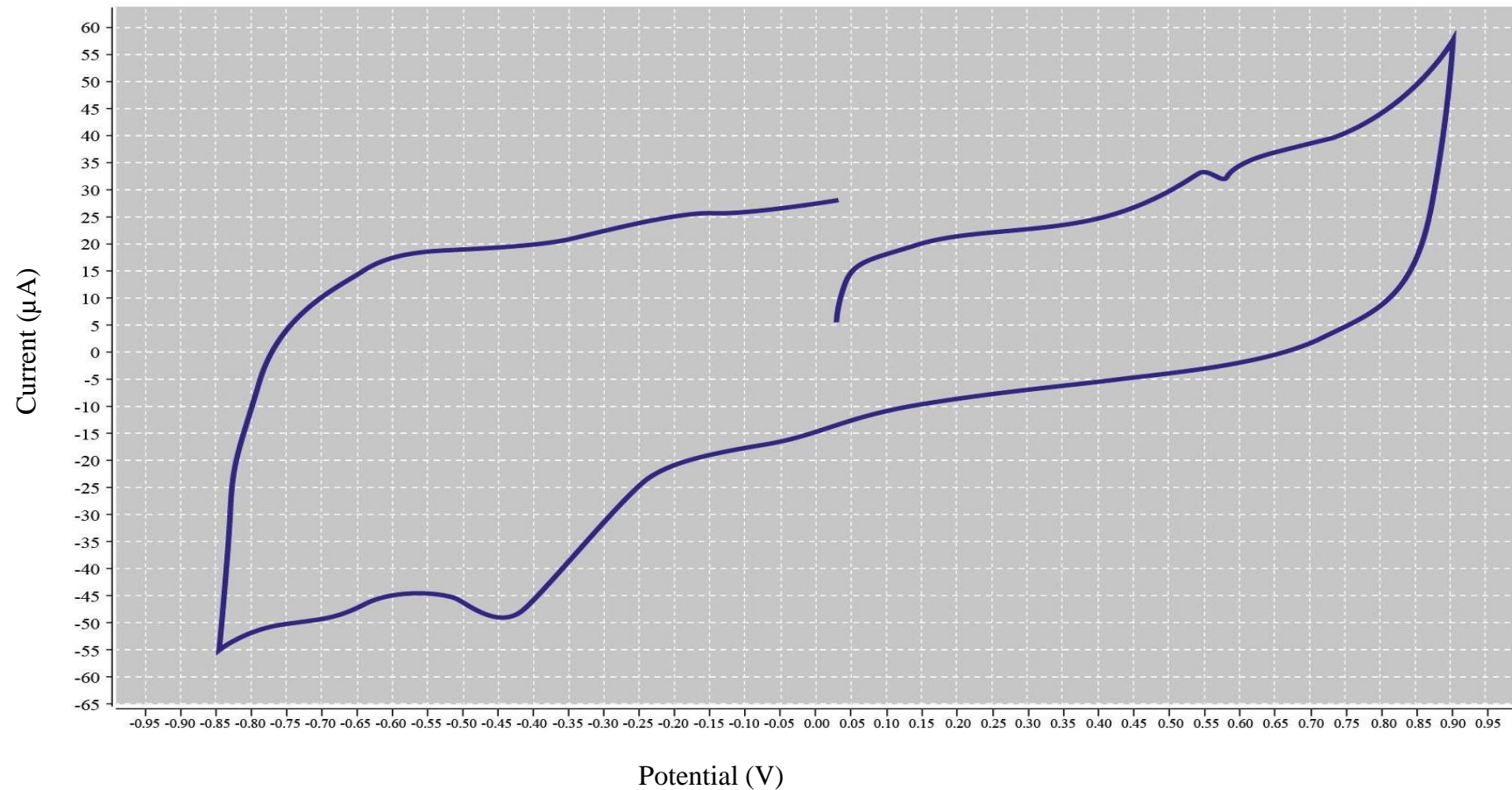
C: E-Step: 0.009 - Srate: 0.09

Figure 14: I-V curves (A-L) obtained from Dropsens software. Using different values for Estep and Srate. Low values of Srate and Estep does not allow proper flow of current as shown in A. High values of Srate does not allow sufficient charge of the sample as shown in G to L. Equal values of Estep and Srate do not give correct shape for cyclic voltammetry graph as shown in D and E (Continued).



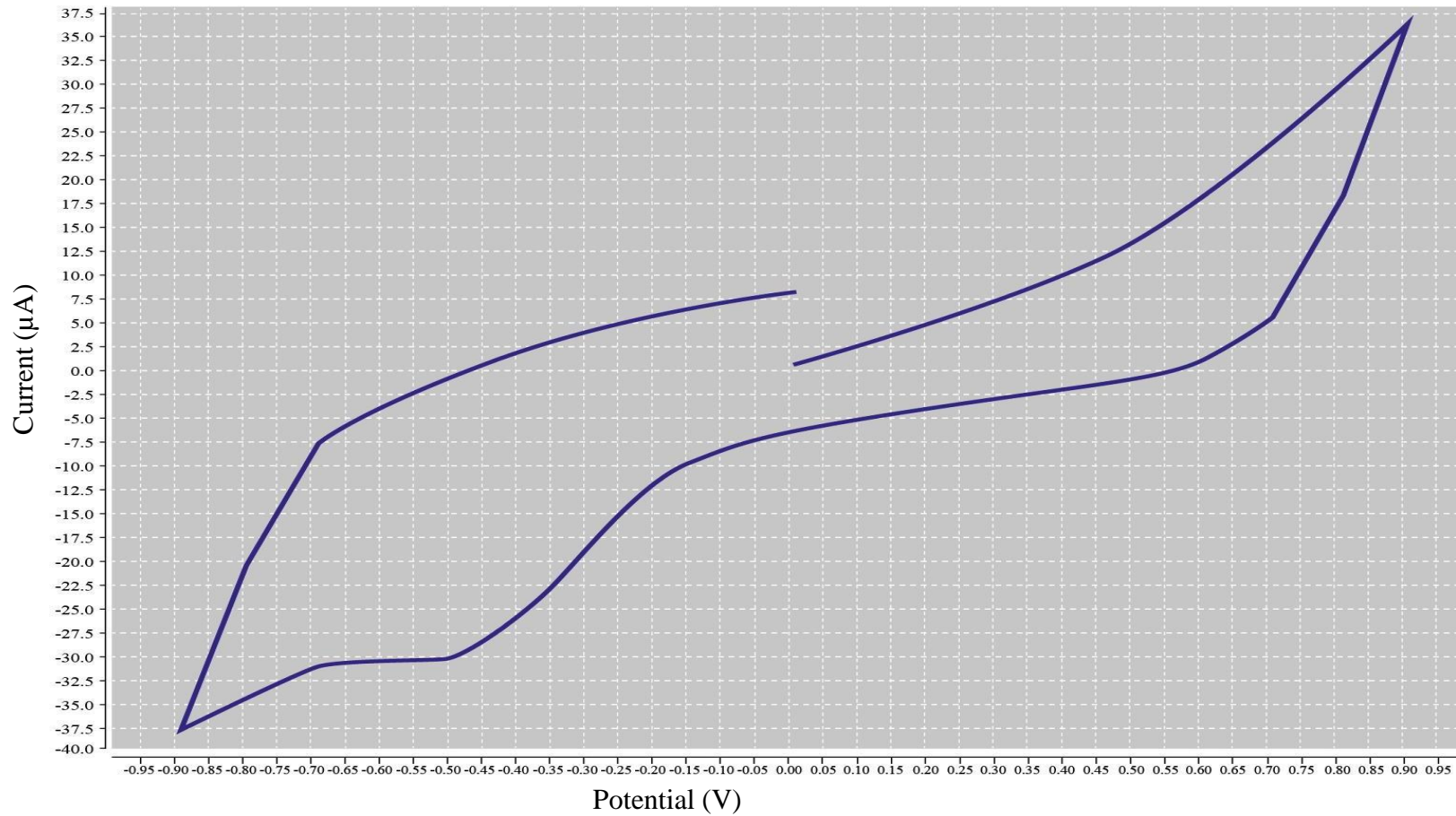
D: E-Step: 0.09 - Srate: 0.09

Figure 14: I-V curves (A-L) obtained from Dropsens software. Using different values for Estep and Srate. Low values of Srate and Estep does not allow proper flow of current as shown in A. High values of Srate does not allow sufficient charge of the sample as shown in G to L. Equal values of Estep and Srate do not give correct shape for cyclic voltammetry graph as shown in D and E (Continued).



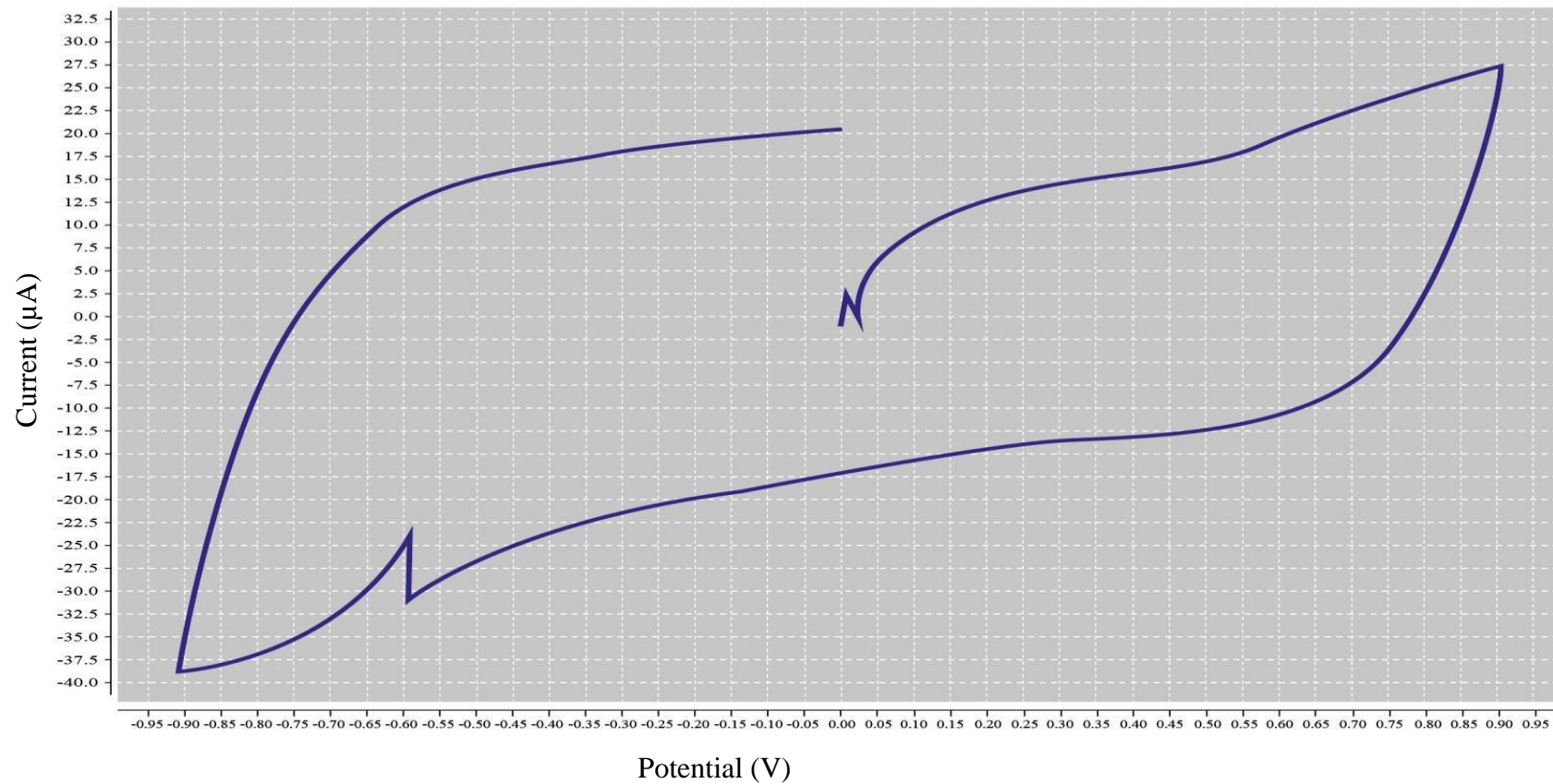
E: E-Step: 0.01 - Srate: 0.1

Figure 14: I-V curves (A-L) obtained from Dropsens software. Using different values for Estep and Srate. Low values of Srate and Estep does not allow proper flow of current as shown in A. High values of Srate does not allow sufficient charge of the sample as shown in G to L. Equal values of Estep and Srate do not give correct shape for cyclic voltammetry graph as shown in D and E (Continued).



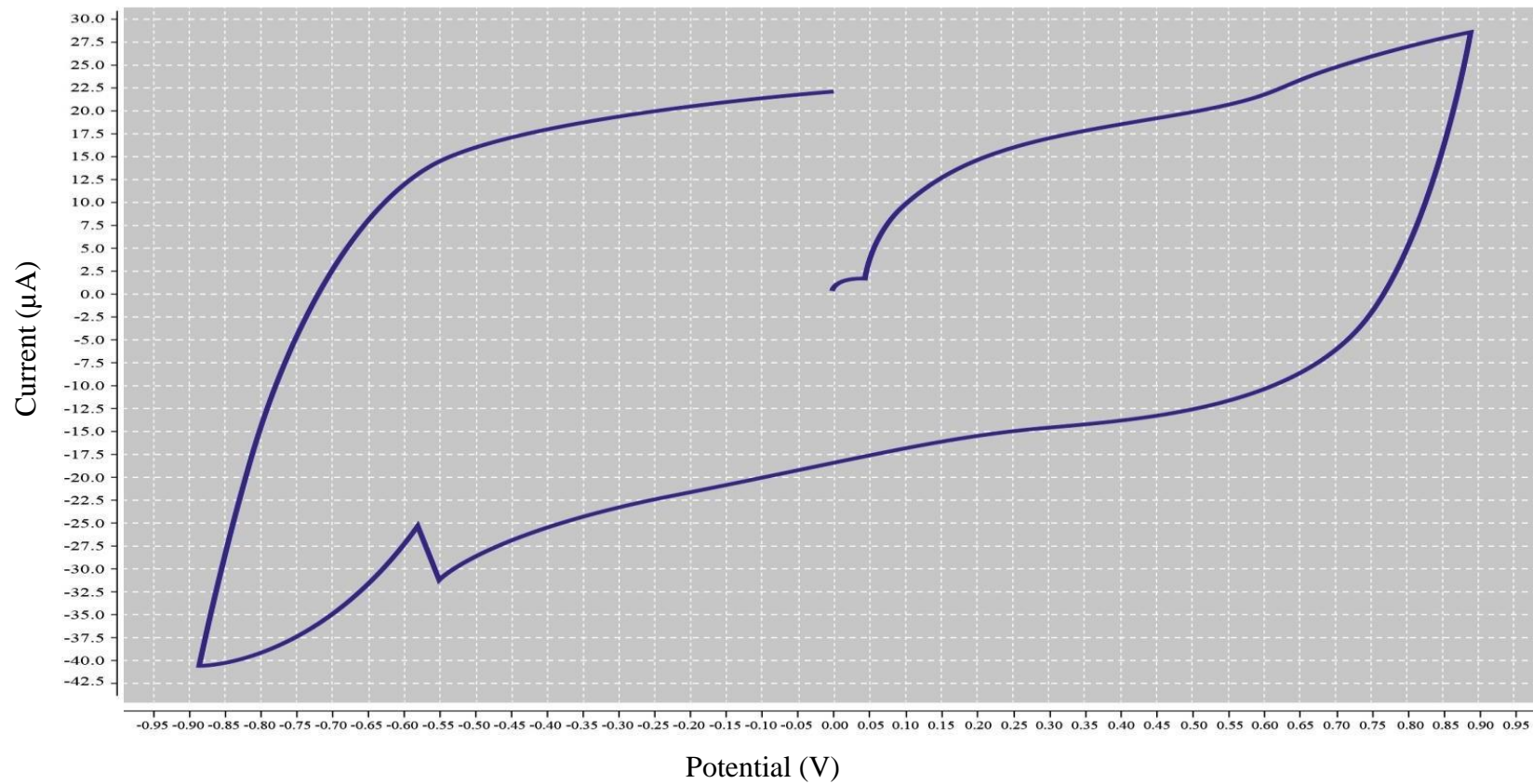
F: E-Step: 0.1 - Srate: 0.1

Figure 14: I-V curves (A-L) obtained from Dropsens software. Using different values for Estep and Srate. Low values of Srate and Estep does not allow proper flow of current as shown in A. High values of Srate does not allow sufficient charge of the sample as shown in G to L. Equal values of Estep and Srate do not give correct shape for cyclic voltammetry graph as shown in D and E (Continued).



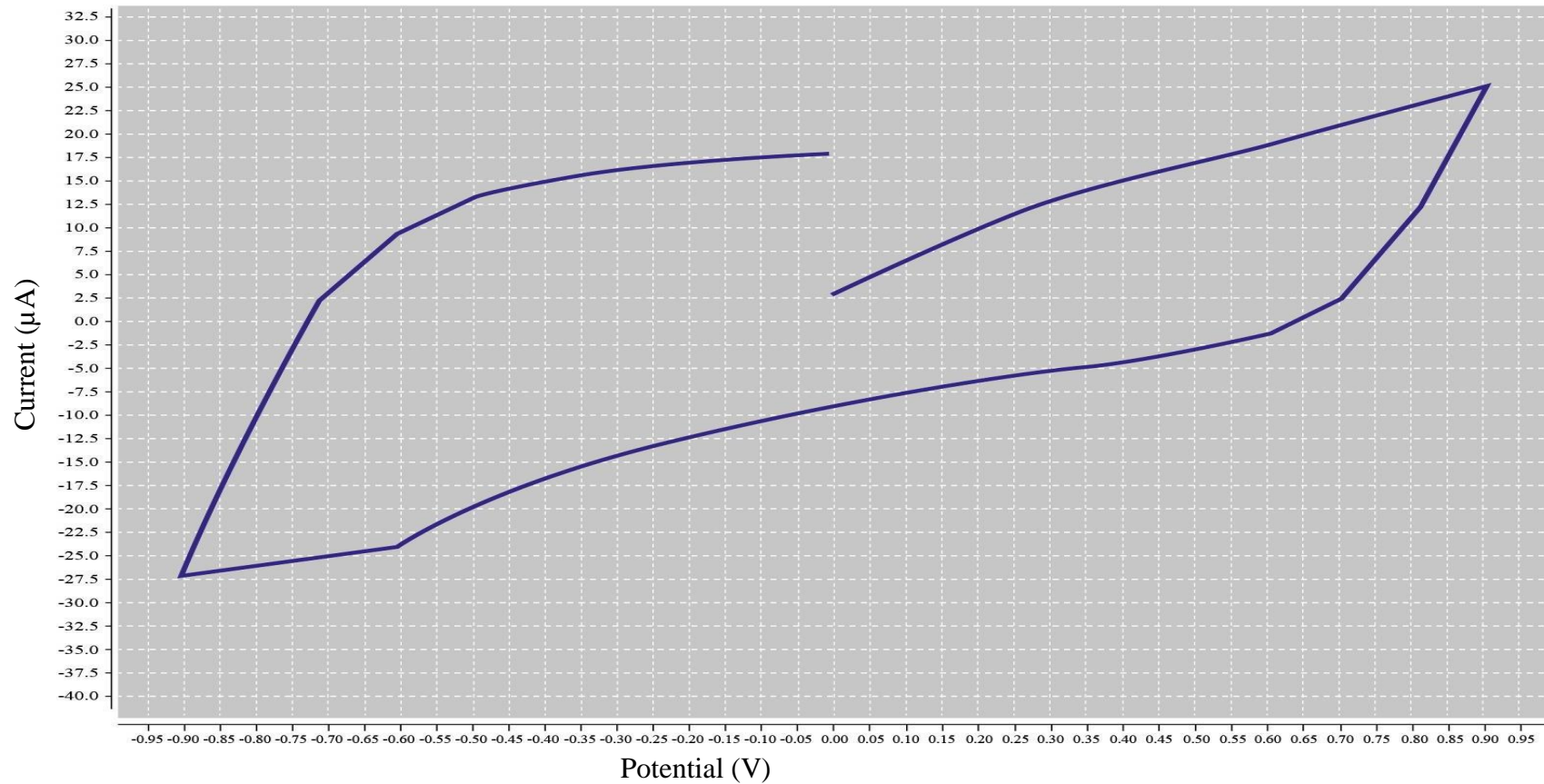
G: E-Step: 0.001 - Srate: 0.9

Figure 14: I-V curves (A-L) obtained from Dropsens software. Using different values for Estep and Srate. Low values of Srate and Estep does not allow proper flow of current as shown in A. High values of Srate does not allow sufficient charge of the sample as shown in G to L. Equal values of Estep and Srate do not give correct shape for cyclic voltammetry graph as shown in D and E (Continued).



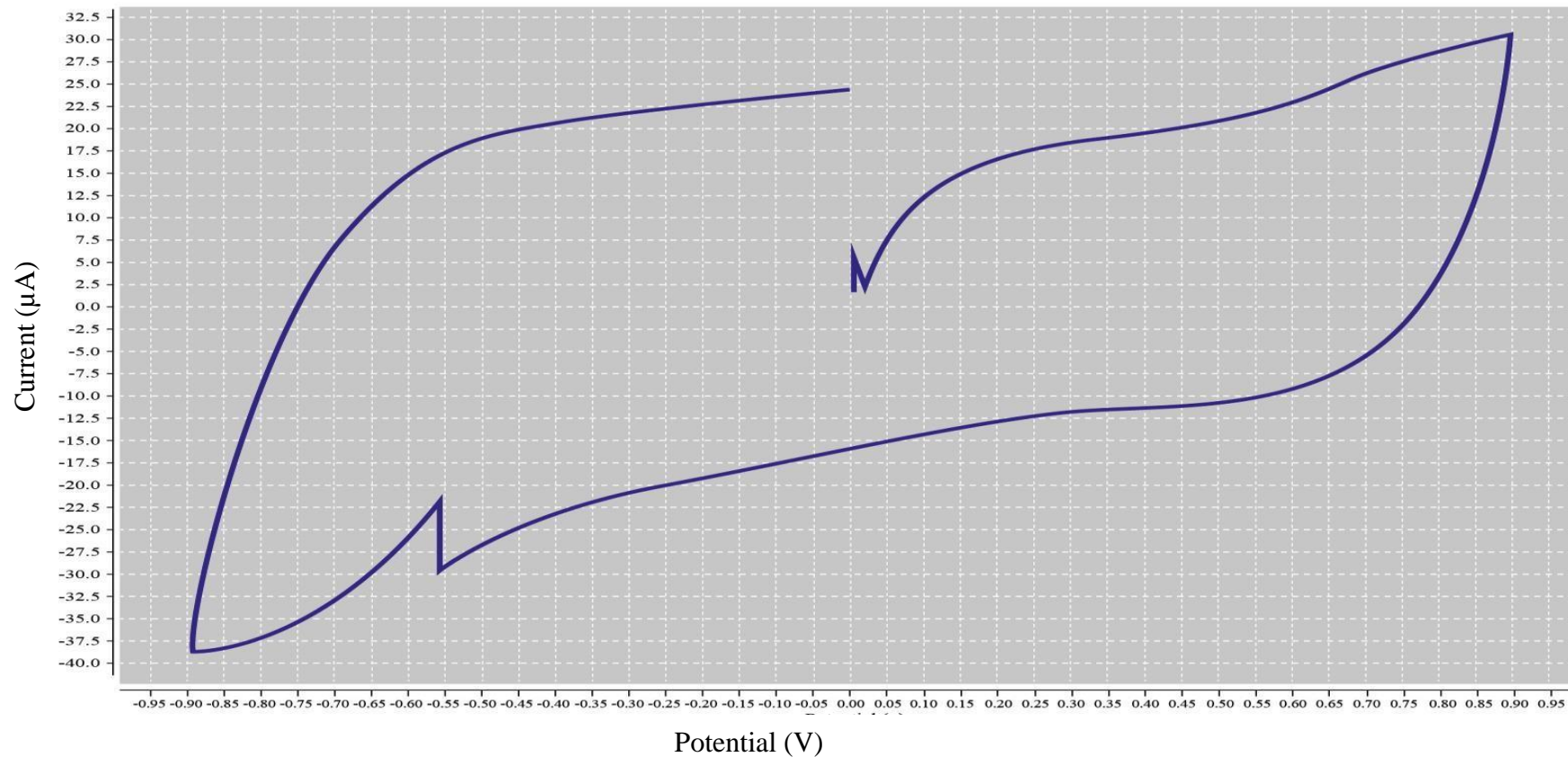
H: E-Step: 0.01 - Srate: 0.9

Figure 14: I-V curves (A-L) obtained from Dropsens software. Using different values for Estep and Srate. Low values of Srate and Estep does not allow proper flow of current as shown in A. High values of Srate does not allow sufficient charge of the sample as shown in G to L. Equal values of Estep and Srate do not give correct shape for cyclic voltammetry graph as shown in D and E (Continued).



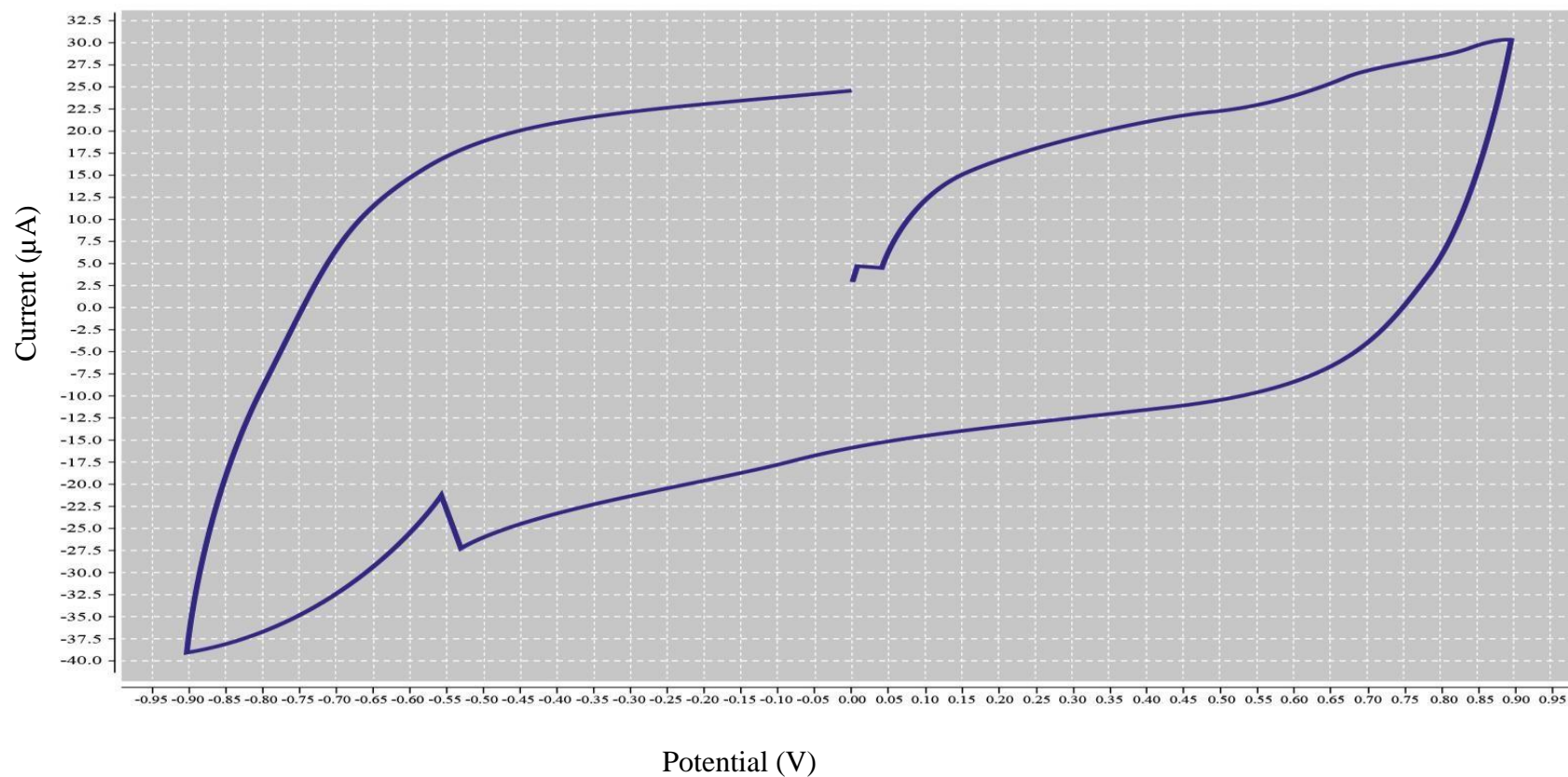
I: E-Step: 0.1 - Srate: 0.9

Figure 14: I-V curves (A-L) obtained from Dropsens software. Using different values for Estep and Srate. Low values of Srate and Estep does not allow proper flow of current as shown in A. High values of Srate does not allow sufficient charge of the sample as shown in G to L. Equal values of Estep and Srate do not give correct shape for cyclic voltammetry graph as shown in D and E (Continued).



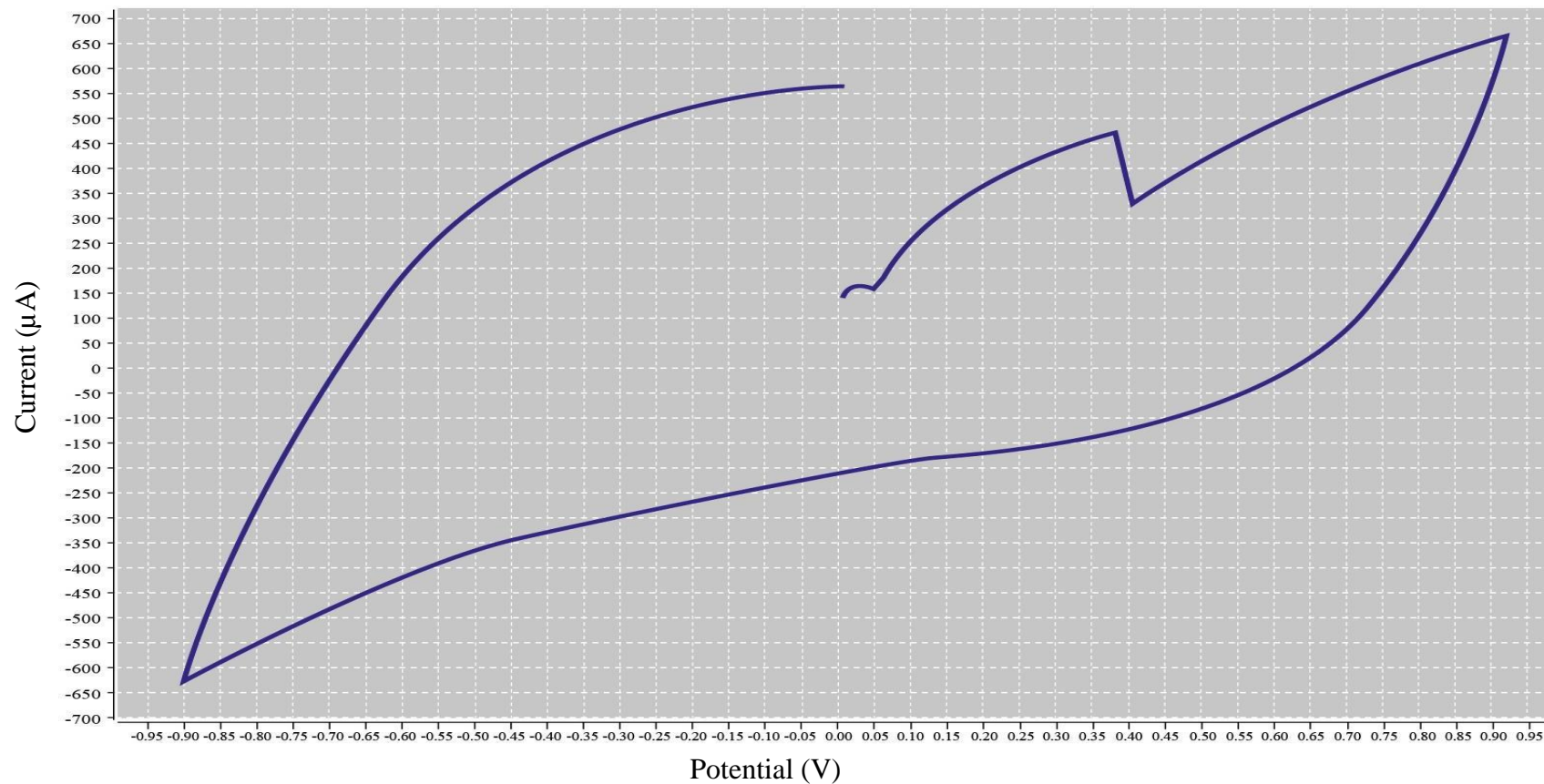
J: E-Step: 0.001 - Srate: 1

Figure 14: I-V curves (A-L) obtained from Dropsens software. Using different values for Estep and Srate. Low values of Srate and Estep does not allow proper flow of current as shown in A. High values of Srate does not allow sufficient charge of the sample as shown in G to L. Equal values of Estep and Srate do not give correct shape for cyclic voltammetry graph as shown in D and E (Continued).



K: E-Step: 0.01 - Srate: 1

Figure 14: I-V curves (A-L) obtained from Dropsens software. Using different values for Estep and Srate. Low values of Srate and Estep does not allow proper flow of current as shown in A. High values of Srate does not allow sufficient charge of the sample as shown in G to L. Equal values of Estep and Srate do not give correct shape for cyclic voltammetry graph as shown in D and E (Continued).



L: E-Step: 0.002 - Srate: 0.004

Figure 14: I-V curves (A-L) obtained from Dropsens software. Using different values for Estep and Srate. Low values of Srate and Estep does not allow proper flow of current as shown in A. High values of Srate does not allow sufficient charge of the sample as shown in G to L. Equal values of Estep and Srate do not give correct shape for cyclic voltammetry graph as shown in D and E (Continued).

Figure 14 displays the I-V curves obtained from changing Estep and Srate in parallel. High values of Srate does not allow the sample to be sufficiently charged and this fact does not change when changing the Estep. This is presented in Figures 14 (G to L). When equating the values of Estep and Srate, the graphs lack any data and fail to get the correct shape of the cyclic voltammetry graph, as shown in Figure 14 (D and E). Low values for Srate with low values of Estep allows no flow of current in the sample Figure 14 (A). In conclusion and from the past optimization experiments, the best values for Estep and Srate are Estep= 0.002 Srate 0.04. This allows for sufficient flow of current without damaging the cells and displays graphs that can be interpreted accurately.

B. Optimization for cable connection using the coaxial cable:

Before trying the connection with the coaxial cable, screen-printed electrodes that allows the sample measurement were used. Figure 15 displays the screen printed electrode used in this optimization experiment.

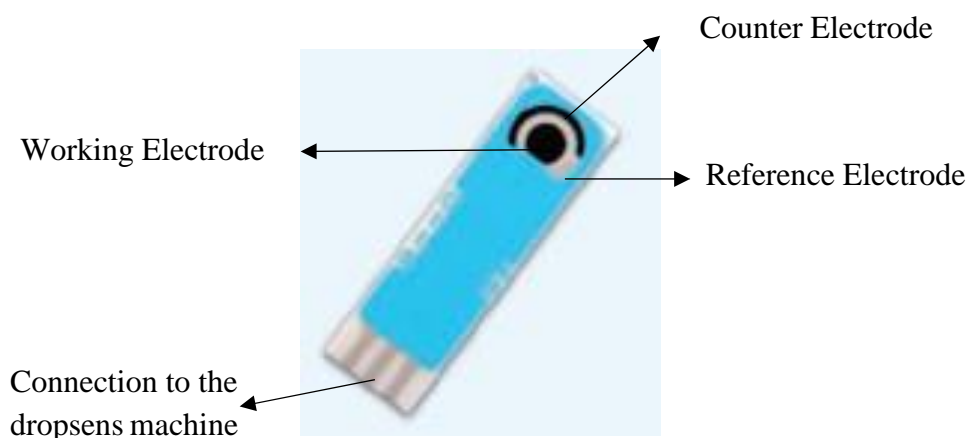


Figure 15: Screen printed electrode. The sample will be put on top of the counter electrode, working electrode and reference electrode. The electrode is connected to the machine by silver contacts.

Advantages of using these electrodes is their low cost, disposable and can give results for microvolumes. However, a disadvantage is interfering with the current flow in the sample, therefore, not all cells within the sample will be charged. Hence a coaxial cable that allows for the use of volumes up to 500 μl was used, is easy to clean between trials and most importantly ensuring that the current flow is equal in all the sample. For this experiment, the cables were connected in different ways to find the best way for connection. The system itself has a cable of five connections that are linked to a two connection cable directly connected to the PC with the software, as shown in Figure 16. Table 7 explains the functionality for each cable. Several connection were tried and the results are presented in Figure 17.

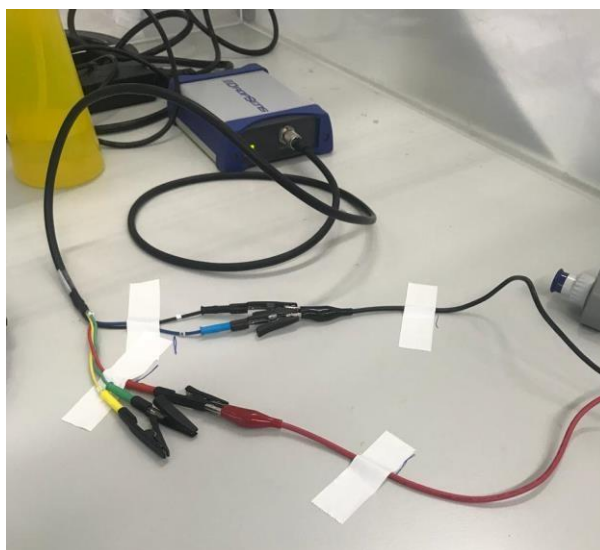
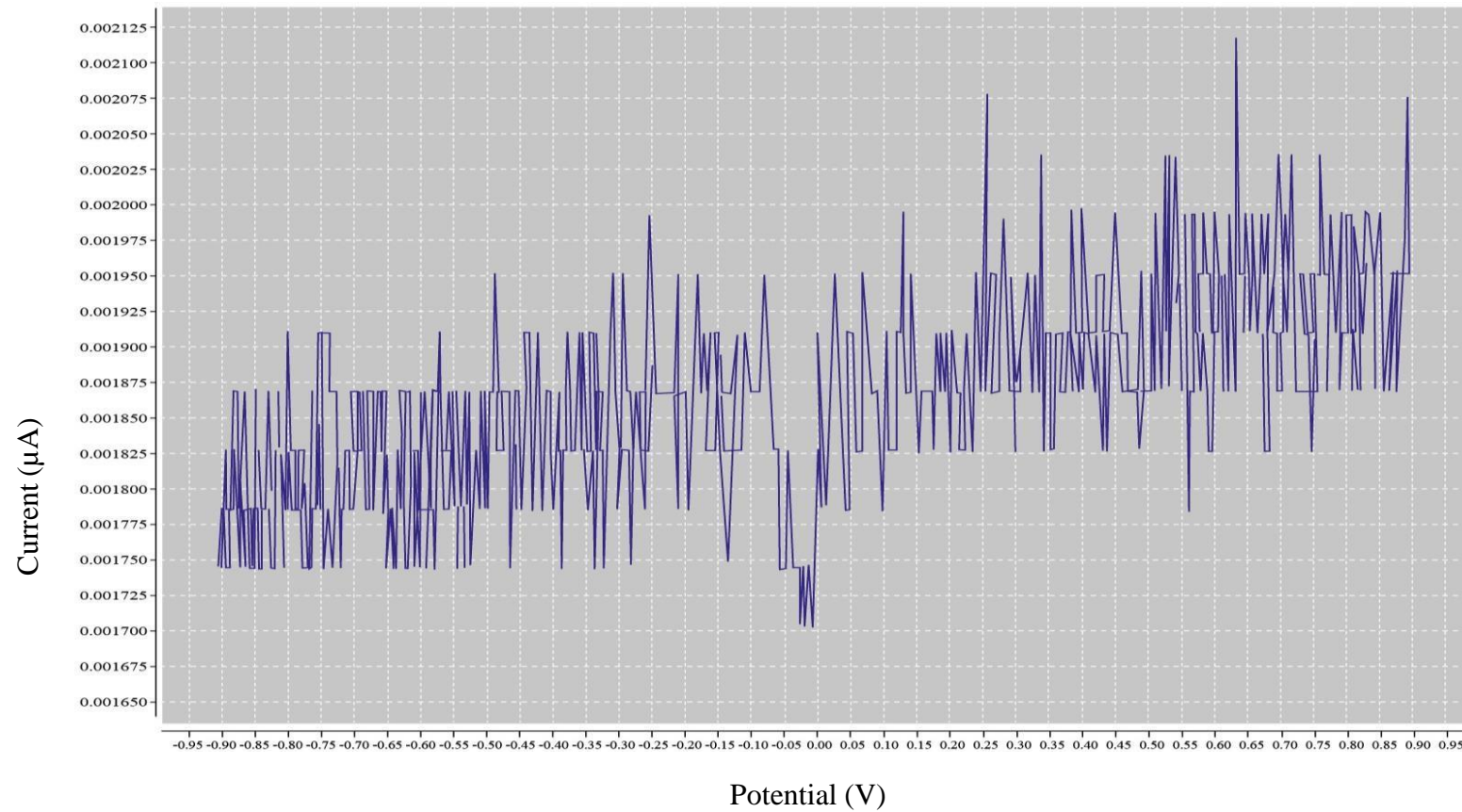


Figure 16: Connection between the system and the software. The system has 5 main colors (Black, Blue, Red, Green, Yellow that are connected to the software by two main cables Black, Red).

Table 7: Functionality for each cable.

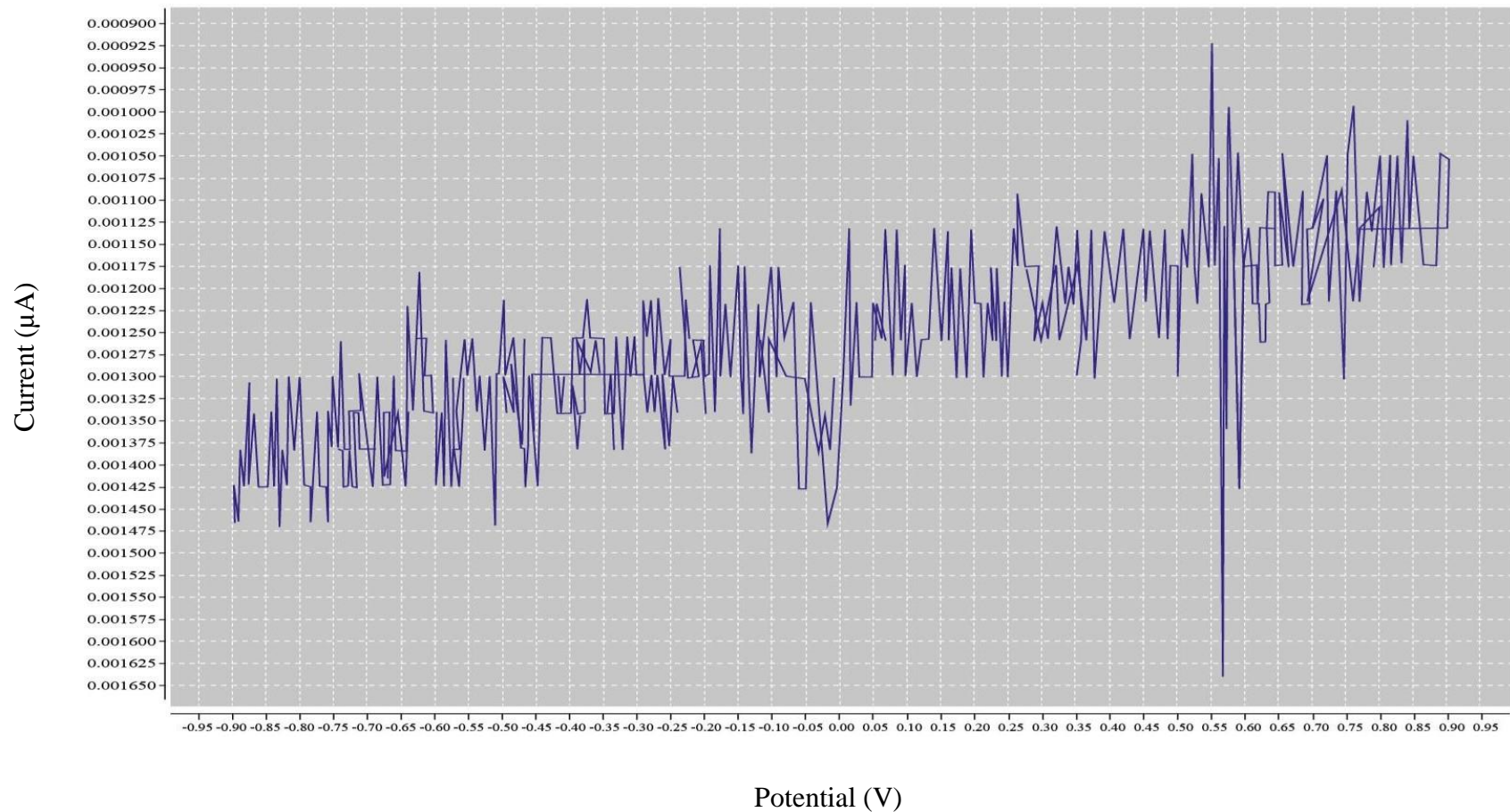
Cable Color	Function
Blue	Reference
Red	Working electrode 1
Yellow	Working electrode 2
Black	Counter electrode
Green	Ground cable

As shown in Figure 17 nothing gives the correct cyclic voltammetry graph except for Figure 17 (C), with the connection black with black and red with red. Hence this was the suitable choice of connection for the rest of the experiments.



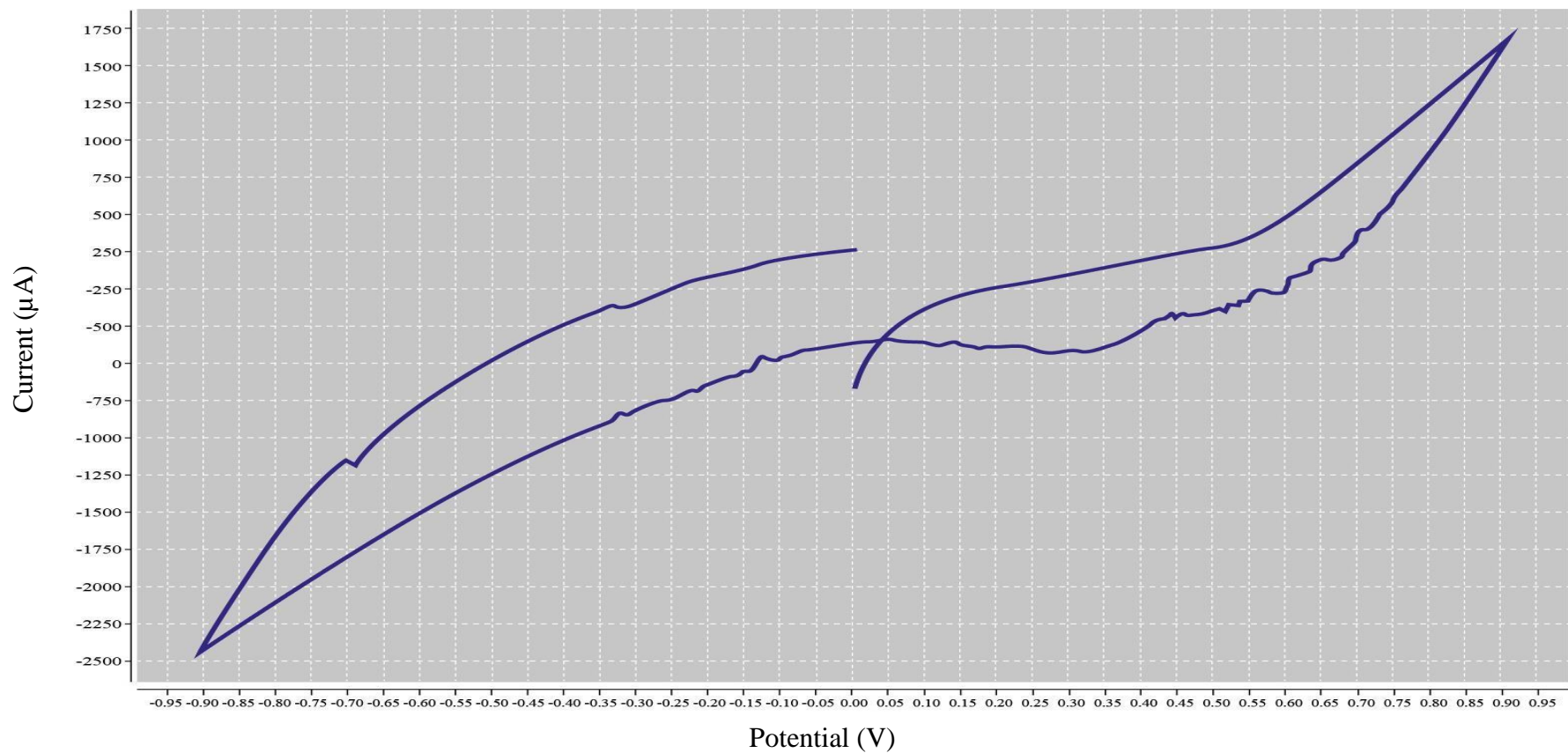
A: Black with Black, Red with Blue

Figure 17: I-V curves (A-L) obtained from the different cable connections. The only connection that shows the cyclic voltammetry curve that can be used for the electrical experiment is graph C of the connection Black with Black, Red with Red. The rest of the graphs show no useful data as they are not cyclic voltammetry graphs.



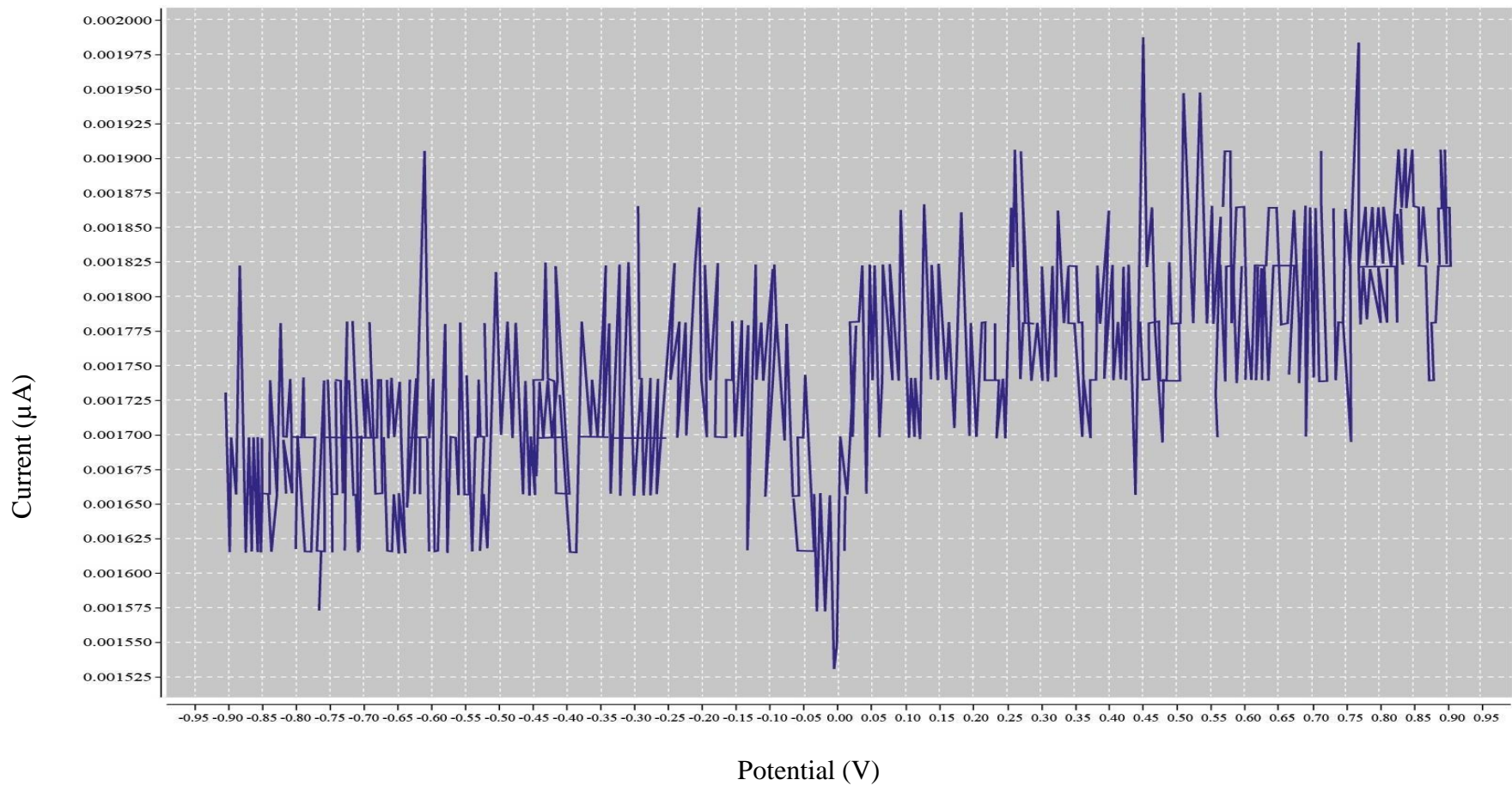
B: Blue with Black, Red with Green

Figure 17: I-V curves (A-L) obtained from the different cable connections. The only connection that shows the cyclic voltammetry curve that can be used for the electrical experiment is graph C of the connection Black with Black, Red with Red. The rest of the graphs show no useful data as they are not cyclic voltammetry graphs (Continued).



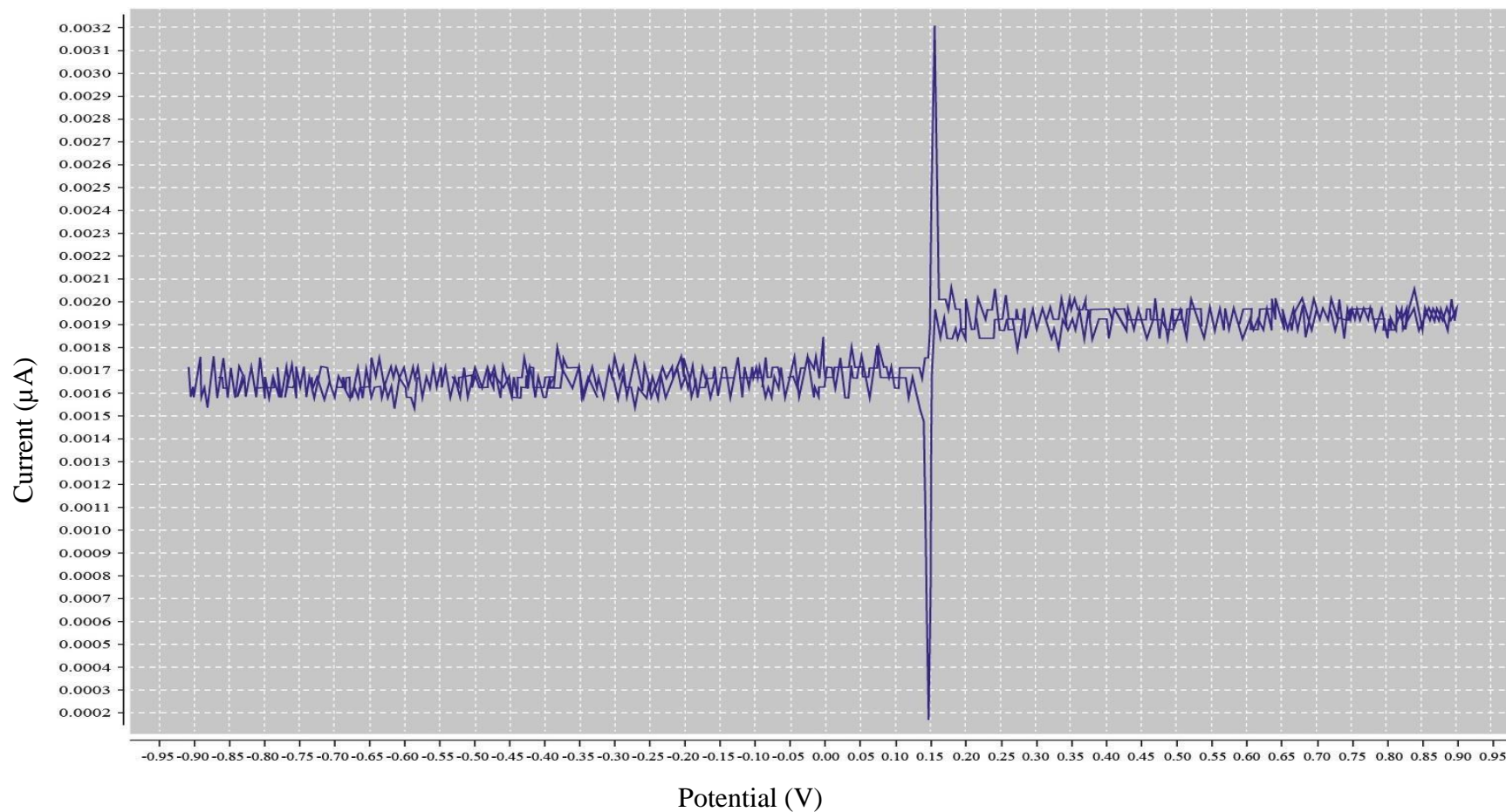
C: Black with Black, Red with Red

Figure 17: I-V curves (A-L) obtained from the different cable connections. The only connection that shows the cyclic voltammetry curve that can be used for the electrical experiment is graph C of the connection Black with Black, Red with Red. The rest of the graphs show no useful data as they are not cyclic voltammetry graphs (Continued).



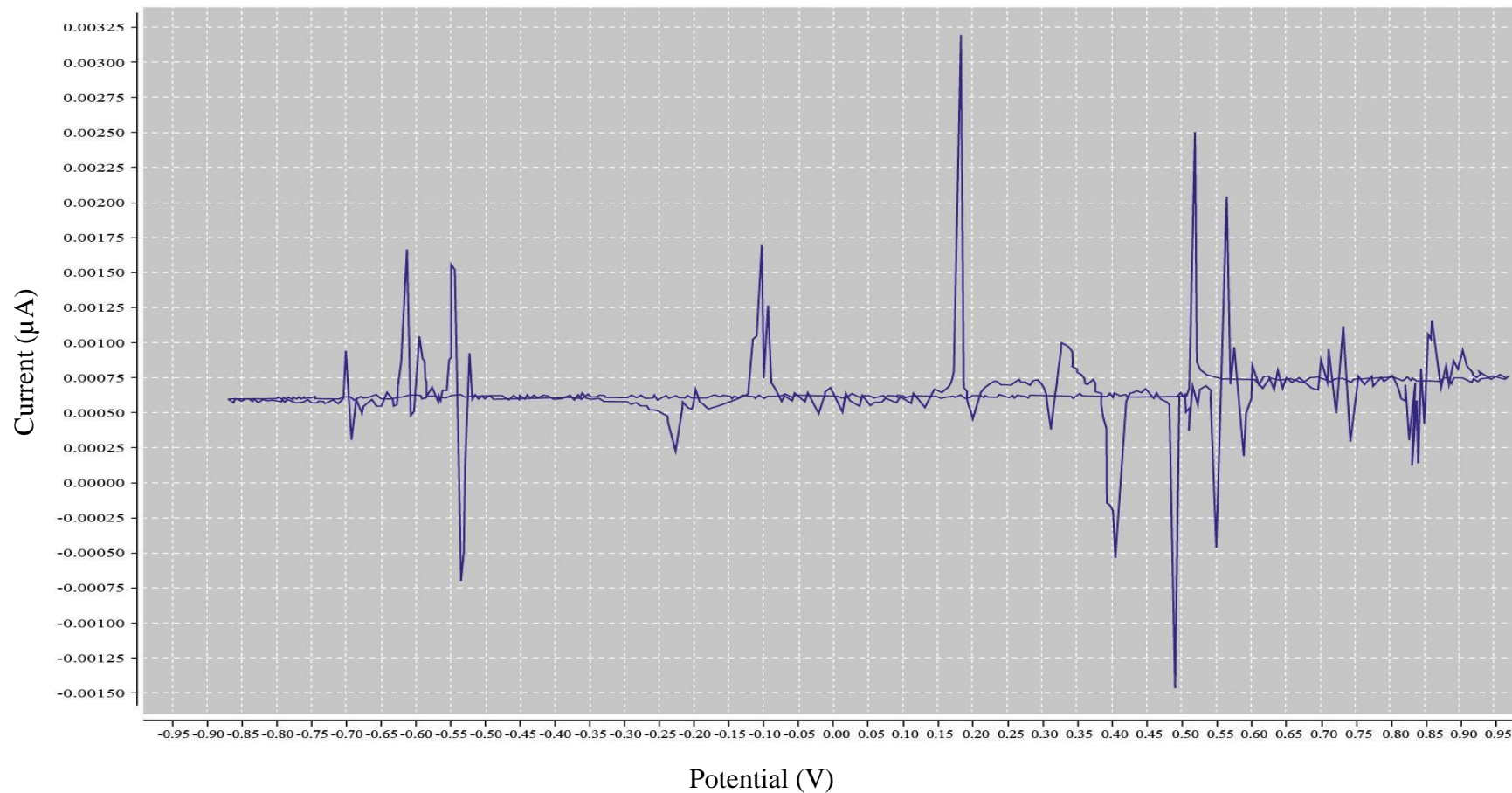
D: Black with Black, Red with Black

Figure 17: I-V curves (A-L) obtained from the different cable connections. The only connection that shows the cyclic voltammetry curve that can be used for the electrical experiment is graph C of the connection Black with Black, Red with Red. The rest of the graphs show no useful data as they are not cyclic voltammetry graphs (Continued).



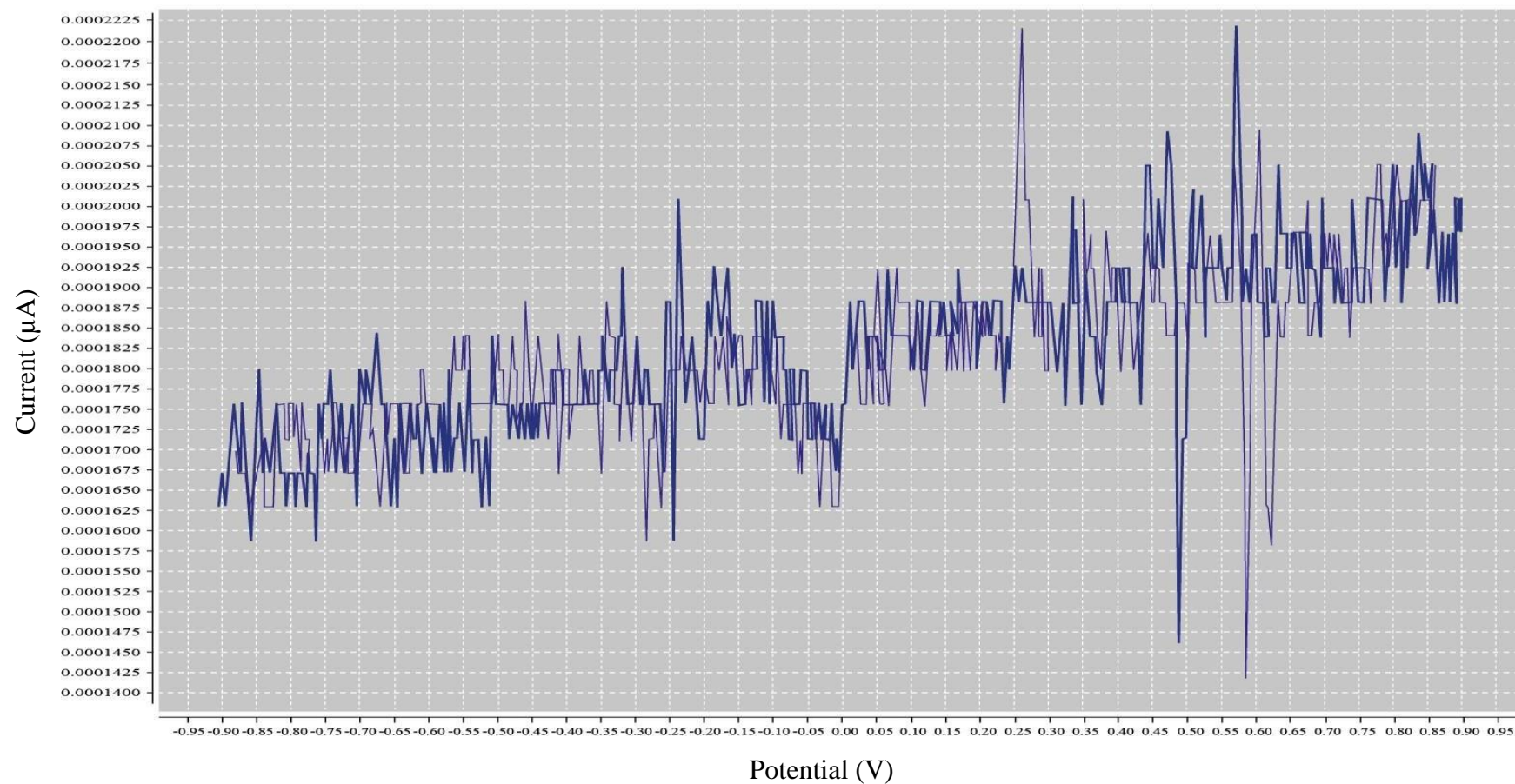
E: Black with Black, Red with Green

Figure 17: I-V curves (A-L) obtained from the different cable connections. The only connection that shows the cyclic voltammetry curve that can be used for the electrical experiment is graph C of the connection Black with Black, Red with Red. The rest of the graphs show no useful data as they are not cyclic voltammetry graphs (Continued).



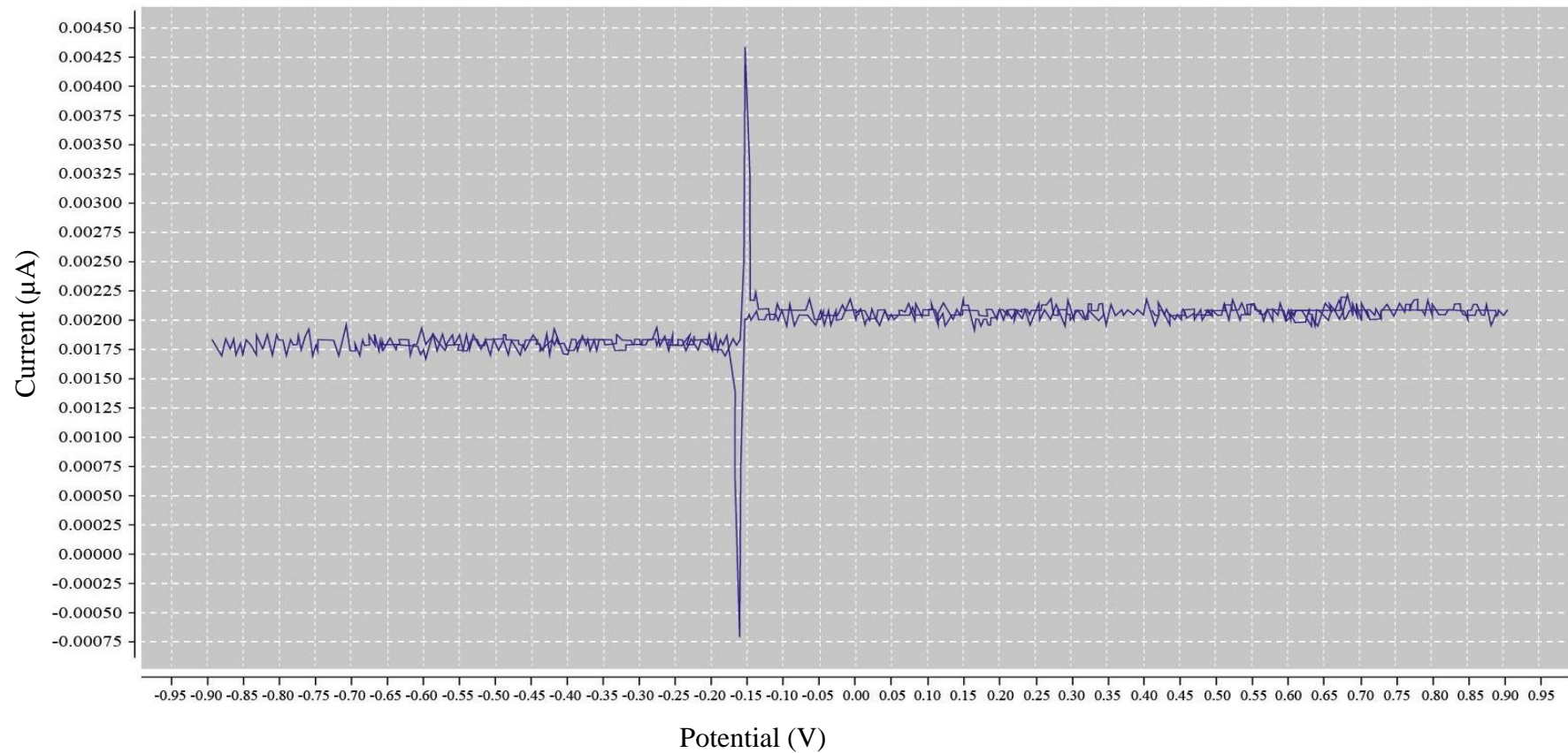
F: Black with Blue, Red with Red

Figure 17: I-V curves (A-L) obtained from the different cable connections. The only connection that shows the cyclic voltammetry curve that can be used for the electrical experiment is graph C of the connection Black with Black, Red with Red. The rest of the graphs show no useful data as they are not cyclic voltammetry graphs (Continued).



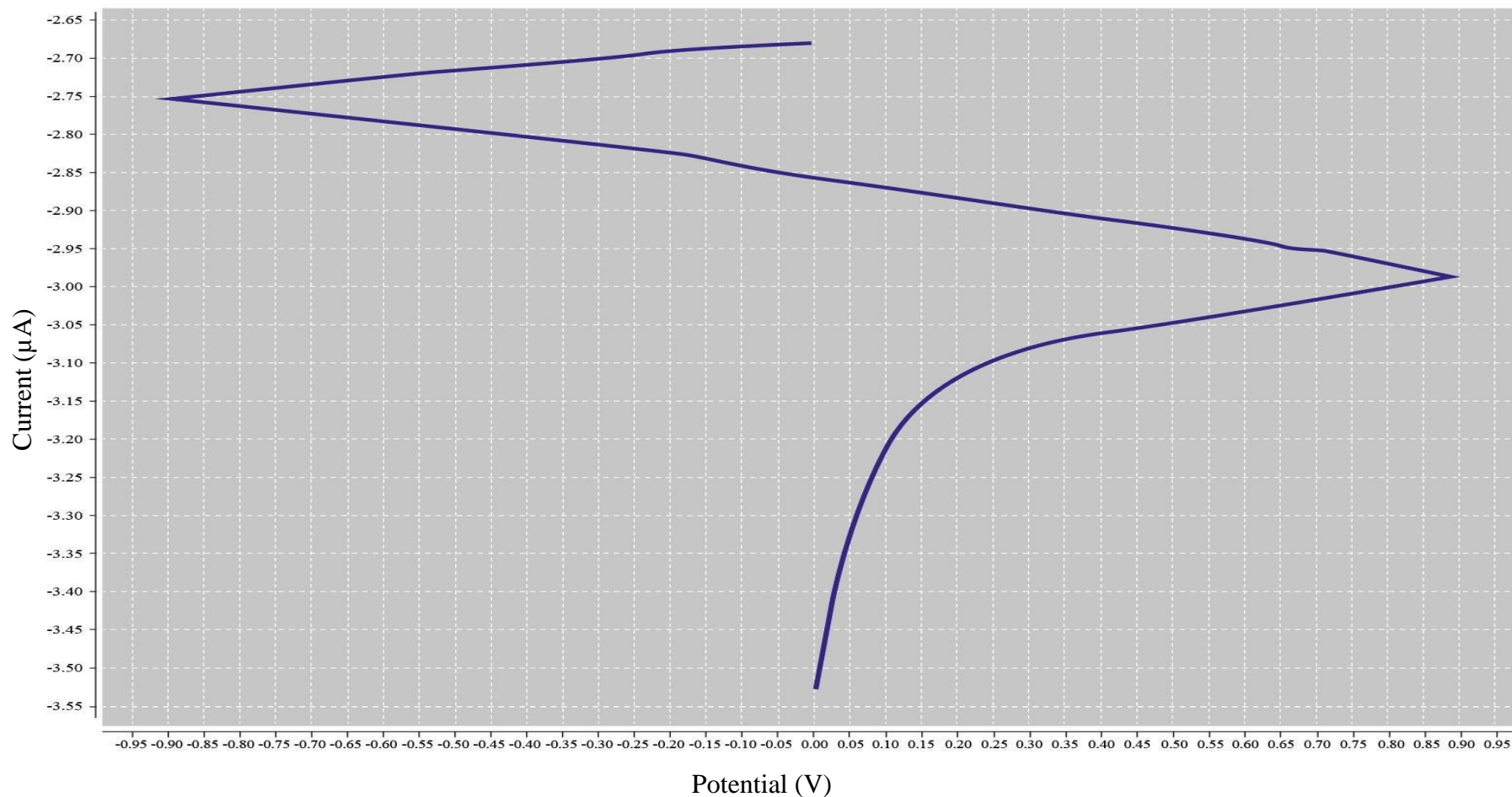
G: Black with Green, Red with Black

Figure 17: I-V curves (A-L) obtained from the different cable connections. The only connection that shows the cyclic voltammetry curve that can be used for the electrical experiment is graph C of the connection Black with Black, Red with Red. The rest of the graphs show no useful data as they are not cyclic voltammetry graphs (Continued).



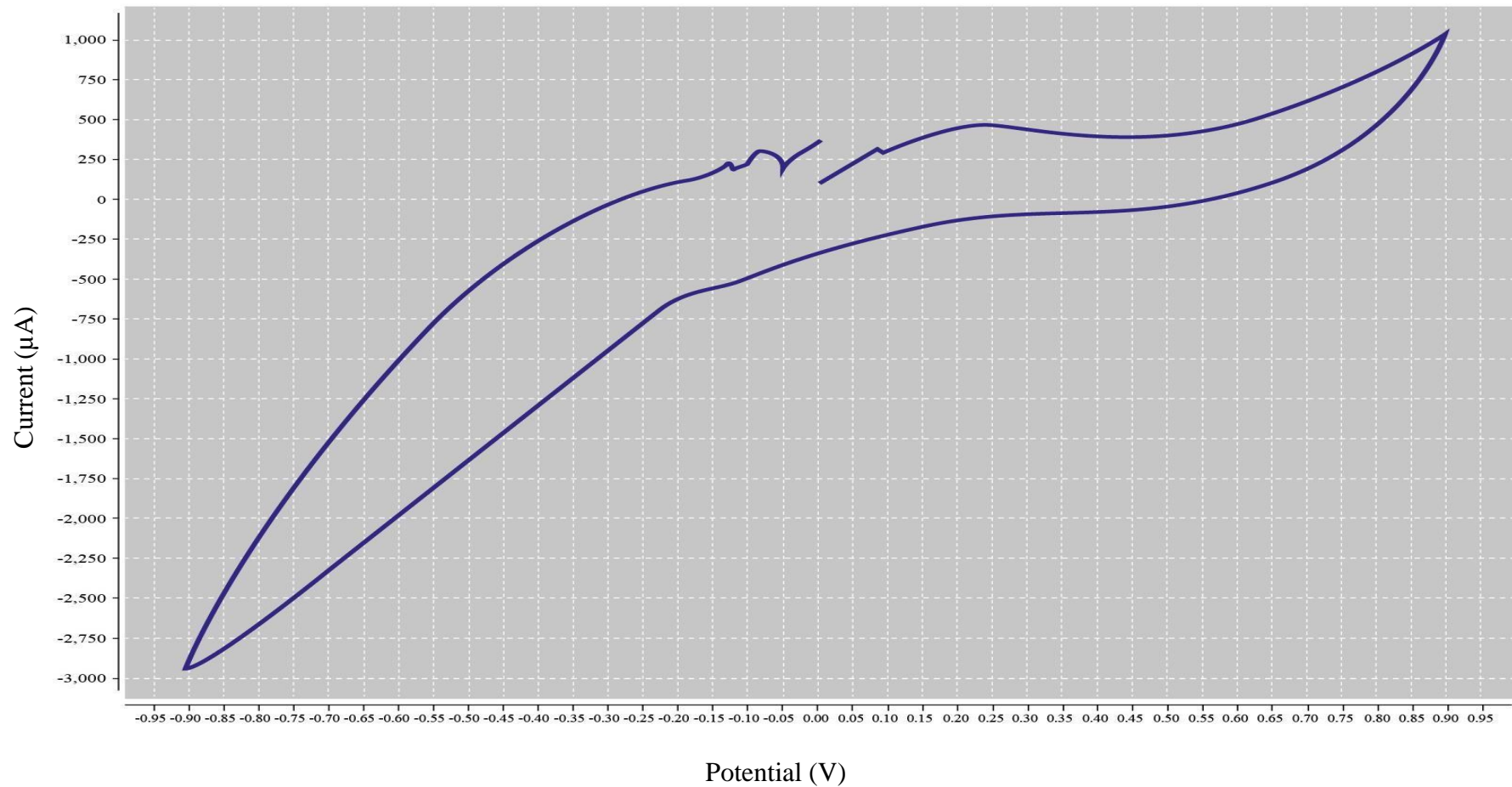
H: Black with Green, Red with Blue

Figure 17: I-V curves (A-L) obtained from the different cable connections. The only connection that shows the cyclic voltammetry curve that can be used for the electrical experiment is graph C of the connection Black with Black, Red with Red. The rest of the graphs show no useful data as they are not cyclic voltammetry graphs (Continued).



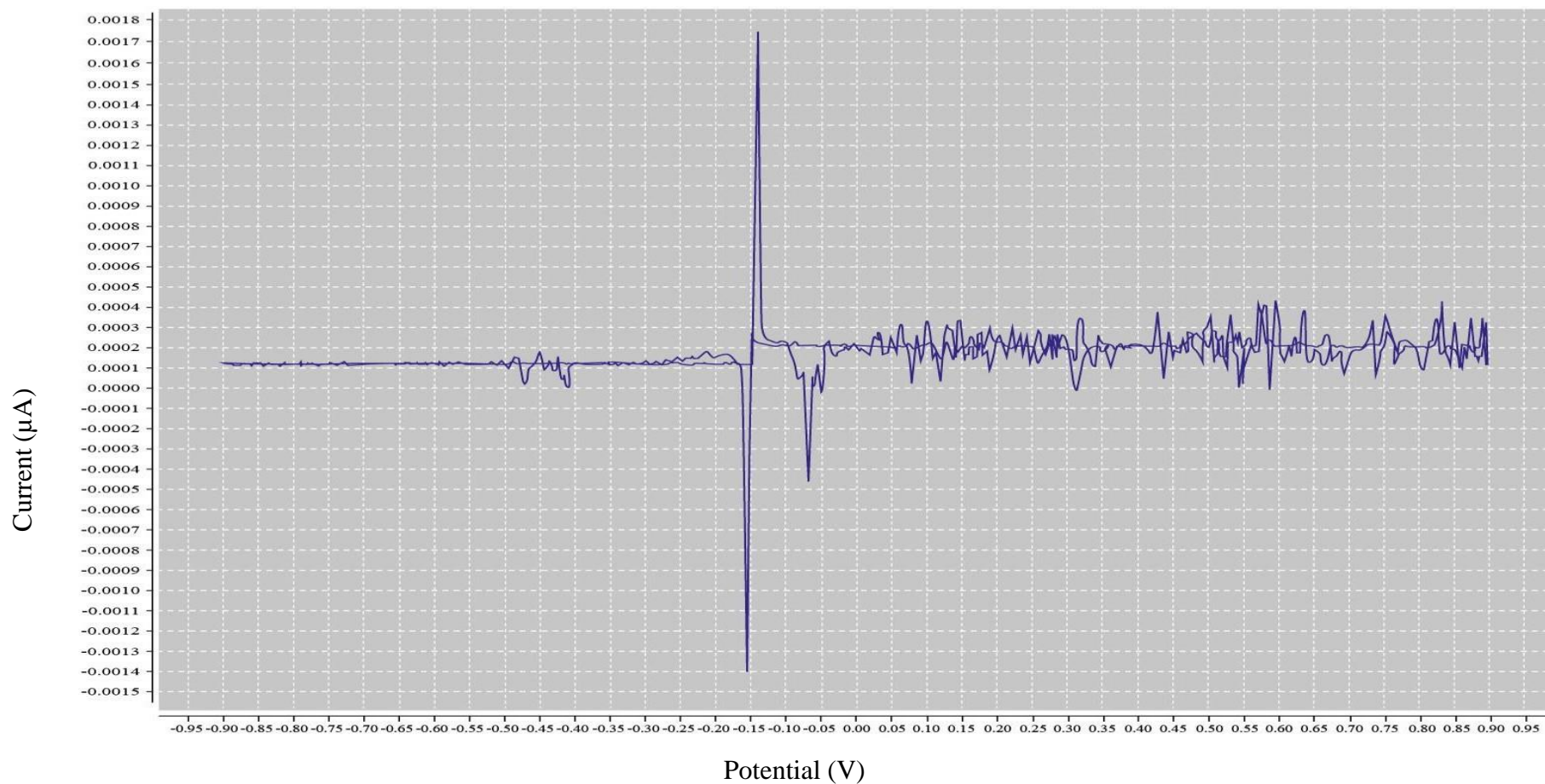
I: Black with Green, Red with Red

Figure 17: I-V curves (A-L) obtained from the different cable connections. The only connection that shows the cyclic voltammety curve that can be used for the electrical experiment is graph C of the connection Black with Black, Red with Red. The rest of the graphs show no useful data as they are not cyclic voltammety graphs (Continued).



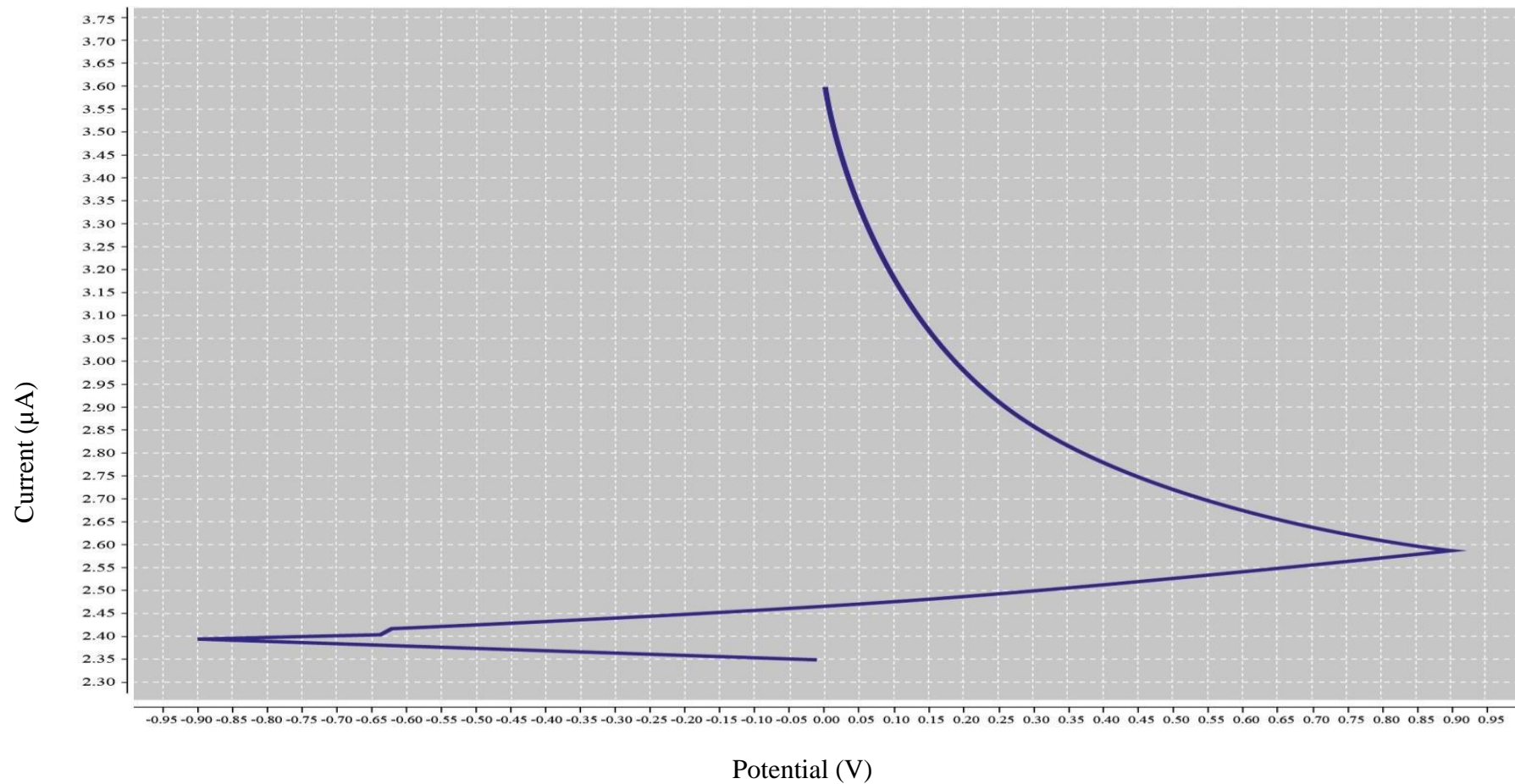
J: Black with Black, Red with Black

Figure 17: I-V curves (A-L) obtained from the different cable connections. The only connection that shows the cyclic voltammetry curve that can be used for the electrical experiment is graph C of the connection Black with Black, Red with Red. The rest of the graphs show no useful data as they are not cyclic voltammetry graphs (Continued).



K: Black with Red, Red with Blue

Figure 17: I-V curves (A-L) obtained from the different cable connections. The only connection that shows the cyclic voltammetry curve that can be used for the electrical experiment is graph C of the connection Black with Black, Red with Red. The rest of the graphs show no useful data as they are not cyclic voltammetry graphs (Continued).



L: Black with Red, Red with Green

Figure 17: I-V curves (A-L) obtained from the different cable connections. The only connection that shows the cyclic voltammetry curve that can be used for the electrical experiment is graph C of the connection Black with Black, Red with Red. The rest of the graphs show no useful data as they are not cyclic voltammetry graphs (Continued).

3.4.2 Electrochemical Experiment

After finalizing the optimization experiments, electrochemical experiments were done to measure the capacitance for each cell, using the configuration that was optimized before. A coaxial cable was used with Estep 0.002 and Srate 0.04. Figure 18 shows the I-V curves for the three immune cells. This was done on different cell concentrations; however, the results show no significant difference within the three types. Hence, extracting the capacitance as an identification tool was done for the three types of cells. Using the matlab code explained in the methods section, to get the capacitance Ohm's law was used. Figure 19 shows the capacitance vs time for the three types of cells. It was clear that with the different concentrations the values overlap and that DCs and Macrophages lack a consistent trend; this is probably due to the lack of a homogenous suspension as cells might not have fully differentiated. To get a better picture of the capacitance data, the value of the media was de-embedded from the other samples (10^{-10} - 10^{-2} - 10^{-3} - 10^{-5}). Figure 20 displays the data for the three immune cells after the de-embedding process, and it clearly shows that there is consistency in capacitance with the concentration. The de-embedding process involves subtracting the value of the media from all the samples, to make sure the capacitance measured is the capacitance of the cells and not the solution. The main goal of this work is to find a way to identify immune cells without the drawback of cross-referencing. Figure 21 is the conclusion of the experiments done for this thesis, it shows that the capacitance increases with the concentration for all cells. In addition to that, it shows that the highest value of capacitance is for macrophages followed by THP-1 cells and dendritic cells, this is supported by data from literature that supports the fact that the capacitance increases with area.

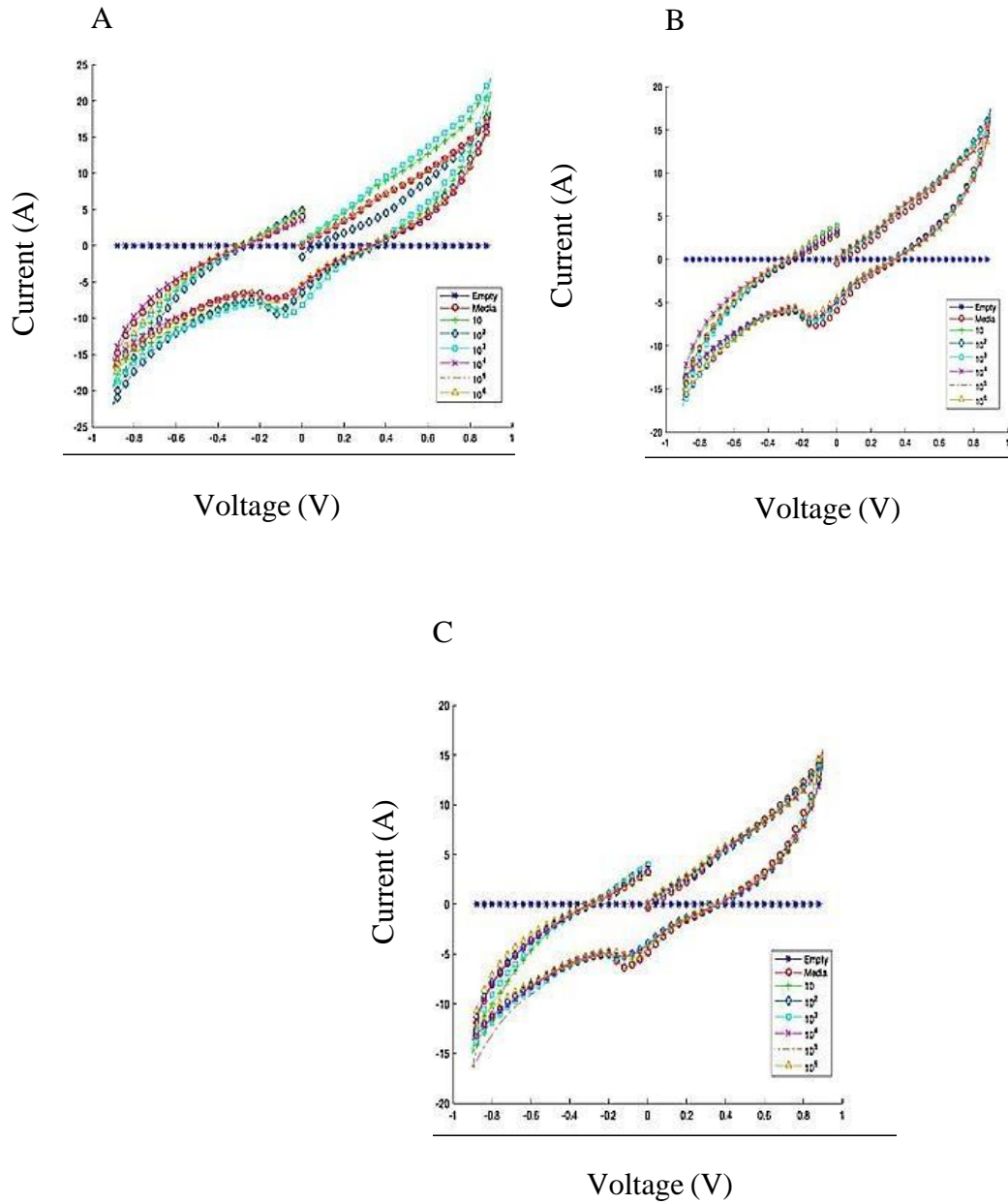


Figure 18: I-V curve for the three types of cells using drop sense technology. A: THP-1, B: Dendritic cells, C: Macrophages. There are no clear differences between the three graphs. Also, no trend is shown with the concentration in each graph.

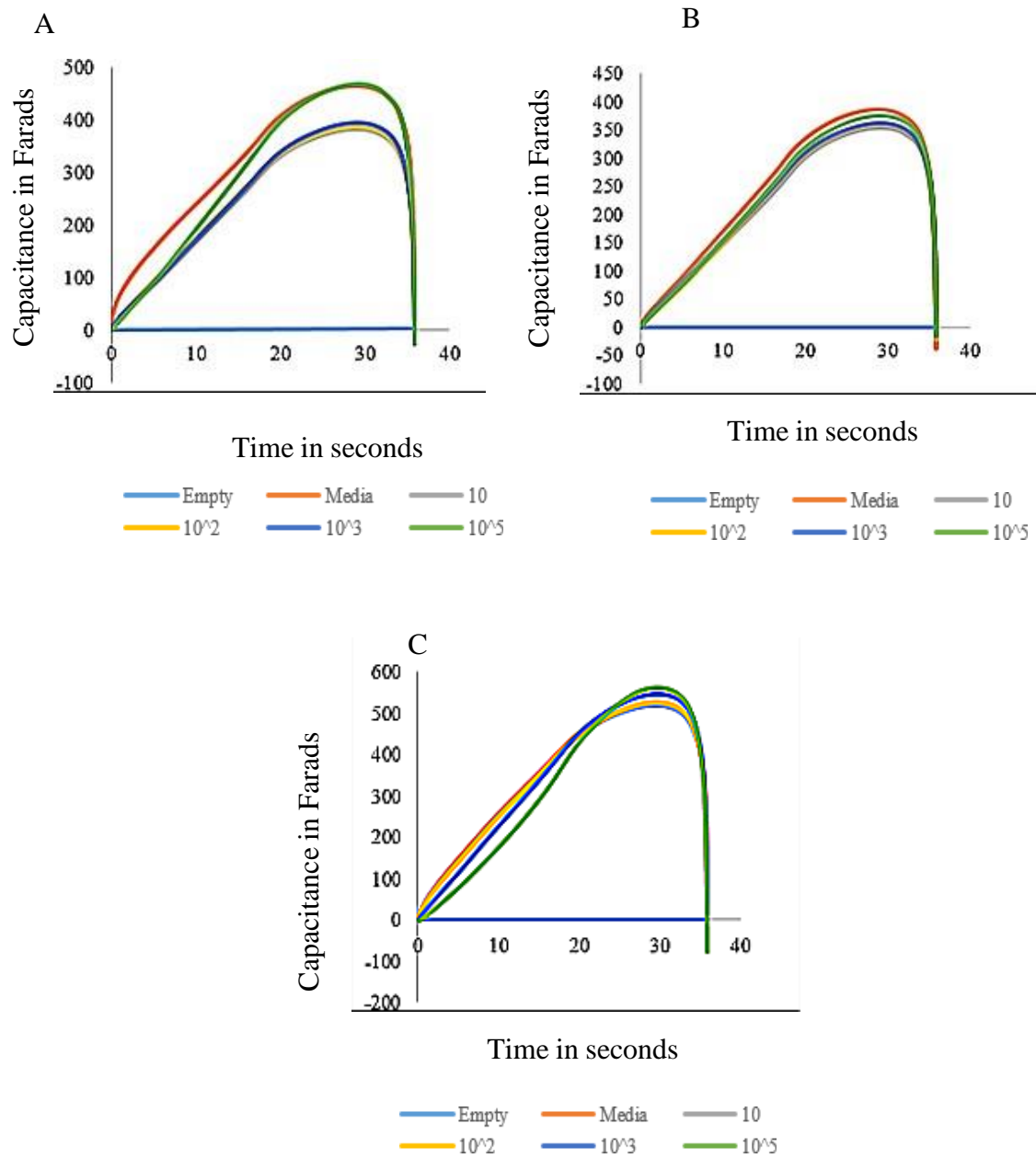


Figure 19: Capacitance-time curve for the three types of cells before media de-embedding. A: THP-1, B: Dendritic cells, C: Macrophages. There is no consistency between the concentration and capacitance.

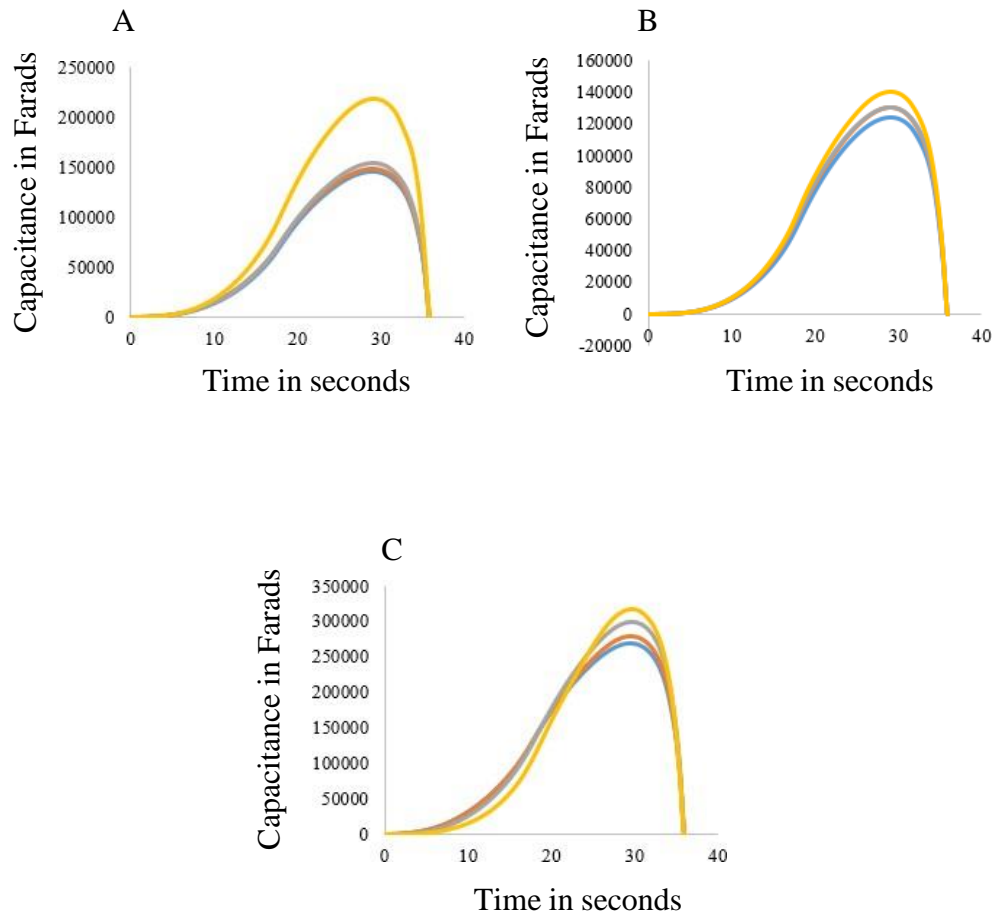


Figure 20: Capacitance-time curve for the three types of cells after media de-embedding. A: THP-1, B: Dendritic cells, C: Macrophages. The capacitance increases with the concentration for the three types of cells. Macrophages have the highest value followed by THP-1 cells then Dendritic cells.

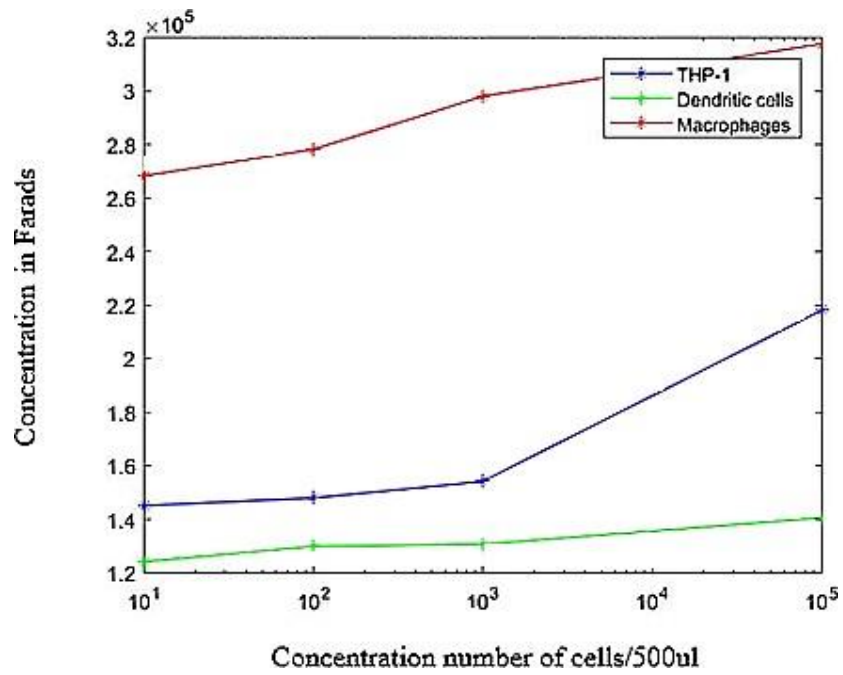


Figure 21: Capacitance vs concentration for the three types of cells. After the de-embedding process, the values of capacitance for each type of cell was extracted vs the concentration. Macrophages have the highest values and dendritic cells have the lowest values.

Chapter 4: Conclusions

A new and easy way to differentiate and characterize immune cells is suggested, tested and developed in this study. The experiments in the thesis started with differentiating THP-1 cells into DCs and macrophages using the Berges protocols. After that the process of optimizing the new system to find the correct configuration and connection for the electrical measurement started. The Dropsens technology used applies current to the sample and measures the output which is the voltage. The I-V curves for the three cells do not show any differences, hence no comparisons were done. From there the capacitance-voltage measurements to characterize the three different biological samples were used. The capacitance was then extracted using a MATLAB code after solving the non-homogeneous linear equation. This method is promising since immune cells face the problem of cross referencing when analyzed with flow cytometry and other conventional methods. The proposed method helps in accurately defining each cell type with a capacity label without the need of the long tedious preparation process. The capacitance results show that each cell has a unique value, and that the capacitance increases with the value of the area, as proven by the known equations.

Chapter 5: Challenges and Future work

Many challenges were faced while doing this work, the main issue was with the optimization of the system to find the best values that represents the data clearly. The second challenge faced during this work was with merging the biological experiments with the electrical measurements. This took extensive planning to find the best time points to do the experiments and countless repeats. The third challenge faced was with the mathematical modeling and deriving the equations that extract the correct values from the data obtained. Matlab training was needed for the coding and revision for the derivation techniques was done to reach for the final equations. The last challenge was faced, was because of university restrictions due to the pandemic caused by COVID-19, the limited lab access at the end of the journey stopped me from planning and executing more experiments.

As for future work, this field opens the door to endless experiments in the same area or in different biological areas. To characterize all the immune cells in the innate and adaptive immune system this technique can be used. Moving forward, more biological samples can be characterized using this method, such as the different types of viruses. Each virus has a different size and from there the capacitance for each virus can be measured using the same technique used in the thesis. However the optimization should be done again for it to be suitable to the biological sample used. The big goal for this new technique is to characterize a mixture biological samples accurately that further aids in modeling diseases and treating them. This requires extensive optimization experiments with the Matlab codes that can give the correct values for each biological sample.

References

- [1] J. L. Goldberg and P. M. Sondel, “Enhancing Cancer Immunotherapy Via Activation of Innate Immunity Introduction/Background: Rationale for targeting innate immunity for,” *Semin. Oncol.*, vol. 42, no. 4, pp. 562–572, 2015, doi: 10.1053/j.seminoncol.2015.05.012.Enhancing.
- [2] O. Donini, “Innate immunity as an alternative immunotherapy approach.” <https://www.nature.com/articles/d42473-018-00172-3> (accessed Jan. 28, 2021).
- [3] O. Donini, R. Straube, and C. Schaber, “Targeting innate immunity to treat disease: potential therapeutic applications,” vol. 4, no. 4, pp. 42–44, 2018, Accessed: Jan. 28, 2021. [Online]. Available: <https://www.drugtargetreview.com/article/37410/targeting-innate-immunity/>.
- [4] B. Alberts, A. Johnson, J. Lewis, M. Raff, K. Roberts, and P. Walter, “Innate Immunity,” *The cell*, vol 91, pp. 401–405, 2002, Accessed: Jan. 28, 2021. [Online]. Available: <https://www.ncbi.nlm.nih.gov/books/NBK26846/>.
- [5] D. A. Hume, “Macrophages as APC and the Dendritic Cell Myth,” *J. Immunol.*, vol. 181, no. 9, pp. 5829–5835, Nov. 2008, doi: 10.4049/jimmunol.181.9.5829.
- [6] D. Ferenbach and J. Hughes, “Macrophages and dendritic cells: what is the difference?,” *Kidney Int.*, vol. 74, pp. 5–7, 2008, doi: 10.1038/ki.2008.189.
- [7] T. Mahmood and P. C. Yang, “Western blot: Technique, theory, and trouble shooting,” *N. Am. J. Med. Sci.*, vol. 4, no. 9, pp. 429–434, Sep. 2012, doi: 10.4103/1947-2714.100998.
- [8] G. Cordier, “Flow cytometry for immunology,” *Biol. Cell*, vol. 58, no. 2, pp. 147–150, Jan. 1986, doi: 10.1111/j.1768-322X.1986.tb00499.x.
- [9] D. M. Haines and K. H. West, “Immunohistochemistry: Forging the links between immunology and pathology,” in *Veterinary Immunology and Immunopathology*, vol. 108, no. 1-2 SPEC. ISS., pp. 151–156, Oct. 2005, doi: 10.1016/j.vetimm.2005.08.007.
- [10] A. M. Lew, R. B. Brandon, M. Panaccio, and C. J. Morrow, “The polymerase chain reaction and other amplification techniques in immunological research and diagnosis,” *Immunology*, vol.75, no1, pp. 3-9, Jan. 1992.
- [11] Healio, “The Innate vs. Adaptive Immune Response.” <https://www.healio.com/hematology-oncology/learn-immuno-oncology/the-immune-system/the-innate-vs-adaptive-immune-response> (accessed Jan. 28, 2021).

- [12] T. Kambayashi and T. M. Laufer, "Atypical MHC class II-expressing antigen-presenting cells: Can anything replace a dendritic cell?," *Nature Reviews Immunology*, vol. 14, no. 11. Nature Publishing Group, pp. 719–730, Jan. 01, 2014, doi: 10.1038/nri3754.
- [13] I. I. Witzel *et al.*, "Deconstructing Immune Microenvironments of Lymphoid Tissues for Reverse Engineering," *Adv. Healthc. Mater.*, vol. 8, no. 4, pp. 1–22, 2019, doi: 10.1002/adhm.201801126.
- [14] C. Gelmetti, "Il Giornale Italiano di Dermatologia e Venereologia," in *Storia Della Dermatologia e Della Venereologia in Italia*, C. Gelmetti, Ed. Milano: Springer Milan, 2015, pp. 181-192.
- [15] A. Matejuk, "Skin Immunity," *Archivum Immunologiae et Therapiae Experimentalis*, vol. 66, no. 1. Birkhauser Verlag AG, pp. 45–54, Feb. 01, 2018, doi: 10.1007/s00005-017-0477-3.
- [16] T. Nochi and H. Kiyono, "Innate Immunity in the Mucosal Immune System," *Curr. Pharm. Des.*, vol. 12, no. 32, pp. 4203–4213, Oct. 2006, doi: 10.2174/138161206778743457.
- [17] P. Aich and Dwivedy, "Importance of innate mucosal immunity and the promises it holds," *Int. J. Gen. Med.*, p. 299, Apr. 2011, doi: 10.2147/ijgm.s17525.
- [18] Nature, "The different types of cell junctions | Learn Science at Scitable." <https://www.nature.com/scitable/content/the-different-types-of-cell-junctions-14714296/> (accessed Jan. 28, 2021).
- [19] "The innate and adaptive immune systems," Jul. 2020, Accessed: Jan. 28, 2021. [Online]. Available: <https://www.ncbi.nlm.nih.gov/books/NBK279396/>.
- [20] "Defenses Against Infection - Infections," *MSD Manual Consumer Version*. <https://www.msmanuals.com/home/infections/biology-of-infectious-disease/defenses-against-infection> (accessed Feb. 23, 2021).
- [21] Bio.libretexts, "13.1: First Line defense- Physical, Mechanical and Chemical Defenses - Biology LibreTexts." [https://bio.libretexts.org/Courses/Manchester_Community_College_\(MCC\)/Remix_of_Openstax%3AMicrobiology_by_Parker%2C_Schneegurt%2C_et_al/13%3A_Innate_Nonspecific_Host_Defenses/13.01%3A_1st_Line_defense_Physical_and_Chemical_Defenses](https://bio.libretexts.org/Courses/Manchester_Community_College_(MCC)/Remix_of_Openstax%3AMicrobiology_by_Parker%2C_Schneegurt%2C_et_al/13%3A_Innate_Nonspecific_Host_Defenses/13.01%3A_1st_Line_defense_Physical_and_Chemical_Defenses) (accessed Jan. 30, 2021).
- [22] Y. Belkaid and T. W. Hand, "Role of the microbiota in immunity and inflammation," *Cell*, vol. 157, no. 1. Cell Press, pp. 121–141, Mar. 27, 2014, doi: 10.1016/j.cell.2014.03.011.
- [23] K. L. Alexander, S. R. Targan, and C. O. Elson, "Microbiota activation and regulation of innate and adaptive immunity," *Immunological Reviews*, vol. 260, no. 1. Blackwell Publishing Ltd, pp. 206–220, Jul. 2014, doi: 10.1111/imr.12180.

- [24] J. Charles A Janeway, P. Travers, M. Walport, and M. J. Shlomchik, "The major histocompatibility complex and its functions," 2001, Accessed: Jan. 28, 2021. [Online]. Available: <https://www.ncbi.nlm.nih.gov/books/NBK27156/>.
- [25] P.Hamrah, R.Dana, "Antigen Presenting Cell - an overview | ScienceDirect Topics." <https://www.sciencedirect.com/topics/medicine-and-dentistry/antigen-presenting-cell> (accessed Jan. 28, 2021).
- [26] J. M. M. den Haan, R. Arens, and M. C. van Zelm, "The activation of the adaptive immune system: Cross-talk between antigen-presenting cells, T cells and B cells," *Immunology Letters*, vol. 162, no. 2. Elsevier, pp. 103–112, Dec. 01, 2014, doi: 10.1016/j.imlet.2014.10.011.
- [27] G. J. Clark *et al.*, "The role of dendritic cells in the innate immune system," *Microbes and Infection*, vol. 2, no. 3. Elsevier Masson SAS, pp. 257–272, 2000, doi: 10.1016/S1286-4579(00)00302-6.
- [28] M. Guilliams *et al.*, "Dendritic cells, monocytes and macrophages: A unified nomenclature based on ontogeny," *Nature Reviews Immunology*, vol. 14, no. 8. Nature Publishing Group, pp. 571–578, Aug. 18, 2014, doi: 10.1038/nri3712.
- [29] A. G. Jegalian, F. Facchetti, and E. S. Jaffe, "Plasmacytoid dendritic cells physiologic roles and pathologic states," *Advances in Anatomic Pathology*, vol. 16, no. 6. pp. 392–404, Nov. 2009, doi: 10.1097/PAP.0b013e3181bb6bc2.
- [30] khanacademy, "Innate immunity (article) | Immune system | Khan Academy." <https://www.khanacademy.org/test-prep/mcat/organ-systems/the-immune-system/a/innate-immunity> (accessed Jan. 28, 2021).
- [31] H. L. Twigg, "Macrophages in Innate and Acquired Immunity," *Seminars in Respiratory and Critical Care Medicine*, vol. 25, no. 1. pp. 21–31, Feb. 2004, doi: 10.1055/s-2004-822302.
- [32] P. J. Murray and T. A. Wynn, "Protective and pathogenic functions of macrophage subsets," *Nature Reviews Immunology*, vol. 11, no. 11. pp. 723–737, Nov. 14, 2011, doi: 10.1038/nri3073.
- [33] N. Oppenheimer-Marks and P.Lipsky, "Leukocyte Extravasation - an overview | ScienceDirect Topics." <https://www.sciencedirect.com/topics/medicine-and-dentistry/leukocyte-extravasation> (accessed Jan. 28, 2021).
- [34] C. L. Sokol and A. D. Luster, "The chemokine system in innate immunity," *Cold Spring Harb. Perspect. Biol.*, vol. 7, no. 5, pp. 1–20, 2015, doi: 10.1101/cshperspect.a016303.
- [35] S. Greenberg and S. Grinstein, "Phagocytosis and innate immunity," *Current Opinion in Immunology*, vol. 14, no. 1. Elsevier Ltd, pp. 136–145, Feb. 01, 2002, doi: 10.1016/S0952-7915(01)00309-0.

- [36] K. Palucka and J. Banchereau, "Dendritic cells: A link between innate and adaptive immunity," *J. Clin. Immunol.*, vol. 19, no. 1, pp. 12–25, 1999, doi: 10.1023/A:1020558317162.
- [37] C. Rachna, "Difference Between T Cells and B Cells (with Comparison Chart and Similarities) - Bio Differences." <https://biodifferences.com/difference-between-t-cells-and-b-cells.html> (accessed Jan. 28, 2021).
- [38] M. I. Vazquez, J. Catalan-Dibene, and A. Zlotnik, "B cells responses and cytokine production are regulated by their immune microenvironment," *Cytokine*, vol. 74, no. 2. Academic Press, pp. 318–326, Dec. 03, 2015, doi: 10.1016/j.cyto.2015.02.007.
- [39] V. Golubovskaya and L. Wu, "Different subsets of T cells, memory, effector functions, and CAR-T immunotherapy," *Cancers*, vol. 8, no. 3. MDPI AG, Mar. 15, 2016, doi: 10.3390/cancers8030036.
- [40] H. Ryoung Jang and H. Rabb, "T Cell Subset - an overview | ScienceDirect Topics." <https://www.sciencedirect.com/topics/medicine-and-dentistry/t-cell-subset> (accessed Jan. 30, 2021).
- [41] V. Golubovskaya and L. Wu, "Different subsets of T cells, memory, effector functions, and CAR-T immunotherapy," *Cancers*, vol. 8, no. 3. MDPI AG, p. 36, Mar. 15, 2016, doi: 10.3390/cancers8030036.
- [42] R. A. Seder and R. Ahmed, "Similarities and differences in CD4+ and CD8+ effector and memory T cell generation," *Nature Immunology*, vol. 4, no. 9. pp. 835–842, Sep. 01, 2003, doi: 10.1038/ni969.
- [43] N. Zhang and M. J. Bevan, "CD8+ T Cells: Foot Soldiers of the Immune System," *Immunity*, vol. 35, no. 2. pp. 161–168, Aug. 26, 2011, doi: 10.1016/j.immuni.2011.07.010.
- [44] L. L. Ye, X. S. Wei, M. Zhang, Y. R. Niu, and Q. Zhou, "The significance of tumor necrosis factor receptor type II in CD8+ regulatory T cells and CD8+ effector T cells," *Frontiers in Immunology*, vol. 8, no. MAR. Frontiers Media S.A., Mar. 22, 2018, doi: 10.3389/fimmu.2018.00583.
- [45] B. Shrestha and M. S. Diamond, "Fas Ligand Interactions Contribute to CD8+ T-Cell-Mediated Control of West Nile Virus Infection in the Central Nervous System," *J. Virol.*, vol. 81, no. 21, pp. 11749–11757, Nov. 2007, doi: 10.1128/jvi.01136-07.
- [46] B. Tunland, "Memory T Cell - an overview | ScienceDirect Topics." <https://www.sciencedirect.com/topics/medicine-and-dentistry/memory-t-cell> (accessed Jan. 28, 2021).
- [47] S. C. Jameson and D. Masopust, "Understanding Subset Diversity in T Cell Memory," *Immunity*, vol. 48, no. 2. Cell Press, pp. 214–226, Feb. 20, 2018, doi: 10.1016/j.immuni.2018.02.010.

- [48] J. Charles A Janeway, P. Travers, M. Walport, and M. J. Shlomchik, "The Humoral Immune Response," 2001, Accessed: Jan. 28, 2021. [Online]. Available: <https://www.ncbi.nlm.nih.gov/books/NBK10752/>.
- [49] Sciencedirect.com, "Thymus Independent Antigen - an overview | ScienceDirect Topics." <https://www.sciencedirect.com/topics/medicine-and-dentistry/thymus-independent-antigen> (accessed Jan. 28, 2021).
- [50] Livescience, "Lymphatic System: Facts, Functions & Diseases | Live Science." <https://www.livescience.com/26983-lymphatic-system.html> (accessed Jan. 28, 2021).
- [51] P. Thapa and D. L. Farber, "The Role of the Thymus in the Immune Response," *Thoracic surgery clinics*, vol. 29, no. 2. NLM (Medline), pp. 123–131, May 01, 2019, doi: 10.1016/j.thorsurg.2018.12.001.
- [52] B. F. Haynes and L. P. Hale, "The human thymus. A chimeric organ comprised of central and peripheral lymphoid components," *Immunologic Research*, vol. 18, no. 2. Humana Press, pp. 61–78, Oct. 1998, doi: 10.1007/BF02788750.
- [53] Z. Hu, J. N. Lancaster, and L. I. R. Ehrlich, "The contribution of chemokines and migration to the induction of central tolerance in the thymus," *Frontiers in Immunology*, vol. 6, no. JUL. Frontiers Research Foundation, Aug. 07, 2015, doi: 10.3389/fimmu.2015.00398.
- [54] D. Shah, "T-cell development in thymus | British Society for Immunology." <https://www.immunology.org/public-information/bitesized-immunology/immune-development/t-cell-development-in-thymus> (accessed Jan. 30, 2021).
- [55] T. K. Starr, S. C. Jameson, and K. A. Hogquist, "Positive and negative selection of T cells," *Annual Review of Immunology*, vol. 21, no. 1. pp. 139–176, Apr. 2003, doi: 10.1146/annurev.immunol.21.120601.141107.
- [56] A. D. Griesemer, E. C. Sorenson, and M. A. Hardy, "The role of the thymus in tolerance," *Transplantation*, vol. 90, no. 5. pp. 465–474, Sep. 15, 2010, doi: 10.1097/TP.0b013e3181e7e54f.
- [57] S. M. Lewis, A. Williams, and S. C. Eisenbarth, "Structure and function of the immune system in the spleen," *Science Immunology*, vol. 4, no. 33. American Association for the Advancement of Science, p. eaau6085, Mar. 01, 2019, doi: 10.1126/sciimmunol.aau6085.
- [58] Sciencedirect, "White Pulp - an overview | ScienceDirect Topics." <https://www.sciencedirect.com/topics/veterinary-science-and-veterinary-medicine/white-pulp> (accessed Jan. 28, 2021).
- [59] A. Wluka and W. L. Olszewski, "Innate and adaptive processes in the spleen," *Ann. Transplant.*, vol. 11, no. 4, pp. 22–29, 2006.

- [60] Britannica.com, “lymphoid tissue | Definition, Components, & Function,” *Encyclopedia Britannica*. <https://www.britannica.com/science/lymphoid-tissue> (accessed Feb. 09, 2021).
- [61] A. R. Kherlopian *et al.*, “A review of imaging techniques for systems biology,” *BMC Systems Biology*, vol. 2, no. 1. p. 74, Aug. 12, 2008, doi: 10.1186/1752-0509-2-74.
- [62] J. E. Hornick and E. H. Hinchcliffe, “It’s all about the pentiums: The use, manipulation, and storage of digital microscopy imaging data for the biological sciences,” *Molecular Reproduction and Development*, vol. 82, no. 7–8. John Wiley and Sons Inc., pp. 508–517, Jul. 01, 2015, doi: 10.1002/mrd.22294.
- [63] Themrmofisher, “Introduction to Fluorescence Microscopy | Nikon’s MicroscopyU.” <https://www.microscopyu.com/techniques/fluorescence/introduction-to-fluorescence-microscopy> (accessed Jan. 28, 2021).
- [64] D. A. Basiji, W. E. Ortyrn, L. Liang, V. Venkatachalam, and P. Morrissey, “Cellular Image Analysis and Imaging by Flow Cytometry,” *Clinics in Laboratory Medicine*, vol. 27, no. 3. pp. 653–670, Sep. 2007, doi: 10.1016/j.cll.2007.05.008.
- [65] Khanacademy, “What is Hooke’s Law? (article) | Khan Academy.” <https://www.khanacademy.org/science/physics/work-and-energy/hookes-law/a/what-is-hookes-law> (accessed Jan. 28, 2021).
- [66] G. Binnig, C. F. Quate, and C. Gerber, “Atomic force microscope,” *Phys. Rev. Lett.*, vol. 56, no. 9, pp. 930–933, 1986, doi: 10.1103/PhysRevLett.56.930.
- [67] S. Aryal, “Electron microscope- definition, principle, types, uses, images.” <https://microbenotes.com/electron-microscope-principle-types-components-applications-advantages-limitations/> (accessed Jan. 28, 2021).
- [68] S. Uchida, “Image processing and recognition for biological images,” *Development Growth and Differentiation*, vol. 55, no. 4. pp. 523–549, May 07, 2013, doi: 10.1111/dgd.12054.
- [69] W. Chen, W. Li, X. Dong, and J. Pei, “A Review of Biological Image Analysis,” *Curr. Bioinform.*, vol. 13, no. 4, pp. 337–343, 2018, doi: 10.2174/1574893612666170718153316.
- [70] I. Oguz, M. Sonka, “Image Segmentation - an overview | ScienceDirect Topics.” <https://www.sciencedirect.com/topics/computer-science/image-segmentation> (accessed Jan. 28, 2021).
- [71] Nist, “Quantification of Cells with Specific Phenotypic Characteristics | NIST.” <https://www.nist.gov/programs-projects/quantification-cells-specific-phenotypic-characteristics> (accessed Jan. 28, 2021).

- [72] A. Di Biasio, L. Ambrosone, and C. Cametti, "The dielectric behavior of nonspherical biological cell suspensions: An analytic approach," *Biophys. J.*, vol. 99, no. 1, pp. 163–174, Jul. 2010, doi: 10.1016/j.bpj.2010.04.006.
- [73] D. Noble, "Electrical properties of biological cells," *Nature*, vol. 276, no. 5687, p. 541, 1978, doi: 10.1038/276541a0.
- [74] N. Nasir and M. Al Ahmad, "Cells Electrical Characterization: Dielectric Properties, Mixture, and Modeling Theories," *Journal of Engineering (United Kingdom)*, vol. 2020. Hindawi Limited, pp. 1–17, Jan. 24, 2020, doi: 10.1155/2020/9475490.
- [75] J. J. Goldberger, H. Subacius, I. Sen-Gupta, D. Johnson, A. H. Kadish, and J. Ng, "A new method to determine the electrical transfer function of the human thorax," *Am. J. Physiol.-Heart Circ. Physiol.*, vol. 293, no. 6, pp. H3440–H3447, Dec. 2007, doi: 10.1152/ajpheart.00707.2007.
- [76] S. Orfanidis, "Introduction to Signal Processing." <https://www.ece.rutgers.edu/~orfanidi/intro2sp/> (accessed Jan. 30, 2021).
- [77] Electronicsclub, "AC, DC and Electrical Signals," 2006. Accessed: Jan. 28, 2021. [Online]. Available: <http://www.kpsec.freeuk.com/acdc.htm>.
- [78] C. A. O. Regan, "(12) United States Patent," vol. 2, no. 12, 2013.
- [79] K. Chu, "Benign Disorders and Diseases of the Breast: concepts and clinical management, ed 2.," *J. Laparoendosc. Adv. Surg. Tech.*, vol. 10, no. 6, pp. 347–348, Dec. 2000, doi: 10.1089/lap.2000.10.347.
- [80] H. D. Cheng, J. Shan, W. Ju, Y. Guo, and L. Zhang, "Automated breast cancer detection and classification using ultrasound images: A survey," *Pattern Recognit.*, vol. 43, no. 1, pp. 299–317, Jan. 2010, doi: 10.1016/j.patcog.2009.05.012.
- [81] Fda, "Ultrasound Imaging | FDA." <https://www.fda.gov/radiation-emitting-products/medical-imaging/ultrasound-imaging> (accessed Jan. 29, 2021).
- [82] Nibib.nih, "Magnetic Resonance Imaging (MRI)." <https://www.nibib.nih.gov/science-education/science-topics/magnetic-resonance-imaging-mri> (accessed Jan. 29, 2021).
- [83] N. Dey, A. S. Ashour, and A. S. Althoupey, "Thermal Imaging in Medical Science," 2017, pp. 87–117.
- [84] M. J. M. Harrap, N. Hempel de Ibarra, H. M. Whitney, and S. A. Rands, "Reporting of thermography parameters in biology: a systematic review of thermal imaging literature," *R. Soc. Open Sci.*, vol. 5, no. 12, p. 181281, Dec. 2018, doi: 10.1098/rsos.181281.
- [85] R. Saunders and E. van Rongen, "Radiofrequency Field - an overview | ScienceDirect Topics." <https://www.sciencedirect.com/topics/medicine-and-dentistry/radiofrequency-field> (accessed Jan. 29, 2021).

- [86] J. P. Leitzke and H. Zangl, "A review on electrical impedance tomography spectroscopy," *Sensors (Switzerland)*, vol. 20, no. 18, pp. 1–19, 2020, doi: 10.3390/s20185160.
- [87] D. Holmes and H. Morgan, "Single cell impedance cytometry for identification and counting of CD4 T-cells in human blood using impedance labels," *Anal. Chem.*, vol. 82, no. 4, pp. 1455–1461, Feb. 2010, doi: 10.1021/ac902568p.
- [88] M. Nadi, "Dielectric characterization of biological tissues: Constraints related to Ex Vivo measurements," in *Lecture Notes in Electrical Engineering*, vol. 21 LNEE, pp. 75–90, 2008, doi: 10.1007/978-3-540-69033-7_5.
- [89] D. G. Grier, "A revolution in optical manipulation," *Nature*, vol. 424, no. 6950, pp. 810–816, 2003, doi: 10.1038/nature01935.
- [90] Y. Nahmias, R. E. Schwartz, C. M. Verfaillie, and D. J. Odde, "Laser-guided direct writing for three-dimensional tissue engineering," *Biotechnol. Bioeng.*, vol. 92, no. 2, pp. 129–136, Oct. 2005, doi: 10.1002/bit.20585.
- [91] D. Bazou, G. P. Dowthwaite, I. M. Khan, C. W. Archer, J. R. Ralphs, and W. T. Coakley, "Gap junctional intercellular communication and cytoskeletal organization in chondrocytes in suspension in an ultrasound trap," *Mol. Membr. Biol.*, vol. 23, no. 2, pp. 195–205, Mar. 2006, doi: 10.1080/09687860600555906.
- [92] M. Tanase, E. J. Felton, D. S. Gray, A. Hultgren, C. S. Chen, and D. H. Reich, "Assembly of multicellular constructs and microarrays of cells using magnetic nanowires," *Lab Chip*, vol. 5, no. 6, pp. 598–605, 2005, doi: 10.1039/b500243e.
- [93] Nanoscience, "Scanning Electron Microscopy - Nanoscience Instruments." <https://www.nanoscience.com/techniques/scanning-electron-microscopy/> (accessed Jan. 29, 2021).
- [94] Ł. Mielańczyk, N. Matysiak, O. Klymenko, and R. Wojnicz, "Transmission Electron Microscopy of Biological Samples," in *The Transmission Electron Microscope - Theory and Applications*, InTech, pp. 193-194, 2015, doi: 10.5772/60680.
- [95] S. Vahabi, B. Nazemi Salman, and A. Javanmard, "Atomic force microscopy application in biological research: A review study," *Iran. J. Med. Sci.*, vol. 38, no. 2, pp. 76–83, 2013, Accessed: Jan. 29, 2021. [Online]. Available: [/pmc/articles/PMC3700051/?report=abstract](https://pmc/articles/PMC3700051/?report=abstract).
- [96] Nanomotion, "The Piezoelectric Effect - Piezoelectric Motors & Motion Systems." <https://www.nanomotion.com/nanomotion-technology/piezoelectric-effect/> (accessed Jan. 29, 2021).

- [97] J. Stetefeld, S. A. McKenna, and T. R. Patel, “Dynamic light scattering: a practical guide and applications in biomedical sciences,” *Biophysical Reviews*, vol. 8, no. 4. Springer Verlag, pp. 409–427, Dec. 01, 2016, doi: 10.1007/s12551-016-0218-6.
- [98] R. Harwood and E. Smith, “Absorption Spectroscopy - an overview | ScienceDirect Topics.” <https://www.sciencedirect.com/topics/medicine-and-dentistry/absorption-spectroscopy> (accessed Jan. 29, 2021).
- [99] L. Johnson, “Voltage vs Current: What are the Similarities & Differences?” <https://sciencing.com/voltage-vs-current-what-are-the-similarities-differences-13721181.html> (accessed Jan. 29, 2021).
- [100] Courses.lumenlearning, “Capacitors and Dielectrics | Physics.” <https://courses.lumenlearning.com/physics/chapter/19-5-capacitors-and-dielectrics/> (accessed Jan. 29, 2021).
- [101] M. M. Robinson, J. M. Martin, H. L. Atwood, and R. L. Cooper, “Modeling biological membranes with circuit boards and measuring electrical signals in axons: Student laboratory exercises,” *J. Vis. Exp.*, no. 47, p. 2325, 2010, doi: 10.3791/2325.
- [102] J. Golowasch *et al.*, “Membrane capacitance measurements revisited: Dependence of capacitance value on measurement method in nonisopotential neurons,” *J. Neurophysiol.*, vol. 102, no. 4, pp. 2161–2175, Oct. 2009, doi: 10.1152/jn.00160.2009.
- [103] Electrical4U, “Bipolar Junction Transistor (BJT): What is it & How Does it Work? | Electrical4U,” <https://www.electrical4u.com/bipolar-junction-transistor-or-bjt-n-p-n-or-p-n-p-transistor/> (accessed Feb. 09, 2021).
- [104] ATCC, “THP-1 ATCC® TIB-202™.” <https://www.atcc.org/products/all/TIB-202.aspx> (accessed Jan. 29, 2021).
- [105] C. Berges *et al.*, “A cell line model for the differentiation of human dendritic cells,” *Biochem. Biophys. Res. Commun.*, vol. 333, no. 3, pp. 896–907, Aug. 2005, doi: 10.1016/j.bbrc.2005.05.171.
- [106] O. Helm, J. Held-Feindt, H. Schäfer, and S. Sebens, “M1 and M2: There is no ‘good’ and ‘bad’-How macrophages promote malignancy-associated features in tumorigenesis,” *Oncoimmunology*, vol. 3, no. 7, 2014, doi: 10.4161/21624011.2014.946818.
- [107] Metrohm, “Metrohm Autolab Modules for electrochemical instruments | Metrohm Autolab.” https://www.metrohm.com/en-ae/products-overview/electrochemistry/autolab-modules/?gclid=CjwKCAiAgc-ABhA7EiwAjev-j8Y4hH_5FAENEIWWuunoHd5QAX_6EvOLByxnQyfXN9Hbc1MuyUAEzBoC4jcQAvD_BwE (accessed Jan. 29, 2021).

- [108] Chem.libretexts, “Cyclic Voltammetry - Chemistry LibreTexts.” [https://chem.libretexts.org/Bookshelves/Analytical_Chemistry/Supplemental_Modules_\(Analytical_Chemistry\)/Instrumental_Analysis/Cyclic_Voltammetry](https://chem.libretexts.org/Bookshelves/Analytical_Chemistry/Supplemental_Modules_(Analytical_Chemistry)/Instrumental_Analysis/Cyclic_Voltammetry) (accessed Jan. 29, 2021).
- [109] C. A. Schneider, W. S. Rasband, and K. W. Eliceiri, “NIH Image to ImageJ: 25 years of image analysis,” *Nature Methods*, vol. 9, no. 7. NIH Public Access, pp. 671–675, Jul. 2012, doi: 10.1038/nmeth.2089.
- [110] M. Cole, “What Are the Advantages & Disadvantages of Flow Cytometry?” <https://sciencing.com/advantages-disadvantages-flow-cytometry-10050486.html> (accessed Jan. 29, 2021).
- [111] N. Weidner and F. Hasteh, “HLA DR Antigen - an overview | ScienceDirect Topics.” <https://www.sciencedirect.com/topics/medicine-and-dentistry/hla-dr-antigen> (accessed Jan. 29, 2021).
- [112] F. Krombach, S. Münzing, A. M. Allmeling, J. T. Gerlach, J. Behr, and M. Dörger, “Cell size of alveolar macrophages: an interspecies comparison,” *Environ. Health Perspect.*, vol. 105 Suppl 5, no. suppl 5, pp. 1261–1263, Sep. 1997, doi: 10.1289/ehp.97105s51261.
- [113] H. Dumortier *et al.*, “Antigen Presentation by an Immature Myeloid Dendritic Cell Line Does Not Cause CTL Deletion In Vivo, but Generates CD8 + Central Memory-Like T Cells That Can Be Rescued for Full Effector Function,” *J. Immunol.*, vol. 175, no. 2, pp. 855–863, Jul. 2005, doi: 10.4049/jimmunol.175.2.855.

Appendix

```

filename = "data Dr.Mahmoud.xlsx"; %filename of the
dataset

%filename = "Experiment-23-Daughter Cell one.xlsx";
%filename = "Experiment-24- Daughter Cell two.xlsx";
range = "A1:G1802"; % Range in excel
sheets = ["THP-1", "Dendritic cells", "Macrophages"];
% Sheet name in excel

shapes = ["-r", "-g", "-b", "-c", "-m", "-y", "-k", "-d"];
% colors of the lines

columns = ["A1", "B1", "C1", "D1", "E1", "F1", "G1", "H1"];
ySize = 7; %

for sIndex=1:length(sheets)
    [NUM, TXT, RAW] =
xlsread(filename, sheets(sIndex), range);

    TXT(3) = cellstr("10");

    tspan = 0.04 : 0.04 : 36-0.04; % Time duration ->
initial value : step size : final value

    N = 3:901; % NUMBER OF ROWS (2+1 : 901 - 1 )

    v = NUM(N,1); % Voltage

```



```
g = 0.05/v; % g-function (dv/dt) / v
ic = 0; % initial conditions
opts = odeset('RelTol',1e-2,'AbsTol',1e-4);
%options for ode solver, Relative tolerance/Absolute
Tolerance

yResult(:, :, sIndex) = zeros(6, 899);

%% Loop through all readings
% 2 -> Empty
% 3 -> Media
% 4 -> 10
% 5 -> 10^2
% 6 -> 10^3
% 7 -> 10^4
% 8 -> 10^5
% 9 -> 10^6

sheetName = [char('CAPACITANCE')
char(sheets(sIndex))];

sheetName = char(sheetName);

figure

for i = 2:ySize
    current = NUM(N,i); % current for every step
```

```

        f = current./v; % f function i(t)/v(t);

        [t,yResult(i-1,1:899,sIndex)] = ode45(@(t,y)
myode(t,y,f,g,tspan), tspan, ic, opts); %% ode
solver -> t: time, y is capacitance

        semilogy(t,yResult(i-
1,1:899,sIndex),char(shapes(i-1))); %%Plot
logarithmic scale

        hold on %Plot all graphs together

        %ylim([10e-8 10e4]) % set the limits of the
y-axes

        %    max(yResult);

        if(i == 2)

xlswrite('MatlabResults.xlsx',t,sheetName,char(column
ns(1)));

        end

        xlswrite('MatlabResults.xlsx',yResult(i-
1,1:899,sIndex)',sheetName,char(columns(i)));

        end

        legend(TXT); % Set excel file headings as legend

%%DE-EMBEDDING

```

```

        sheetName = [char('DEEMBED')
char(sheets(sIndex))];

        sheetName = char(sheetName);

        figure

        for k = 3:6 %range of concentrations

            % ydiff = (yResult(k,:))./min(yResult(2,:));

            ydiff(k-2, :, sIndex) =

(yResult(k, :, sIndex))./max(yResult(2, :, sIndex));

%Divide result of concentration by maximum
capacitance of media

            ydiff(k-2, :, sIndex) = ydiff(k-2, :, sIndex).*

((yResult(k, :, sIndex).*yResult(2, :, sIndex)).^1);

%multiply results by the product of the results

            plot(t, ydiff(k-2, :, sIndex), char(shapes(k-
2))))); %%Plot

            if(k == 3)

xlswrite('MatlabResults.xlsx', t, sheetName, char(column
ns(1)));

            end

            xlswrite('MatlabResults.xlsx', ydiff(k-
2, :, sIndex)', sheetName, char(columns(k-1)));

            hold on %Plot all graphs togetherend

```

```
end

legend(TXT(3:6));

concentrations = TXT(3:end);

for k=1:length(concentrations)
    yMax(sIndex,k) = max(ydiff(k, :, sIndex));
    conct(sIndex,k) =
str2num(char(concentrations(k)));
end

end

shapes1 = ["-*b", "-*g", "-*r"];

figure

for sIndex=1:length(sheets)

semilogx(conct(sIndex, :), yMax(sIndex, :), char(shapes1
(sIndex)))

    if(sIndex == 1)

xlswrite('MatlabResults.xlsx', conct(sIndex, :), 'conc
ap', char(columns(1)));

end
```

```
xlswrite('MatlabResults.xlsx',yMax(sIndex,:),'conca  
p',char(columns(sIndex+1)));  
    hold on  
end  
legend(sheets)
```